Astbury Centre for Structural Molecular Biology

UNIVERSITY OF LEEDS

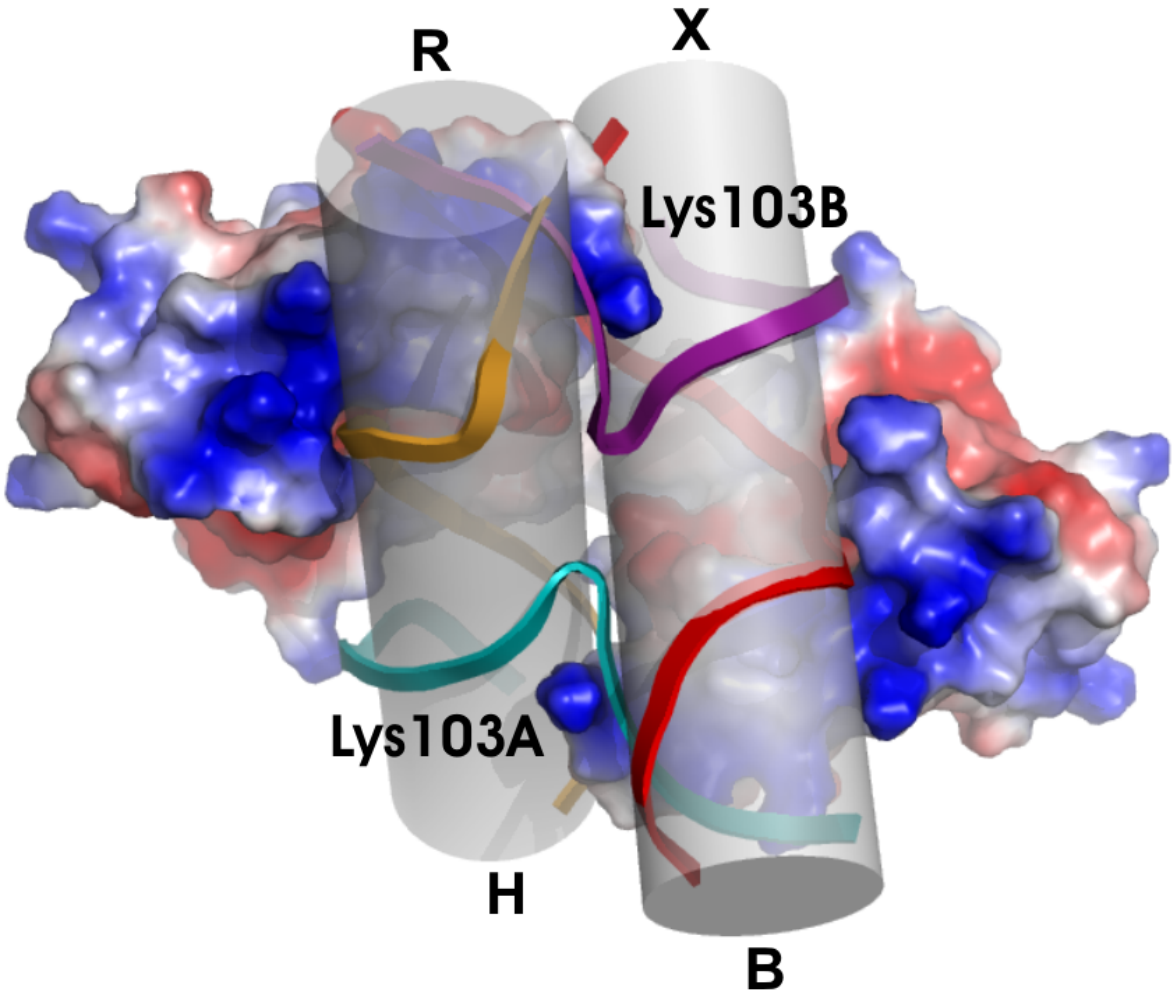

ASTBURY CENTRE

Annual Report 2007

Front cover illustration:

The crystal structure of bacteriophage T7 endonuclease I resolving a Holliday Junction
Jonathan M. Hadden, Stephen B Carr and Simon E.V. Phillips
(see page 62)

Acknowledgement
The Astbury Centre for Structural Molecular Biology thanks its many sponsors for support of the work and its members for writing these reports. The report is edited by Alan Berry.

This report is also available electronically via http://www.astbury.leeds.ac.uk

Mission Statement

The Astbury Centre for Structural Molecular Biology will promote interdisciplinary research of the highest standard on the structure and function of biological molecules, biomolecular assemblies and complexes using physico-chemical, molecular biological and computational approaches.

Introduction

It is once again a great pleasure to write this Introduction to the Annual Report on the activities within the Astbury Centre during 2007. As I described on these pages last year the only constant in life is change and this has been yet another hectic period in our development. In particular we have been preparing for the first visit by our external Scientific Advisory Board, and the visit is now scheduled for the second half of 2008.

The Astbury Society formed by our postdoctoral and postgraduate colleagues has also made major contributions to forging the personal links between laboratories, departments and disciplines essential to our future, with a series of highly enjoyable social and scientific events, including our second Annual Astbury Lecture, given by Dr Tim Hunt of Cancer Research UK and Nobel Laureate for Medicine & Physiology in 2001. Tim's overwhelming enthusiasm for his science and obvious delight in experimental approaches produced a stunning seminar. He then showed the kind of dedication and focus one expects of a Nobel Laureate in beating Kenny McDowall in an egg-and-spoon race at the BBQ and "Sports Day" (see photos on the Astbury Web Site). There is no doubt that the highlight of the year was our first residential research retreat held at the Castle Green Hotel, Kendal, in the Lake District, where we were all entertained and educated by the outstanding science presented by staff at every level of the Centre. I would like to thank Donna Fletcher particularly for her tireless efforts in organisation of this event and all the participants for "pulling out the stops" to present their latest work.

Astbury members continue to be very successful in raising external grant income and it was very encouraging to see some of our newly appointed staff getting their first major grants funded. 2007 also saw the second renewal of our Welcome Trust 4 Year PhD Studentship Scheme on the topic of the Molecular Basis of Biological Mechanisms. Thanks go to Alan Berry, Adam Nelson and Sheena Radford for steering our application successfully home.

The pages that follow describe some of the highlights of our work over the last year. These reports have largely been written by our younger researchers. Their tremendous enthusiasm for this kind of interdisciplinary work augurs well for our future. As always I am particularly struck by the breadth of activity in the Centre, ranging from the sophisticated applications of synthetic organic chemistry to the developments in single molecule biophysics. In between these extremes you will find groundbreaking activity in many traditional areas for structural biology, e.g. the developments in mass spectrometry for analysis of non-covalent self-assembling macromolecular complexes. The Astbury Centre has always been outward looking and this tradition continues with the many external collaborations acknowledged in these pages, from both within the UK and beyond. We would welcome discussions with anyone wishing to collaborate or simply to make use of our facilities, the details of which can be found via our web page (http://www.astbury.leeds.ac.uk/). These brief summaries, however, only scratch the surface of the work of the Centre. I hope you enjoy reading them, and if you wish to learn more please visit our website or contact the Director. The Centre also continues to host a very successful seminar programme that illustrates aspects of work within the Centre.

The Centre produces a regular Newsletter describing its activities. If you would like to receive an electronic copy of this Newsletter it can be downloaded from the Astbury web site. This annual report is also available as an 20.5MB PDF document that can be downloaded from our web site (www.astbury.leeds.ac.uk/Report/All_Reports.htm).

Finally I would like to thank our Editor, Alan Berry, once again for another outstanding job getting the Report together, ably assisted by Donna Fletcher.

Peter G. Stockley
Director, Astbury Centre for Structural Molecular Biology
Leeds, April 2008

Contents

Contributions indexed by Astbury Centre Principal Investigator

Subunit specificity in P pilus assembly studied by mass spectrometry

Rebecca J. Rose, Emanuele Paci, Sheena E. Radford and Alison E. Ashcroft

Introduction

P pili are multi-subunit fibres essential for the attachment of uropathogenic *E. coli* to the kidney. These fibres are formed by the non-covalent assembly of six different homologous subunit types into a final structure that is strictly defined in terms of the number and order of each subunit type. Figure 1 shows the subunits PapG (red), PapF (orange), PapE (yellow), PapK (green), PapA (cyan) and PapH (blue) assembling at the usher (PapC, grey) assisted by the chaperone PapD (brown). Assembly occurs through a mechanism termed "donor-strand exchange (DSE)" in which an N-terminal extension (Nte) of one subunit donates a β-strand to an adjacent subunit, completing its immunoglobulin fold. Despite the structural determination of the different subunits, the specificity of subunit ordering in pilus assembly remains unknown.

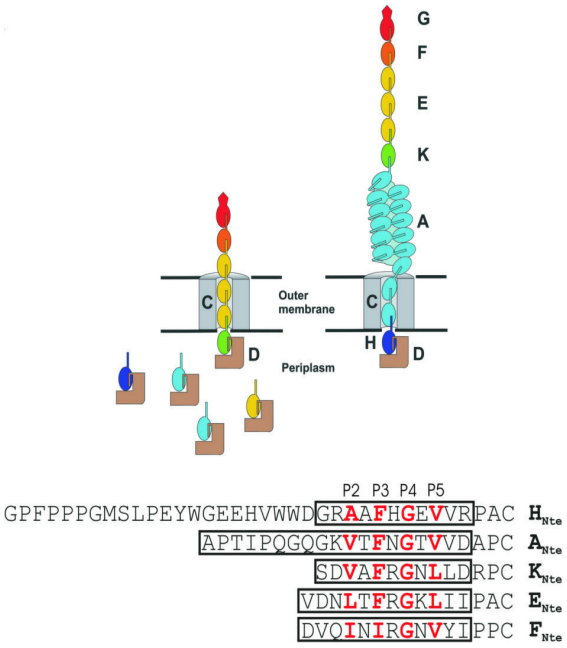

Figure 1: Scheme of P pilus biogenesis

We have used non-covalent mass spectrometry (MS) to monitor DSE between all 30 possible pairs of P pilus subunits (G, F, E, K, A, H) and peptides representing their Ntes (Figure 1: H_{Nte}, A_{Nte}, K_{Nte}, E_{Nte}, F_{Nte}). The results show a striking correlation between the natural order of subunits in pili and their ability to undergo DSE *in vitro*, revealing new insights into the molecular mechanism by which the assembly of this complex is achieved.

Mass spectrometry of non-covalently bound P pilus subunits and Nte peptides

The individual chaperone (PapD)-subunit reactions with the Nte peptides were followed in real-time by nano-electrospray ionisation (nanoESI)-MS. Spectra of the reactions between PapD:PapE and the Nte peptide of PapK (K_{Nte}; a cognate DSE reaction), and PapD:PapF and the Nte peptide of PapH (H_{Nte}; a non-cognate DSE reaction) are shown as examples in Figure 2. The mass spectra of the chaperone:subunit complexes immediately after addition of each Nte (Figure 2a,e) show these species to be the predominant species (red peaks). With time, changes in the spectra reveal the progress of DSE as the peaks corresponding to PapD:PapE and PapD:PapF decrease in intensity and peaks relating to the PapE:K_{Nte} or PapF:H_{Nte} products (blue peaks) and released PapD (yellow peaks) appear and increase in intensity (Figure 2b,c,f,g). Integration of the peaks from each spectrum illustrates the progression of DSE for the cognate and non-cognate pairs (Figure 2d,h). Whilst the reaction between PapD:PapE and K_{Nte} is effectively complete within 28 h, a significant amount of the reactant complex remains in the PapD:PapF plus PapH_{Nte} reaction at this time, with only small peaks relating to PapF:H_{Nte} observed (Figure 2g).

The data demonstrate the effectiveness of ESI-MS to monitor DSE in real-time, allowing the potential of different cognate/ non-cognate pairs to undergo DSE to be compared (Figure 2d,h) and suggest an inherent specificity between different pairs of acceptor subunit grooves and donor subunit Ntes that mirrors subunit order in the intact pilus.

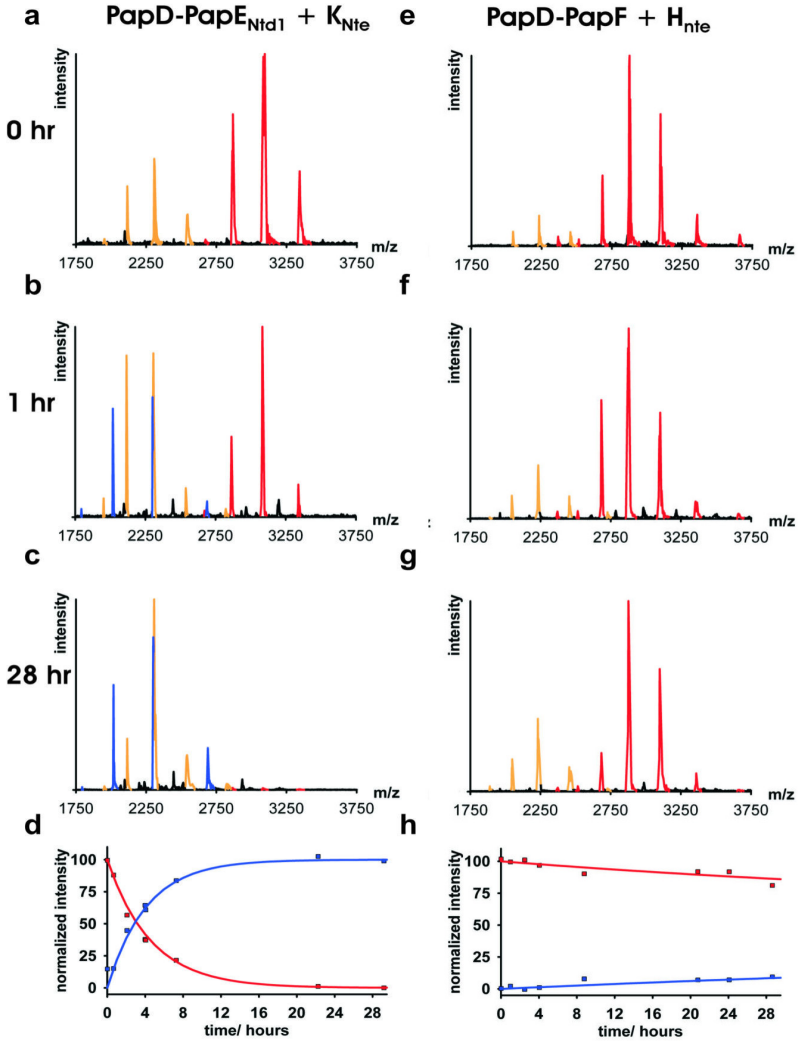

Figure 2: Discrimination in pilus assembly revealed by monitoring the rate of DSE of different chaperone:subunit – Nte pairs in real-time by mass spectrometry**.**

Molecular simulations are also being used to determine at atomic resolution the factors which determine the largely different reactivity between subunits and the consequences on the macroscopic growth of functional pili.

Publications

Remaut, H., Rose, R.J., Hannan, T., Hultgren, S.J., Radford, S.E., Ashcroft, A.E., Waksman, G. (2006) Donor-strand exchange in chaperone-assisted pilus assembly proceeds through a concerted beta-strand displacement mechanism. *Molecular Cell***, 22,** 831-842.

Funding

This work was funded by the BBSRC, the Wellcome Trust, and (Waters Corpn.). We acknowledge with thanks continued support from Robert Bateman (Waters UK Ltd), supporting work by Toshana Foster (Wellcome Trust post-graduate student), and provision of samples and numerous enlightening discussions from our collaborators Gabriel Waksman, Han Remaut, Denis Verger and Tina Daviter of the Institute of Structural Molecular Biology & School of Crystallography, Birkbeck College, London.

Mass spectrometry research group

David P. Smith, Victoria L. Morton, Rebecca J. Rose, John P. Hodkinson, Lynsey N. Jones, Thomas W. Knapman, Jimmy Muldoon and Alison E. Ashcroft

Introduction

The Mass Spectrometry (MS) Facility has five mass spectrometers: a new **Synapt HDMS** orthogonal acceleration quadrupole time-of-flight instrument with a NanoMate nano-electrospray ionisation (ESI) interface and ion mobility spectrometry capabilities (Figure 1), an **LCT Premier** time-of-flight instrument with a NanoMate interface and ion mobility spectrometry capabilities, a **Q-Tof** orthogonal acceleration quadrupole-time-of-flight instrument with nano-ESI and capillary HPLC, a **Platform II** ESI-quadrupole instrument with HPLC, and a surface enhanced/matrix assisted laser desorption ionization (SELDI/MALDI) **ProteinChip Reader.**

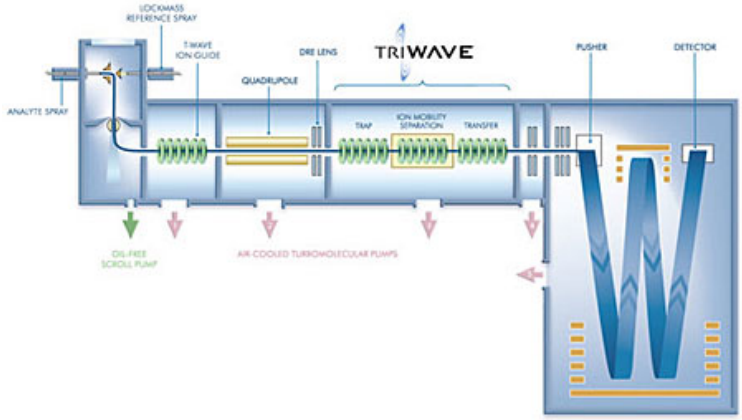

Figure 1: The new Synapt HDMS mass spectrometer has an integral travelling wave ion mobility spectrometry device situated in between the quadrupole and time-of-flight analysers**.**

Research

Our research involves the application of mass spectrometry to the structural elucidation of biomolecules and can be summarised as follows:

i) Mass spectrometry method development. We are developing Ion Mobility Spectrometry (IMS) coupled to mass spectrometry as a method to separate co-populated protein conformers, mixtures of oligomers, and for the structural characterisation of peptides (Figure 2). We have two IMS devices: a high Field Asymmetric waveform IMS (FAIMS) system on the **LCT Premier** and a Travelling Wave IMS (TWIMS) system on the **Synapt HDMS.**

ii) Protein folding. Protein folding is an intriguing area of biochemistry and protein mis-folding is thought to be a contributing factor to several diseases. Working with Sheena Radford's group, ESI-MS is being used to investigate β_2-microglobulin conformations using charge state distribution analysis, proteolysis and H/D exchange to gain insights into folding mechanisms.

iii) Protein-ligand non-covalent interactions and macromolecular assembly. ESI-MS is being used to investigate non-covalently bound macromolecular structures e.g., protein-ligand, protein-protein, and protein-RNA complexes. The latter are important in virus assembly, an area we are investigating in collaboration with Peter Stockley and Nicola Stonehouse. Protein-protein macromolecular complexes are under investigation as an integral part of our pilus assembly and β_2-microglobulin amyloid projects with Sheena Radford. We are also investigating the inhibition of protein-protein interactions in

conjunction with Andrew Wilson, peptide self-assembly in conjunction with Amalia Aggeli, and membrane protein functionality in collaboration with Peter Henderson.

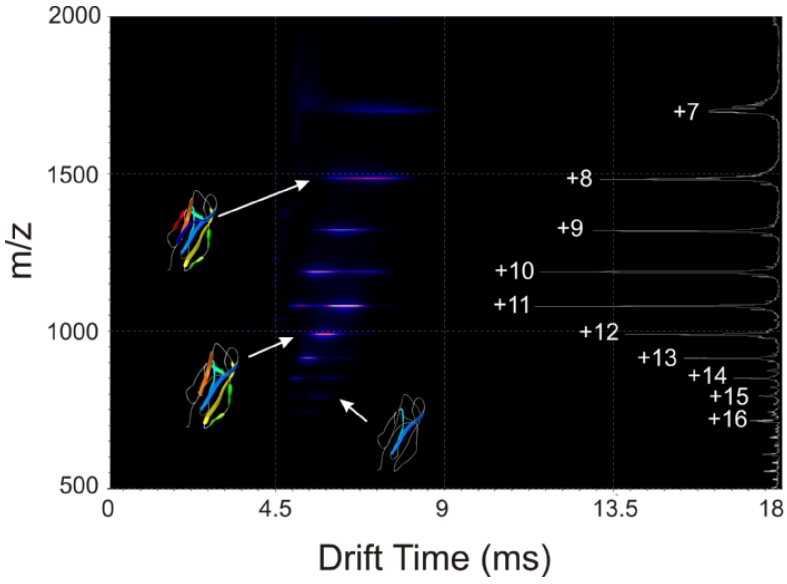

Figure 2: ESI-IMS-MS applied to the separation and quantification of co-populated conformers of the amyloidogenic protein, β_2-microglobulin. The Driftscope plot shows IMS drift time v. m/z for β_2m at pH 2.6 and the folded, partially folded and unfolded conformers are highlighted adjacent to their ESI-IMS-MS signals. Inset at right hand side: the full scan m/z spectra of the protein showing the charge state distribution.

Publications

Legrand, B., Ashcroft, A.E. & Arscott, S. (2007) SOI-based nanoelectrospray emitter tips for mass spectrometry: a coupled MEMS and microfluidic design. *J. Micromech. & Microeng.* **17,** 509-514.

Ironmonger, A., Whittaker, B., Baron, A.J., Clique, B., Adams, C.J., Ashcroft, A.E., Stockley, P.G. & Nelson, A. (2007) Scanning conformational space with a library of stereo- and regiochemically diverse aminoglycoside derivatives: The discovery of new ligands for RNA hairpin sequences. *Org. Biomol. Chem.* **5**, 1081-1086.

Stockley, P.G., Rolfsson, O., Thompson, G.S., Basnak, G**.,** Francese, S., Stonehouse, N.J., Homans, S.W. & Ashcroft, A.E. (2007) A simple, RNA-mediated allosteric switch controls the pathway to formation of a *T*=3 capsid. *J. Mol. Biol.* **369**, 541-552.

White, H.D. & Ashcroft, A.E. (2007) Real-time measurement of myosin–nucleotide noncovalent complexes by nano-electrospray ionisation mass spectrometry. *Biophysical Journal.* **93**, 914-919.

Arscott, S., Legrand, B., Buchaillot, L. & Ashcroft, A.E. (2007) A silicon beam-based microcantilever nanoelectrosprayer. *Sensors and Actuators B.* **125**, 72-78.

Smith, D.P., Giles, K., Bateman, R.H., Radford, S.E. & Ashcroft, A.E. (2007) Monitoring co-populated conformational states during protein folding events using electrospray ionisation – ion mobility spectrometry – mass spectrometry. *J. Am. Soc. Mass Spectrom*. **18,** 2180-2190.

Funding & Acknowledgements

We thank our internal collaborators Sheena Radford, Peter Stockley, Nicola Stonehouse, Peter Henderson, Alison Baker, Amalia Aggeli and Andrew Wilson, and also our external collaborators Steve Arscott (CNRS France), Howard White (Eastern Virginia Medical School, USA) and Kevin Giles and Robert Bateman (Waters UK Ltd).

Financial support from the University of Leeds, the Wellcome Trust, the BBSRC, the EPSRC, Waters Corpn., AstraZeneca, Pfizer and Syngenta is gratefully acknowledged.

New tools for the enzymatic synthesis of complex oligosaccharides.

Nicole Timms, Louise Horsfall, Ieuan Davies, Adam Nelson and Alan Berry

Introduction

Sialylated oligosaccharides, present on mammalian outer cell surfaces, play vital roles in cellular interactions. Bacteria are able to mimic these structures, enabling them to successfully evade the host's immune system. The ability to synthesise various sialylated oligosaccharides would therefore significantly benefit the study of infectious and autoimmune diseases. To this end, our laboratory is primarily aiming to evolve novel enzymes involved in oligosaccharide synthesis and sialylation in order to obtain a library of differentially sialylated sugars, essential for discovering their full roles in biology and as therapeutic targets.

Results

We have previously used structure-guided saturation mutagenesis to create an enzyme variant capable of producing a 6-dipropylcarboxamide sialic acid analogue. We are now investigating subsequent enzymes in the creation of sialylated oligosaccharides including a CMP-NeuAc synthetase (CNS) from *Neisseria meningitidis* and the sialyltransferases CstII from *Campylobacter jejuni* and Pst from *Pasteurella multocida*, with a view to obtaining a one-pot three-enzyme synthetic route to a variety of oligosaccharides.

CNS is responsible for an intermediate step in the creation of sialylated oligosaccharides; wild-type CNS activates sialic acid, using CTP, producing CMP-sialic acid. Using the CNS crystal structure, we have identified six residues Gln104, Lys142, Tyr179, Phe192, Phe193 and Asp209, all of which contact sialic acid in positions that are altered in the 6-dipropylcarboxamide sialic acid analogue. We reasoned that a variant with activity for the analogue may be found in libraries of mutants of these residues. Such libraries, produced by mega-primer PCR, are currently being screened using a high-throughput thiobarbituric acid assay in which mutants with the desired activity produce a pink colour. Any variants found to be active with the 6-dipropylcarboxamide sialic acid analogue will be identified and the activated product will be purified and tested as a novel substrate for the sialyltransferases.

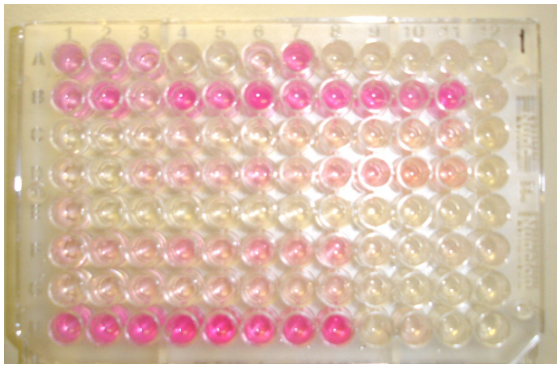

Figure 1: 96 well plate demonstrating the effectiveness of the TBA assay used in the screening of CNS mutants.

Pst, known as both Δ24PmST1 and tPm0188Ph in the literature, is a bifunctional enzyme reportedly showing both α-2,3-sialyltransferase and α-2,6-sialyltransferase activity, dependent upon the pH. This enzyme has been cloned, expressed and purified, with the α-2,3-sialyltransferase activity being confirmed at a range of pHs, the optimum of which has been identified as pH 9.0, whilst the secondary activity remains elusive but is currently under further investigation. Confirmation of the sialylated reaction products has been made possible by the use of a fluorescein-labelled lactose acceptor molecule, which is detectable by HPLC analysis, the sialylated product having a longer retention time than the non-sialylated substrate in the presence of an ion pair reagent. The synthesis of the fluorescent lactose species was undertaken by a stepwise glycosylation/conjugation methodology. A short three-carbon linker unit was glycosylated with acetyl protected lactosyl bromide. Sequential deprotection of the lactose and linker gave an amine which, upon conjugation with fluorescein isothiocyanate (FITC) to give a thiourea, led to fluorescently labelled species **A** (Fig. 2). The

synthesis of alternative fluorescently labelled glycosyl acceptors and donors is also under way.

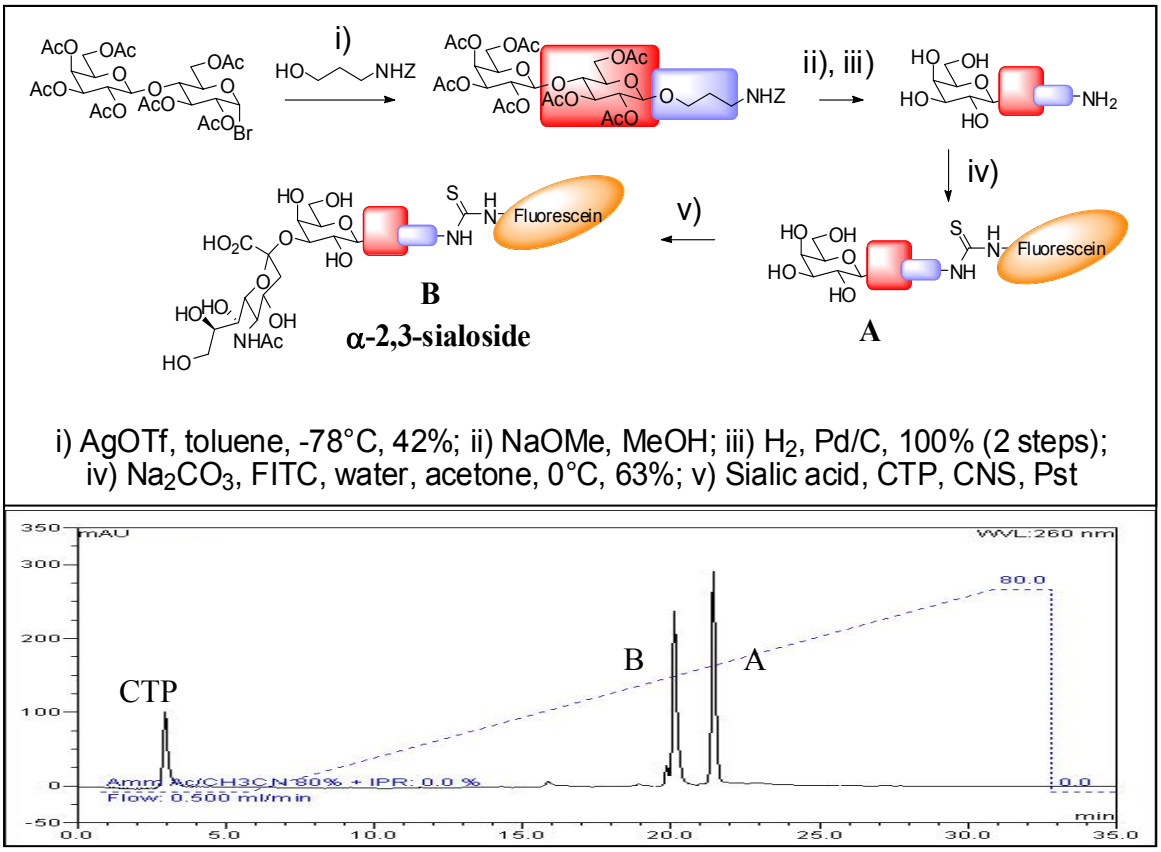

Figure 2 Figure to show (top) the chemical synthesis of fluorescently labelled lactose (A), and the enzymatic addition of sialic acid to give the final reaction product, an α-2,3-sialoside (B). And, below, to show the HPLC chromatogram of substrate (A) and product (B) separation.

CstII is an α-2,3-sialyltransferase which uses a β-galactose moiety as the acceptor sugar. It is also reported to perform a second sialylation on the 8-position of the first sialic acid. This enzyme has been cloned and a single point mutation, reported in the literature to increase activity and stability, introduced before its subsequent expression and purification. The reported α-2,3-sialyltransferase activity has been confirmed with galactose, lactose and fluorescein labelled lactose .

Funding
This work is funded by the BBSRC

Structural analysis of engineered *N*-acetyl-neuraminic acid lyase

Ivan Campeotto, Mandy Bolt, Chi H. Trinh, Alan Berry, Adam Nelson,
Arwen Pearson and Simon E.V. Phillips

Introduction:

Sialic acids play a pivotal role in mediating host-pathogen interactions and therefore drug analogues of sialic acid are exciting prospects as therapeutic agents. One example of clinical relevance is the inhibition of influenza virus attachment and particle release from infected cells targeted by the sialic acid derivatives Relenza® (GSK) and Tamiflu® (Roche). *De novo* chemical synthesis of sialic acid analogues is difficult owing to the number of chiral centers, and their production often relies on the use of the enzyme *N*-acetylneuraminic acid lyase (NAL) also called *N*-acetylneuraminic acid aldolase or sialic acid aldolase. NAL catalyzes the reversible condensation between *N*-acetyl-D-mannosamine and pyruvate to yield sialic acid (Fig.1) but the wild-type enzyme has restricted substrate specificity and limited substrate stereoselectivity.

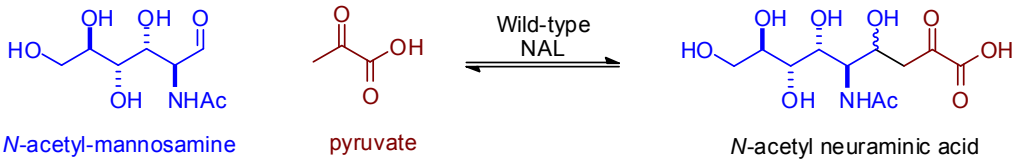

Fig.1 NAL wild-type reaction, showing the condensation between *N*-acetyl-D-mannosamine and pyruvate to yield sialic acid.

Using an approach which encompasses directed evolution and structure guided saturation mutagenesis, NAL variants have been made which have altered substrate specificity and stereoselectivity. The mutant E192N catalyses the aldol reaction between pyruvate and a dipropylamide substrate **1**, whereas the variants NAL-*R* (E192N/T167V/S208V) and NAL-*S* (E192N/T167G) catalyse the same reaction but with stereocontrol at C-4: an *R*-configured centre is the major stereoisomer when NAL-*R* is used, and an *S*-configured centre can be obtained by using the NAL-*S* mutant. X-ray crystallographic studies of these proteins, with and without substrates, has been undertaken in order to offer an insight into the mechanism of substrate specificity and stereocontrol in the NAL variants.

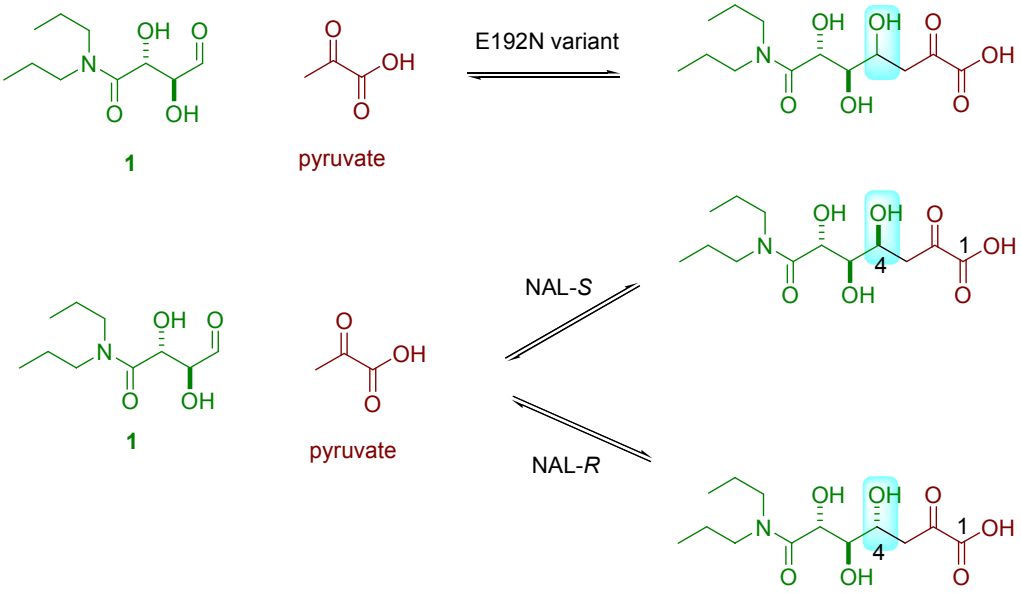

Figure 2. Reactions of NAL variants. The mutant E192N catalyses the aldol reaction between the dipropylamide substrate. **1**, and pyruvate. The variants NAL-*R* and NAL-*S* make *R* and *S* configured carbon centres at C-4 respectively.

Crystallographic studies:
NAL is a tetramer of four-identical subunits, each of which forms an alpha/beta barrel. The active site is characteristically located at C-terminal end of the β-barrel.

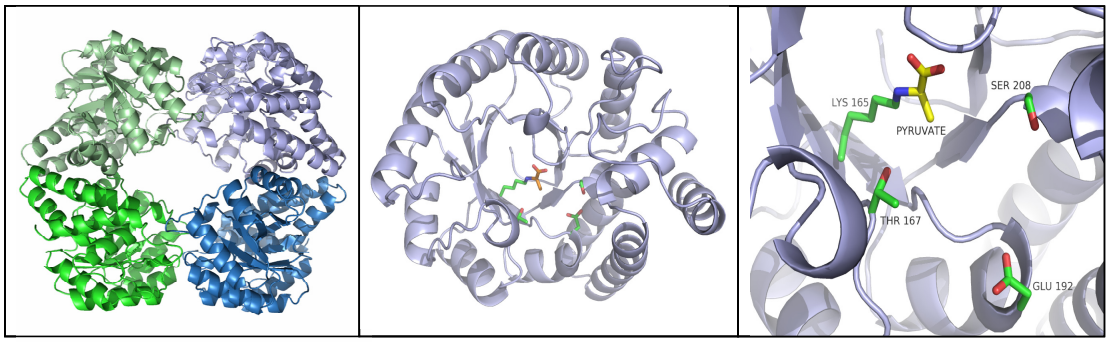

Figure 3. *E.coli* NAL overall X-ray structure of the tetramer, the monomer and the catalytic pocket where the amino acid substitutions are located.

- The crystal structure of the mutant E192N has been solved at 1.5Å and 1.9Å resolution respectively, with and without pyruvate.
- The crystal structure of the NAL-*S* with pyruvate was obtained at 1.9Å resolution, while the structure of the NAL-*R* was obtained in absence of pyruvate at 2.3Å resolution.

These structures form the basis of a structural investigation of the changes in stereochemistry brought about by the mutations found in the evolved enzymes. The crystal structures of the NAL-*S* mutant without pyruvate and the structure of the NAL-*R* mutant with pyruvate will be required in order to complete the first set of crystal structures and to investigate the effects of the protein engineering on the protein structure. However, preliminary structural analysis has suggested a role of residue Tyr137, located in the catalytic pocket in close proximity to the pyruvate. It is postulated that Tyr137 mediates the proton abstraction from the substrate in the *H. influenzae* homologue protein, and structural changes at this position could be critical in determining enzyme stereochemistry.

Synthesis of the following substrates has also been undertaken to explore further the substrate specificity and stereoselectivity of the aldol reaction with evolved NAL mutants:

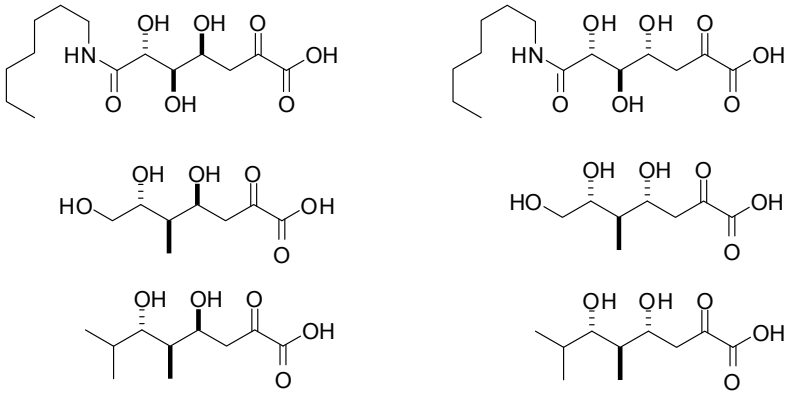

Figure 4 Substrates synthesised for further evolution of NAL

Funding support:
This work has been sponsored by BBSRC and the Wellcome Trust.

Using force to investigate the stability of proteins and their complexes

Eleanore Hann, Jim Pullen, David Sadler, Sheena Radford and David Brockwell

Introduction

Mechanical forces such as those encountered during hydrodynamic flow and cell deformation are ubiquitous in Nature and consequently many proteins are adapted to resist or respond to a mechanical stimulus. The ability to specifically tether and manipulate single biomolecules using techniques such as optical tweezers and the atomic force microscope has allowed experimentalists to measure the effects of force on the stability (or lifetime) of proteins and their complexes, as well as the measurement of the steps size and the effect of load on a wide variety of processive motors.

The aim of our research is to investigate the fundamental effects of force on model proteins and their complexes and apply this knowledge to understand the many seemingly diverse processes *in vivo* where force has been implicated, such as protein translocation and degradation, the remodelling of complexes and signal transduction. Currently research in the group covers three areas: (i) delineation of the mechanical unfolding transition state and rational engineering of the mechanical stability of the small, topologically simple protein L; (ii) measurement of the effects of complexation on the mechanical unfolding energy landscape of proteins and (iii) direct measurement of the unbinding force and pathway of protein:ligand interactions.

Breaking apart high affinity complexes by application of small forces.

As part of their function many proteins form complexes with other proteins or non-proteinaceous ligands. In some cases, the affinity between ligand and receptor is very high to sequester either toxic substances or nutrients vital to other organisms (biotin:streptavidin, for example) or to inhibit the action of a potentially deleterious enzyme. In many cases the high affinity of the complex results from a rapid, diffusion limited on-rate and an off-rate of the order of tens of hours – far longer than the timescales over which most biochemical processes operate.

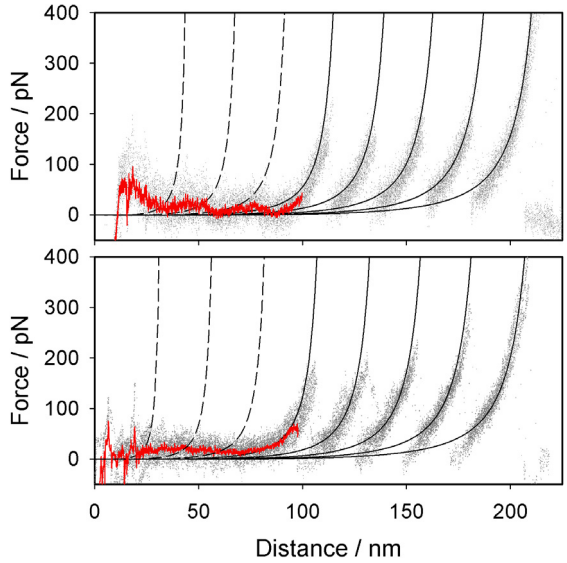

Figure 1: In a heteropolymer comprising of four I27 domains alternating with three Im9 domains, uncomplexed Im9 unfolds at a force below the thermal noise limit of the AFM (bottom). Upon complexation with E9 (top), the mechanical resistance of Im9 increases, but the protein still unfolds at a relatively low force (~35 pN). Multiple force extension profiles (grey dots) are plotted for each experiment. Black continuous and dashed lines show the predicted position of unfolding events for I27 and Im9, respectively. Red lines show a running average of the overlaid plots in the region that Im9 unfolds.

We have been investigating the role that force may play in the remodelling of protein complexes by studying the strong interaction between the colicin nuclease E9 and its ligand, the four helical bacterial immunity protein, Im9. Colicins are bacteriocins produced by some strains of *E.coli* which are toxic to related species, but not the host, owing to the production of an inhibitory immunity protein which binds tightly to the nuclease (K_d ~fM) preventing hydrolysis of the host's DNA. However, once exported out of the host cell, this highly avid interaction must be broken to allow cell invasion and enable catalytic activity. How does this occur on such a

rapid timescale? Many aspects of the colicin import pathway are currently poorly understood but it is thought that force may play an important role *via* either coupling to the proton motive force across the inner membrane or by the action of an energy dependent ATPase protease.

To test this theory the mechanical unfolding strength of Im9 was measured in the absence (Figure 1, bottom) and presence of E9 (Figure 1, top) by constructing a tandem array of alternating Im9 and I27 domains (the latter has previously been shown to display significant mechanical strength and its unfolding profile therefore acts as control to verify the unfolding of Im9). In the absence of E9, Im9 unfolds at a force below the thermal noise limit of the AFM (< 20 pN) in accord with the hypothesis that all α-helical proteins are generally mechanically weak. Surprisingly, complexation with E9 was found to enhance the mechanical strength of Im9 only slightly which still unfolded (and therefore dissociated from E9) under the application of a relatively low level of force (~35 pN). These data suggest that it is possible to disrupt strong complexes *in vivo* by application of a small force to one member of a protein pair. We are now testing this hypothesis by measuring the effects of complexation on the degradation rate of Im9 by a large bacterial protease thought to actively unfold substrate proteins before proteolysis.

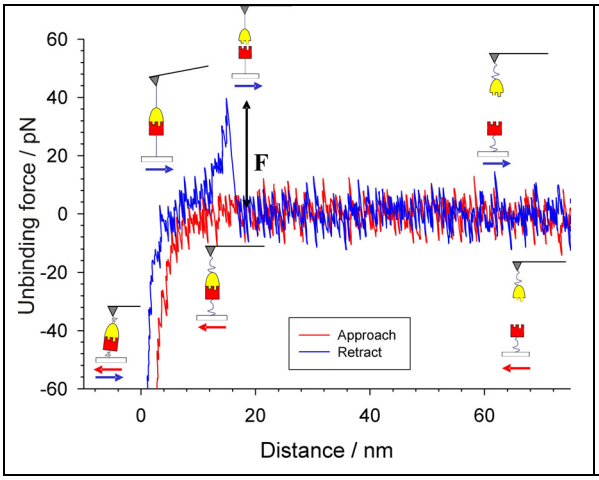

Figure 2: Measurement of the unbinding force (F) for a single E9/Im9 complex by AFM. Upon approach to the surface (red arrows and force-distance trace) a complex is formed between Im9 (yellow) attached to the cantilever tip *via* a polyethylene glycol linker and E9 (red) immobilised to a silicon nitride substrate immobilised in the same manner. Retracting the tip (blue arrows and force-distance trace) increases the force applied across this interaction until it is broken and the force returns to zero.

In addition to measuring the effects of complexation on the mechanical properties of Im9, we have recently developed protocols to specifically immobilise Im9 and E9 to an AFM tip and silicon nitride substrate, respectively (Figure 2). By sequentially approaching and retracting the Im9 labelled tip from an E9 covered surface, it is possible to measure the rupture force of a single protein:protein interaction. Repeating these experiments at different retraction speeds allows the underlying energy landscape of this strong interaction to be mapped, revealing features difficult to detect by standard ensemble methods and allowing estimates of the magnitude of force required to disrupt such complexes *in vivo*.

Collaborators

Emanuele Paci, School of Physics and Astronomy, Stuart Warriner, School of Chemistry, University of Leeds. Colin Kleanthous, Department of Biology, University of York

Publications

The effect of protein complexation on the mechanical stability of Im9. Hann, E., Kirkpatrick, N., Kleanthous, C., Smith, D., Radford, S. and Brockwell, D. (2007) *Biophys. J.*, **92**:L79-L81.

Probing the mechanical stability of proteins using the atomic force microscope. Brockwell, D. (2007) *Biochem. Soc. Trans*. **35**:1564-1568.

Funding
We thank Keith Ainley for technical support and the BBSRC, EPSRC and the University of Leeds for funding. DJB is an EPSRC funded White Rose Doctoral Training Centre lecturer.

Elucidating the folding mechanism of a bacterial outer membrane protein

Gerard H M Huysmans, Sheena E Radford, David J Brockwell and Stephen A Baldwin

Introduction

One of the key questions in structural biology is how the three dimensional structures of proteins are encoded in their amino acid sequences. Although much progress towards understanding the folding process has been made for water-soluble proteins, our understanding of this process for membrane proteins remains very limited. This is mainly because few membrane proteins can be reversibly unfolded and refolded *in vitro* and because of the need for an adequate mimetic for the biological membrane. To increase our understanding of membrane protein biosynthesis, we investigated the bacterial outer membrane protein PagP, which we have shown can be reversibly folded into artificial liposomes. This small, transmembrane, 8-stranded β-barrel protein acts as a lipid A palmitoyltransferase. A unique feature of the PagP-family is an N-terminal α-helix which is suggested to lie parallel to the membrane plane. The roles of this helix in the folding and stability of PagP were investigated using tryptophan fluorescence and circular dichroism (CD) spectroscopy.

PagP folds co-operatively in artificial membranes

PagP was refolded from a guanidinium-Cl denatured state into *di*$C_{12:0}$PC liposomes with a lipid-to-protein ratio of 800:1 in the presence of 7 M urea. Refolding was confirmed by altered migration on SDS-polyacrylamide gels, tryptophan fluorescence, CD and enzymic activity towards the artificial substrate *p*-nitrophenylpalmitate. The presence of a positive band at 232 nm in the CD-spectrum arising from aromatic stacking in the folded protein, in addition to the β-sheet minimum positioned around 218 nm (Figure 1a, inset), enabled the simultaneous monitoring of secondary and tertiary structure formation. The folding kinetics monitored at 218 nm exhibited a burst phase with an amplitude up to 50 % of the total change, followed by a single exponential with a rate constant of 0.92 ± 0.03 min^{-1} (Figure 1a). In contrast, when monitored at 232 nm the folding kinetics did not show a burst and could be fitted to a single exponential with a rate constant of 0.88 ± 0.01 min^{-1} (Figure 1b), showing that in this phase secondary and tertiary structure forms co-operatively.

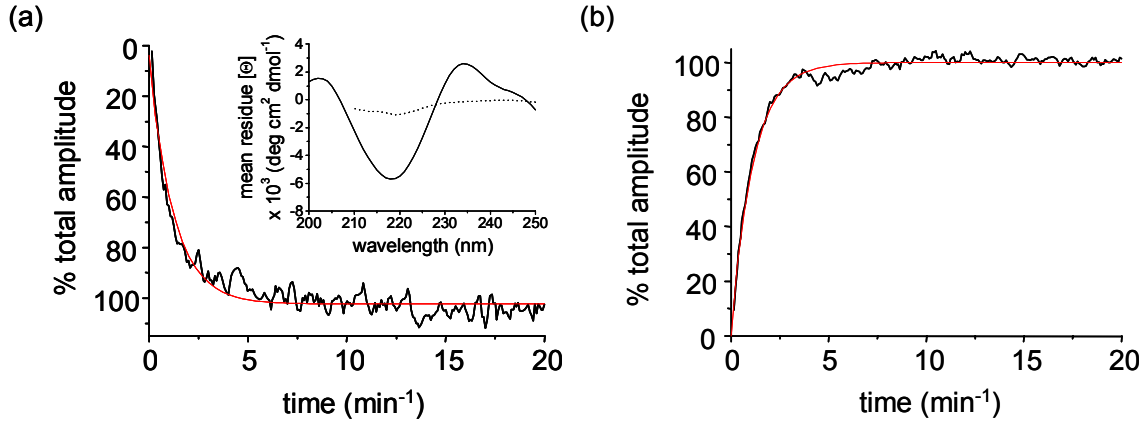

Figure 1: Folding kinetics of wild-type PagP into large unilamellar vesicles of *di*$C_{12:0}$PC, monitored by CD at 218 nm (a) and 232 nm (b). Inset in (a): CD spectrum of folded (full line) and unfolded (dotted line) PagP.

The N-terminal helix acts as a post-assembly clamp

Guided by the structure of PagP (Figure 2a), several mutational variants were created, each deleting potential interactions between the helix and the barrel (W17A; R59L; and W17A/R59L), as well as a variant lacking the entire helix (Δ1-19). The refolding kinetics for

all mutants, measured under the experimental conditions described above, were very similar. In contrast, a significant effect was observed in the unfolding kinetics upon increasing the urea concentration from 7 to 10 M: all variants lacking W17 unfolded substantially faster than wild-type PagP, with rates of 0.76 ± 0.02, 0.71 ± 0.02, 0.65 ± 0.03 and 0.013 ± 0.001 min^{-1} for W17A, W17A/R59L, Δ(1-19) and wild-type, respectively (Figure 2b). Taken together, the refolding and unfolding data suggest that W17 plays a crucial role in modulating PagP stability in the bilayer, possibly because the aromatic ring of W17 is required to complete the periplasmic aromatic girdle (Figure 2a, yellow), clamping the β-barrel in the membrane-inserted state after folding of the barrel itself is complete.

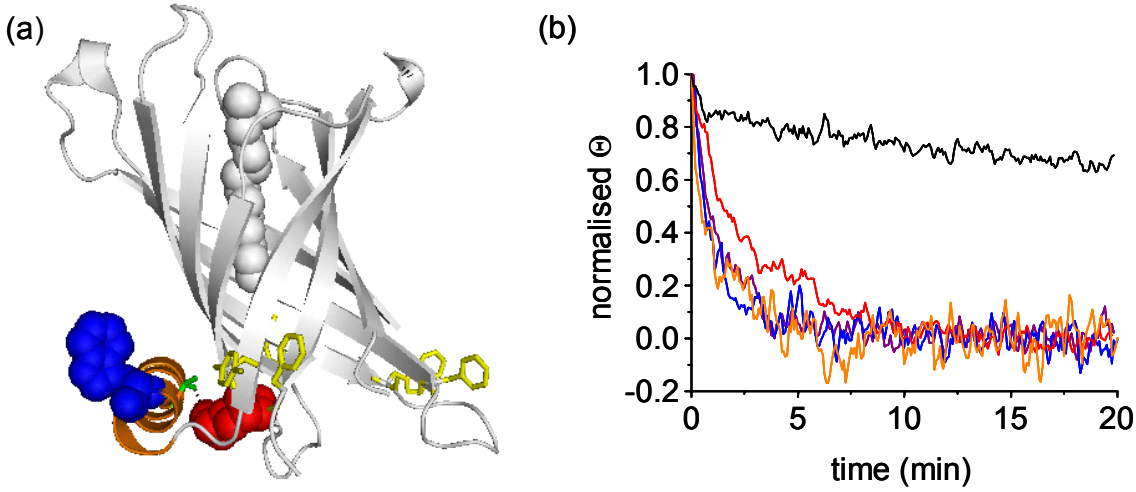

Figure 2: (a) Cartoon of PagP structure. Highlighted features: N-terminal α-helix (orange), R59 (red) which could form a hydrogen bond with T16 (green), W17 (blue) and periplasmic aromatic girdle (yellow). (b) Unfolding kinetics, monitored by circular dichroism at 232 nm, of wild-type PagP (black) and its variants (blue: W17A, red: R59L, purple: W17AR59L and orange: Δ1-19)

Outlook

Ongoing studies are focussing on the different phases in the folding kinetics of PagP and how these are modulated by the protein sequence and the lipid environment.

Publications

Huysmans, G.H., Radford, S.E., Brockwell, D.J. & Baldwin, S.A. (2007). The N-terminal helix is a post-assembly clamp in the outer membrane protein PagP. *Journal of Molecular Biology*, **373**, 529-540.

Funding

This work was funded by the BBSRC and the Wellcome Trust

Structural studies of the motor protein dynein

Anthony J. Roberts, Bara Malkova, Yusuke Kato and Stan A. Burgess

Introduction

Dynein is a family of minus-end directed microtubule motors that function in a wide diversity of cellular processes in eukaryotes including the trafficking of numerous cargoes (e.g. vesicles, mRNA, mitochondria), the positioning of the nucleus, Golgi apparatus and the mitotic spindle as well as driving the propagated-bending waves of cilia and flagella. Dynein is one of three different families of molecular motors, the others being kinesin and the actin-based motor myosin, and by far the least well understood. Dynein is large (~ 520 kDa), with a motor domain ~ten times larger than that of the other microtubule-based motor kinesin and has an evolutionary origin within the AAA+ superfamily of mechanoenzymes, unlike kinesin and myosin.

Little is known about dynein's structure and mechanism. We showed previously by negative stain electron microscopy (EM) that dynein has a stalk-head-tail structure (Fig. 1A). The head is ring-like and contains six AAA+ domains. ATP hydrolysis primarily in AAA1 drives the conformational changes associated with the power stroke and those governing its binding to and release from, the microtubule track via a small domain at the end of the ~12nm long anti-parallel coiled coil of the stalk.

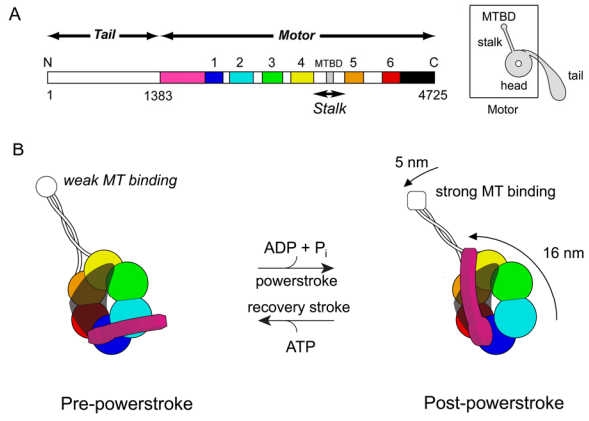

Figure 1
Structure and powerstroke mechanism of dynein. (**A**) Heavy chain sequence showing the subdomain organization including AAA+ modules (1-6), microtubule-binding domain (MTBD) and flanking N- (magenta) and C-terminal (black) sequences essential for motor activity. Inset: cartoon of dynein heavy chain structure. (**B**) New model of dynein motor subdomain organization and power stroke mechanism (unpublished). ATPase activity in AAA1 (blue) drives long-range conformational changes associated with the powerstroke- stalk tilt and linker swing.

Current Research

Structural studies in my lab are focused on understanding the structure and mechanisms of the molecular motors dynein and myosin, with recent emphasis on dynein and its subdomain organization three dimensional (3D) structure.

In collaboration with Prof. Kazuo Sutoh's group (University of Tokyo) we have mapped the locations of key sites within the motor domain using GFP-labeled fusion proteins and truncated motor domain constructs. We have identified three of the AAA+ modules within the ring, as well as the locations of flanking N- and C-terminal sequences (Fig. 1B). We show that the N-terminal sequence defines an elongated lever which swings this lever swings by > 90° during the powerstroke and the stalk tilts by 15° (Fig. 1B).

In collaboration with Prof. Kazuhiro Oiwa's group (KARC, Kobe, Japan) we are also pursuing the 3D structure of the motor domain by cryo-EM. We have obtained 3D density maps of the motor in both pre- and post-powerstroke conformations for the first time. These studies have led us to propose a new model for the structure and mechanism of dynein motors (Fig. 1B).

Finally, in collaboration with Dr. Tom Edwards (University of Leeds) and Dr. Dan Mulvihill (University of Kent), we are pursuing atomic resolution structures of subdomains of the motor. Expression trials of various subdomains are currently underway.

Publications

Kotani, N., Sakakibara, H., Burgess, S.A., Kojima, H. & Oiwa, K. (2007) Mechanical properties of inner-arm Dynein-F (Dynein I1) studied with *in vitro* motility assays. *Biophys. J.* **93**, 886–894.

Burgess, S. A., Yu, S., Walker, M. L., Hawkins, R. J., Chalovich, J. M. & Knight, P. J. (2007). Structures of smooth muscle myosin and heavy meromyosin in the folded, shutdown state. *J. Mol. Biol*. **372**, 1165-1178.

Funding

This work is funded by BBSRC and The Wellcome Trust.

A beta-sheet interaction interface directs the tetramerisation of the Miz-1 POZ domain

Mark Stead, Stephanie Wright and Thomas Edwards

Introduction

The POZ/BTB domain is an evolutionarily conserved motif found in approximately 40 zinc-finger transcription factors (POZ-ZF factors). Several POZ-ZF factors are implicated in human cancer, and POZ domain interaction interfaces represent an attractive target for therapeutic intervention. Miz-1 (Myc-interacting zinc-finger protein) is a POZ-ZF factor that regulates DNA-damage-induced cell cycle arrest and plays an important role in human cancer by virtue of its interaction with the c-Myc and BCL6 oncogene products. The Miz-1 POZ domain mediates both self-association and the recruitment of non-POZ partners. POZ-ZF factors generally function as homodimers, although higher-order associations and heteromeric interactions are known to be physiologically important; crucially, the interaction interfaces in such large complexes have not been characterised.

Structure of the Miz-1 POZ domain

We have solved the 2.1 Å resolution crystal structure of the Miz-1 POZ domain (Figure 1). The tetrameric organisation of Miz-1 POZ reveals two types of interaction interface between subunits; an interface of alpha-helices resembles the dimerisation interface of reported POZ domain structures, whereas a novel beta-sheet interface directs the association of two POZ domain dimers. We have shown that the beta-sheet interface directs the tetramerisation of the Miz-1 POZ domain in solution and therefore represents a newly described candidate interface for the higher-order homo- and hetero-oligomerisation of POZ-ZF proteins *in vivo*.

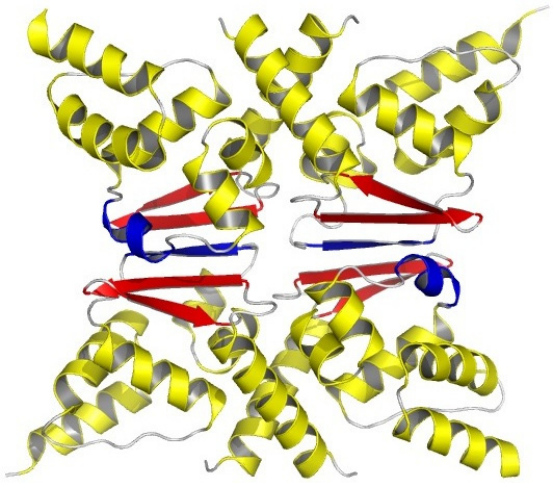

Figure 1. POZ domain tetramer
Secondary structure of the Miz-1 POZ domain tetramer. Helices and sheets from homologous POZ dimers are coloured in yellow and red respectively. At the tetramerisation interface, highlighted in blue, a strand from one monomer contributes to the shared β-sheet whereas the equivalent residues from the opposite monomer are extruded and form an α-helix.

Funding

This work was funded by Yorkshire Cancer Research, the Royal Society, European Union, and the University of Leeds.

Publications

Stead MA, Trinh CH, Garnett JA,Carr SB, Baron AJ, Edwards TA, Wright SC (2007). A beta-sheet interaction interface directs the tetramerisation of the Miz-1 POZ domain. *J. Mol. Biol.* **373,** 820-6.

The structure of the Pumilio homology domain of murine Pum2

Huw Jenkins and Thomas Edwards

Introduction

Human fertility is directly affected by the regulation of gene expression during gamete formation. Post-transcriptional regulation of gene-expression through control of translation by RNA-binding proteins has recently been implicated as a critical factor in this process. Two RNA-binding proteins that have been shown to interact in order to control translation during spermatogenesis are the deleted in azoospermia (DAZ) family member, DAZ-like (Dazl) and a homologue of the *Drosophila* Pumilio Puf protein – Pum2. Members of the Puf family of RNA-binding proteins bind to the 3' UTR of selected transcripts causing repression of translation. The RNA is bound to a C-terminal Puf (Pum and FBF) domain. This domain is also the interaction site for Dazl.

Structure of murine Pum2

In order to start to examine the detail of the interaction between Dazl and Pum2 on target RNAs we have solved the 2.8 Å resolution crystal structure of the murine Pum2 Puf domain (Figure 1). Crystals of mPum2 Puf domain belong to space-group $P6_3$ (a = b = 150.6 Å, c= 77.1 Å, $\alpha = \beta = 90^\circ$, $\gamma = 120^\circ$) and contain two molecules per asymmetric unit. The structure was solved by molecular replacement using the human Pum1 Puf domain structure as a search model. We are currently attempting to produce crystals that diffract to higher resolution. We are also using fluorescence polarisation assays to screen RNA sequences that were bound with high affinity by Pum2 in SELEX experiments with the aim of solving the co-crystal structure of Pum2 bound to a high affinity target RNA sequence. Future work will focus on solving the structure of the Dazl:Pum2:RNA complex.

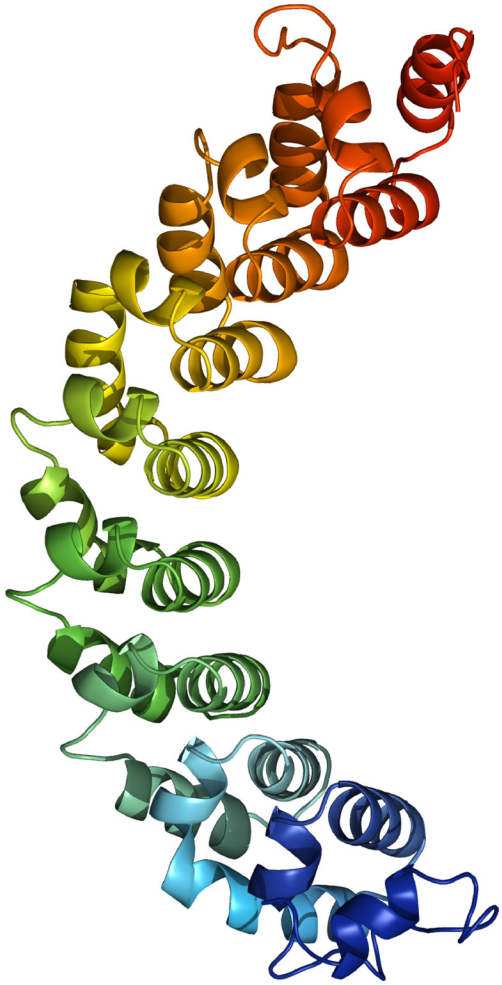

Figure 1. Mouse Pum2 Puf domain
Cartoon of the cystal structure of the murine Pum2 Puf domain. The Puf domain contains 8 tandem Puf repeats coloured from blue (Puf 1) to red (Puf8).

Collaborators

Howard Cooke and Nicola Gray (MRC Human Genetics Unit, Edinburgh).

Funding

This work was funded by the BBSRC.

Publications

Edwards, T.A., Wilkinson, B.D., Wharton, R.P. & Aggarwal, A.K. (2003) Model of the brain tumor-Pumilio translation repressor complex. *Genes Dev*. **17**, 2508-2513.

The p7 ion channel of hepatitis C virus (HCV) as a therapeutic target

Corine StGelais, Toshana Foster, Philip Tedbury, Barnabas King, Lynsey Corless,
Marko Noerenberg, David Rowlands, Mark Harris and Stephen Griffin

Hepatitis C virus (HCV) chronically infects 170-200 million individuals causing severe liver disease such as cirrhosis and hepatocellular carcinoma. Accordingly, HCV is now the leading indicator for liver transplant surgery and incurs massive health costs due to its associated high morbidity and mortality rates. The majority of positive individuals, however, are unaware that they carry the virus as acute infection is almost always asymptomatic, resulting in clinical intervention only at late stages of disease when liver damage has already occurred. Current therapy based on a combination of interferon α and the guanosine analogue, ribavirin, is expensive, poorly tolerated and effective in only 50% of cases due to a high level of innate viral resistance. A small number of new, virus-specific therapies are forthcoming, yet their development has been severely hampered by our inability to grow the virus in culture. Recently, however, an infectious culture system for HCV has become available which we have established in the category III facility at Leeds, enabling investigation of the processes involved in virus assembly and entry.

In 2003 we demonstrated that the HCV p7 protein formed an oligomeric ion channel whose activity was blocked by the antiviral drug, amantadine. Since then, alternative inhibitory compounds have been identified and the arrival of the HCV culture system has allowed us to investigate p7 as a drug target in the context of a complete virus life cycle. We and others have found p7 to be critical to the process of virus assembly. Viruses with mutations in p7 are severely impaired in their ability to secrete infectious virions, despite being able to replicate their genomes as wild type virus. Recent data suggests that the way p7 acts during assembly is by its interaction with the viral glycoproteins (Figure 1) which line the surface of the enveloped virus and mediate entry, and also with the NS2 protein. In collaboration with Prof. Steven Weinman (UTMB, Galveston), we have determined that p7 acts to alter proton permeability in cellular vesicles, providing a mechanism by which p7 can direct vesicle trafficking or alternatively protect viral glycoproteins from low pH during cell surface transport. We also have evidence that p7 may be incorporated into HCV particles (Figure 2), thus acting during the entry process. p7 inhibitors, therefore, could act to block two distinct stages of the virus life cycle.

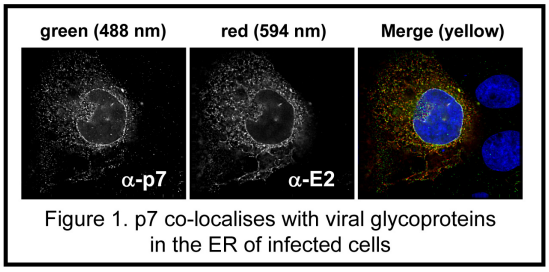

Figure 1. p7 co-localises with viral glycoproteins in the ER of infected cells

Exploiting p7 as a therapeutic target has been greatly aided by our development of an *in vitro* assay for p7 activity based on fluorescent dye release from liposomes. Using this and the cell culture system, we have shown that the sensitivity of HCV to p7 inhibitors is dependent on the p7 sequence itself; therefore varying according to virus genotype. This has profound implications for the development of p7 inhibitors by the pharmaceutical industry as compounds will have to display activity against multiple strains of the virus. To this end, our liposome assay forms the basis of a high-throughput drug screen being developed in partnership with Pfizer. We are also pursuing structure-based rational drug design using NMR in collaboration with Prof. Steven Homans (Leeds). p7 inhibitors could greatly expand the repertoire of treatments available for HCV patients in the near future.

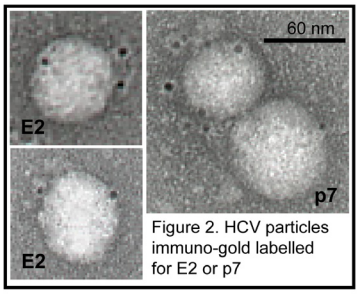

Figure 2. HCV particles immuno-gold labelled for E2 or p7

Publications:

St Gelais, C., Tuthill, T., Clarke, D., Rowlands, D., Harris, M. & Griffin, S.**.** (2007) Inhibition of hepatitis C virus p7 membrane channels in a liposome based assay system. *Antiviral Research* **76**,48-58.

Clarke, D., Griffin, S., Beales, L., Burgess, S., Harris, M. & Rowlands, D. (2006) Evidence for the formation of a heptameric ion channel complex by the HCV p7 protein *in vitro*. *Journal of Biological Chemistry* **281**, 37057-68.

Collaborators:

Prof. Steven Homans (University of Leeds)
Prof. Steven Weinman (UTMB, Galveston, USA)
Dr Victoria Flores & Dr Helen Bright (Pfizer, Sandwich, UK)

Funding:

Stephen Griffin holds an MRC New Investigator Award and Corine StGelais was the recipient of a Pfizer-funded CASE studentship. Other funding was provided by the Wellcome Trust and the Royal Society.

Studies on the HIV-1 Nef protein

Matthew Bentham and Mark Harris

HIV-1 Nef is a 205 amino acid N-terminally myristoylated protein that plays a critical role in viral pathogenesis. Myristoylation is an eukaryotic specific co-translational modification that is catalysed by a ribosomal associated enzyme - N-myristoyltransferase (NMT). Two projects are ongoing. Firstly we are attempting to understand the mechanisms by which Nef interacts with cellular membranes – using a combination of *in vitro* liposome binding assays and sucrose gradient fractionation of lysates from Nef-expressing cells we have determined that both the myristate and basic amino acids near the N-terminus of the protein are required. In further experiments we have anchored Nef irreversibly to the membrane with a C-terminal farnesyl tag and shown that this abrogates the ability of Nef to down-modulate cell-surface CD4.

Secondly we are raising RNA aptamers to native, myristoylated Nef. The latter can be co-expressed in *E.coli* with N-myristoyl transferase to generate large amounts of purified myristoylated Nef. This has been used to select out pools of randomised RNA aptamers and we are currently in the process of characterising these aptamers. They will be tested out for the ability to inhibit Nef functions – both *in vitro* (using ELISA based protein-protein interaction assays to measure effects on the interactions of Nef with cellular SH3 domains or CD4 cytoplasmic tail), and *in vivo*. The latter include FACS analysis of down-modulation of cell surface CD4 by Nef, and effects of Nef on virus replication - these experiments are being carried out in the Category III containment facility.

Publication:

Bentham, M., Mazaleyrat S. and Harris, M. (2006) A cluster of arginine residues near the N-terminus of the HIV-1 Nef protein is required both for membrane association and CD4 down-modulation. *Journal of General Virology,* **87**:563-571.

Collaborators:

Kalle Saksela, University of Tampere, Finland
Matthias Geyer, Max Planck Institute, Dortmund
J Victor Garcia, University of Texas at Dallas

Funding:
This work is funded by the MRC.

Studies on the hepatitis C virus non-structural proteins NS2 and NS5A

Jamel Mankouri, Anna Nordle, Andrew Milward, Sarah Gretton, Philip Tedbury, Mair Hughes, Barnabas King, Lynsey Corless, Steve Griffin and Mark Harris

Hepatitis C virus (HCV) infects 170 million individuals and is a major cause of chronic liver disease, including fibrosis, cirrhosis and hepatocellular carcinoma. The virus has a single stranded positive sense RNA genome of 9.5kb that contains a long open reading frame encoding a single polyprotein of 3000 amino acids which is cleaved into 10 individual polypeptides by a combination of host cell and virus specific proteases. The molecular mechanisms of virus replication and pathogenesis remain to be elucidated, however, recently a clone of the virus that is able to replicate in cell culture has been identified and we are using this model extensively to understand how viral protein products function within the viral lifecycle.

A major focus of work is the NS5A protein, firstly in terms of perturbation of cellular signalling pathways - we have previously shown that NS5A perturbs two key mitogenic pathways within the cell; it inhibits the Ras-ERK MAP kinase pathway and stimulates PI3K signalling pathways, the latter promotes cell survival and activates the proto-oncogene β-catenin with implications for the link between HCV and hepatocellular carcinoma. We are currently funded by the MRC and Yorkshire Cancer Research to analyse these signalling events in more detail. Recent data demonstrate that NS5A blocks Ras-Erk signalling by perturbing the endocytotic profile of the epidermal growth factor receptor, and we have also demonstrated a direct interaction between NS5A and β-catenin that may facilitate activation of the latter and contribute to carcinogenesis. We are also investigating the role of NS5A in virus replication. We are generating a series of NS5A mutants – particularly in PxxP motifs that interact with cellular SH3 domains – to characterise the role of these interactions in viral replication. These data have revealed genotype specific differences with regard to the requirement for specific proline residues. We are also addressing the role of NS5A phosphorylation in viral replication initially by using mass spectrometry to identify phosphorylation sites.

We are analysing a novel autoproteolytic event in the virus lifecycle – the cleavage between the NS2 and NS3 proteins. We have shown that this protease requires zinc and have identified a key cysteine residue that is required for cleavage, current work is addressing the role of NS2 in both viral RNA replication and assembly of new virus particles. Our data point to a pivotal role of NS2 in linking these two processes and furthermore suggest direct physical interactions between NS2 and the p7 ion channel protein.

Publications:

Shelton, H & Harris, M. (2008) Hepatitis C virus NS5A protein binds the SH3 domain of the Fyn tyrosine kinase with high affinity: Mutagenic analysis of residues within the SH3 domain that contribute to the interaction. *Virology Journal* **5**:24

Mankouri, J., Milward, A., Pryde, K., Warter, L., Martin, A. & Harris, M. (2008) A comparative cell biological analysis reveals only limited functional homology between the NS5A proteins of hepatitis C virus and GB virus B *Journal of General Virology, in press*

Tedbury, P. and Harris, M. (2007) Characterisation of the role of zinc in the hepatitis C virus NS2/3 auto-cleavage and NS3 protease activities. *Journal of Molecular Biology*. **366**:1652-1660.

Collaborators:
Kalle Saksela, University of Helsinki, Finland
John McLauchlan, MRC Virology Unit, Glasgow
Annette Martin, Institute Pasteur, Paris
Mair Hughes holds an Arrow Therapeutics CASE studentship (NS5A).

Funding:
This work is funded by the Wellcome Trust, MRC, Yorkshire Cancer Research and BBSRC. Further CASE studentships with Pfizer and Glaxo-Smith-Kline will commence in 2008.

Structural genomics of bacterial membrane proteins

Kim Bettaney, Pikyee Ma, Gerda Szakonyi, Halina Norbertszak, Ryan Hope, Peter Roach, Simon Patching, Richard Herbert, Nick Rutherford, Mary Phillips-Jones and Peter Henderson

Introduction

Many bacterial membrane transport proteins are essential for metabolism and some contribute to emerging antibiotic resistance. Some have potential applications in biotechnology. Two-component system (TCS) receptor membrane proteins also play key roles in metabolism and in the sensitivity to antibiotics of many microorganisms. The design of novel antibacterial drugs and the operation of fermentation processes would be greatly enhanced by knowledge of the structures and functions of these membrane proteins, which are poorly understood because of the difficulties of obtaining purified protein and crystals of quality. We have devised and implemented a structural genomics strategy for the amplified expression, purification and characterisation of such proteins.

Results

Over seventy transport and TCS membrane proteins have been expressed and over thirty have been purified from *Bacillus cereus, Bacillus subtilis, Brucella melitensis, Campylobacter jejuni, Escherichia coli, Enterococcus faecalis, Helicobacter pylori*, *Microbacterium liquefaciens, Neisseria meningitides, Pseudomonas aeruginosa, Staphylococcus aureus, and Streptomyces coelicolor*. Twelve of the proteins are in crystallisation trials, and three so far yielded crystals that diffract. The structure of one of these has been elucidated by colleagues at Imperial College. Some of the proteins have also been employed in the development of novel applications of NMR technology to determine features of their structure-activity relationships.

The success of this strategy is an important step towards reproducible production of membrane transport and receptor proteins for the screening of drug binding and for optimisation of crystallisation conditions to enable subsequent structure determination.

Collaborators

Professors Baldwin, Bushby, Chopra, Evans, and Homans and Drs Baldwin, Fishwick, Jeuken and Phillips-Jones at Leeds. Professor Iwata and Drs Byrne, Cameron, Weyand, and Carpenter at the Diamond Synchrotron, Didcot. Dr David Middleton in Liverpool. Professor Malcolm Levitt in Southampton. Professor Essen and Dr Psakis in Marburg, Germany. Dr Butaye in Brussels, Belgium. Professor Anna-Brit Kolsto in Oslo, Norway. Professor Arakawa and Dr Shibayama in the NIH, Tokyo, and Dr Suzuki in Ajinomoto Co., Kawasaki, Japan.

Publications

Jeuken, L..J.C., Connell, S.D., Henderson, P.J.F., Gennis, R.B., Evans, S.D. and Bushby, R.J. (2006) Redox enzymes in tethered membranes. *J. Am. Chem. Soc.* **128**, 1711-1716.

Spencelayh, M.J., Cheng, Y., Bushby, R.J. Bugg, T.D., Li, J.J., Henderson, P.J.F., O'Reilly, J. and Evans, S.D. (2006) Antibiotic action and peptidoglycan formation on tethered lipid bilayer membranes. *Angew. Chem.* **45**, 2111-2116.

Clough, J., Saidijam, M., Bettaney K.E., Szakonyi, G., Meuller, J., Suzuki, S., Bacon, M., Barksby, E., Ward, A., Gunn-Moore, F., O'Reilly, J., Rutherford, N.G., Bill, R.M. and Henderson, P.J.F. (2006) Prokaryote membrane transport proteins: amplified expression and purification. In *Structural genomics of membrane proteins* (ed. Lundstrom, K.) pp.21-42. CRC Press, USA.

Saidijam, M., Benedetti, G., Ren, Q., Zhiqiang, X., Hoyle, C.J., Palmer, S.L., Ward, A., Bettaney, K.E., Szakonyi, G., Meuller, J., Morrison, S., Pos' M.K., Butaye, P, Walravens,

K., Langton, K., Herbert, R.B., Skurray, R.A., Paulsen, I.T., O'Reilly, J., Rutherford, N.G., Brown, M.H., Bill, R.M. and Henderson, P.J.F. (2006) Microbial drug efflux proteins of the Major Facilitator Superfamily, in *Current Drug Targets* **7**, pp. 793-811.

Suzuki, S and Henderson, P.J.F. (2006) The hydantoin transport protein from *Microbacterium liquefaciens. J. Bacteriol*. **188**, 3329-3336.

Everberg. H., Clough, J., Henderson, P.J.F., Jergil, B. and Tjerneld, F. Barinaga-Rementeria Ramírez, R. (2006) Isolation of *Escherichia coli* inner membranes by metal affinity two-phase partitioning. *J. Chromatogr A*. **1118**, 244-252.

Potter, C., Jeong, E-L., Williamson, M.P., Henderson, P.J.F. and Phillips-Jones, M.K. (2006) Redox-responsive in vitro modulation of the signalling state of the isolated PrrB sensor kinase of *Rhodobacter sphaeroides* NCIB 8253. *FEBS Lett.* **580**, 3206-3210.

Szakonyi G., Dong, L., Ma, P., Bettaney K.E., Saidijam M., Ward, A., Zibaei, S., Gardiner, A.T., Cogdell, R.J., Butaye, P., Kolsto, A-B., O'Reilly J., Hope, R.J., Rutherford N.G., Hoyle C.J. and Henderson P.J.F. (2007). A genomic strategy for cloning, expressing and purifying efflux proteins of the major facilitator superfamily. *J. Antimicrob. Chemother*. **59**, 1265-1270.

Shibayama, K., Wachino, J-i., Arakawa, Y., Saidijam, M., Rutherford N.G, and Henderson, P.J.F. (2007) Metabolism of glutamine and glutathione via gamma-glutamyltranspeptidase and glutamate transport in *Helicobacter pylori*: Possible significance in the pathophysiology of the organism. *Molec. Microbiol*. **64**, 396-406.

Gutman, D.A.P., Mizohata, E., Newstead, S., Ferrandon, S., Henderson, P.J.F., van Veen, H.W. and Byrne, B. (2007) A high-throughput method for membrane protein solubility screening: the ultracentrifugation dispersity sedimentation dispersion assay. *Protein Sci.* **16**, 1422-1428.

Reig, N., del Rio, C., Casagrande, F., Ratera, M., Gelpi, J.L., Torrents, D., Henderson, P.J.F., Baldwin, S.A., Zorzano, A., Fotiadis, D. and Palacin, M. (2007). Functional and structural characterisation of the first prokaryotic member of the Lat family: a model for APC transporters. *J. Biol. Chem*. **282**, 13270-13281.

Patching, S.G., Henderson, P.J.F., Herbert, R.B. and Middleton, D.A. (2008) Solid-state NMR spectroscopy detects interactions between tryptophan residues of the *E. coli* sugar transporter GalP and the alpha-anomer of the D-glucose substrate. *J. Am. Chem. Soc*. **130**, 1236-1244.

Dunsmore, C.J., Miller, K., Blake, K.L., Patching, S.G., Henderson, P.J.F., Garnett, J.A., Stubbings, W.J., Phillips, S.E.V., Palestrant, D.J., De Los Angeles, J., Leeds, J.A., Chopra, I. and Fishwick, C.W.G. (2008). 2-Aminotetralones: Novel Inhibitors of MurA and MurZ *Bioorganic & Med. Chem. Lett.* **18**, 1730-1734.

Roach, P.C.J., O'Reilly, J., Norbertczak, H., Hope, R.A., Venter, H., Patching, S.G., Jamshad, M., Stockley, P.G., Baldwin, S.A., Herbert, R.B., Rutherford, N.G., Bill, R.M. and Henderson, P.J.F. (2008) Equipping a research scale fermentation laboratory for production of membrane proteins. In *Practical fermentation technology* (McNeil, B. and Harvey, L.M.) pp. 37-67. J. Wiley, Chichester, UK.

Funding

This research is supported by the BBSRC, the EU European Membrane Protein Consortium EMeP, EU COST Action B16, Japan Society for Promotion of Science, and the Wellcome Trust.

Investigation into the role of macrophages in formation and degradation of β_2-microglobulin amyloid fibrils

Isobel J. Morten, Walraj Gosal, Sheena E. Radford and Eric W. Hewitt

Introduction

β_2-microglobulin (β_2m) is a small 99 residue soluble protein and is the non-covalently bound subunit of the major histocompatibility complex class I molecule, which is expressed on the surface of all nucleated cells. Cells continually shed β_2m from their surface, whereupon the protein is normally removed from the serum by degradation in the proximal tubule of the kidney. In patients with end stage renal disease, however, neither the kidney nor the dialysis membrane can remove β_2m from the circulation, resulting in a 10-50-fold increase in the concentration of β_2m in the serum. The sustained high concentration of β_2m therein appears to be one key initiating factor in the aggregation of this protein into insoluble amyloid fibrils, which typically accumulate in the musculoskeletal system resulting in bone and joint destruction. How β_2m forms amyloid fibrils *in vivo* is poorly understood, although macrophages are found in association with the β_2m amyloid deposits and β_2m amyloid fibrils have been observed in the lysosomes of these cells. This raises the intriguing possibility that the macrophage lysosome may be a site for β_2m amyloid formation. Alternatively, the macrophages associated with β_2m amyloid deposits may play a protective role by capturing extracellular amyloid by phagocytosis for degradation

Are macrophage lysosomes a site of β_2m amyloid fibril formation?

In order to determine whether macrophage lysosomes are a potential site for β_2m amyloid formation, we analysed the endocytic uptake of monomeric β_2m by the model macrophage cell line RAW 264.7. In live cell imaging experiments RAW 264.7 macrophages internalised monomeric β_2m, whereupon it was sorted to lysosomes. Next we examined whether β_2m self-associates to form amyloid-like fibrils when incubated at the acidic pH of lysosomes (pH 4.5). At pH 4.5 β_2m self-associated to form amyloid-like fibrils; however, when monomeric β_2m was incubated at this pH with lysosomal proteases, isolated from RAW 264.7 macrophages, this resulted in the rapid degradation of the monomeric protein and the consequent inhibition of fibril formation. Consistent with this observation, monomeric β_2m internalised by RAW 264.7 macrophages was also rapidly degraded (Fig. 1). Together these data demonstrate that whilst the pH of the macrophage can promote β_2m fibril formation, lysosomal proteases degrade the monomeric protein before it can self assemble into amyloid fibrils. Thus rather than acting as a site for fibril formation, lysosomes may instead play a protective role by eliminating amyloid precursors before β_2m fibrils can accumulate in what is an otherwise fibrillogenic environment (Fig. 2).

Do macrophage lysosomes degrade β_2m amyloid fibrils?

Live cell imaging experiments demonstrated that RAW 264.7 macrophages can internalise β_2m fibrils, but in marked contrast to the monomeric protein, these fibrils were not degraded within the lysosomes of these cells (Fig. 1). Correspondingly β_2m fibrils were highly resistant to degradation when incubated at pH 4.5 in the presence of high concentrations of lysosomal proteases. Based on these observations we conclude that despite their substantial degradative capacity macrophage lysosomes cannot degrade the internalised β_2m amyloid fibrils and as consequence β_2m fibrils accumulate in this organelle (Fig. 2). We therefore predict that macrophages found in association with β_2m amyloid deposits *in vivo* are unable to prevent amyloid accumulation in the osteoarticular tissues of dialysis patients.

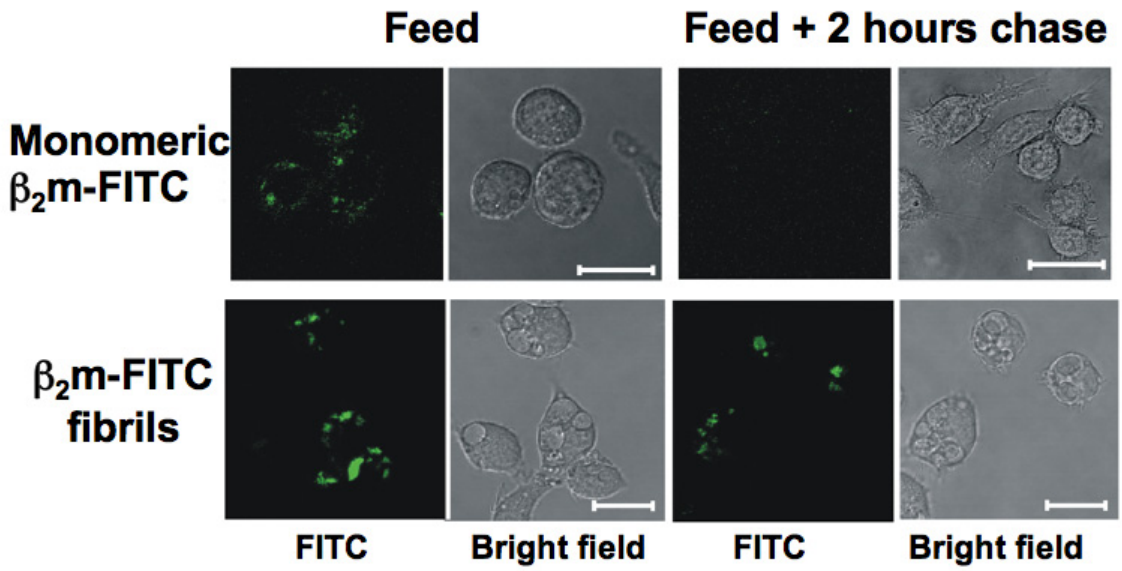

Figure 1. RAW 264.7 macrophages were incubated with either monomeric β_2m labelled with fluorescein-5-isothiocyanate (β_2m-FITC) (upper panels) or with β_2m-FITC fibrils (lower panels) for 2 hours at 37°C, washed to remove non-cell associated β_2m-FITC and then incubated for a further 2 hours at 37°C. Cell associated fluorescence was visualised by confocal microscopy.

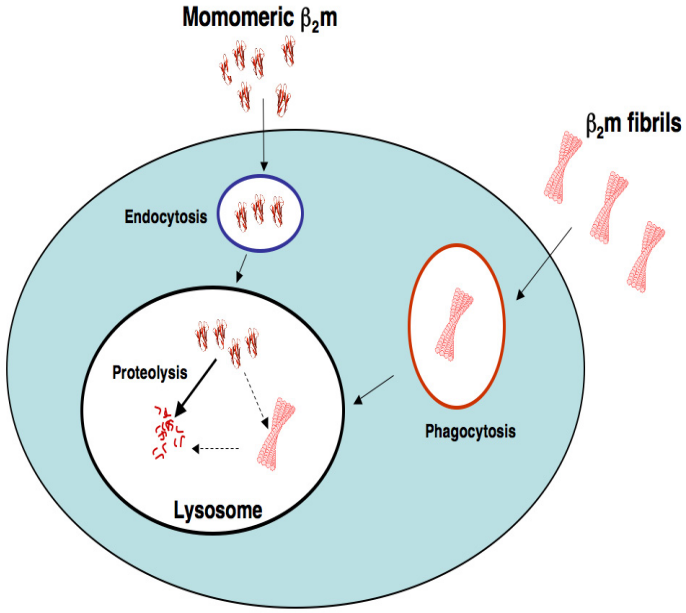

Figure 2. Schematic diagram of the potential role(s) of macrophage lysosomes in β_2m amyloid formation and degradation. Monomeric β_2m is internalised by macrophages and then sorted to lysosomes. At the low pH of the lysosomes β_2m can assemble into amyloid-like fibrils, however lysosomal proteases protect against amyloid formation by degrading the vast majority, if not all, of monomeric β_2m before it can self-assemble into fibrils. Macrophages can internalise extracellular β_2m amyloid fibrils, but unlike the monomeric form of the protein, these fibrils are resistant to lysosomal proteolysis and hence accumulate in these cells.

Publications

Morten I.J., Gosal W.S., Radford S.E. and Hewitt E.W. (2007). Investigation into the role of macrophages in the formation and degradation of β_2-microglobulin amyloid fibrils. *J. Biol. Chem.* **282**, 29691-29700.

Funding

We gratefully acknowledge Kidney Research UK for financial support.

Interaction of coronaviruses with the host cell

Julian A. Hiscox

Introduction

Coronaviruses cause diseases relevant to both animal and human health. Examples of coronaviruses range from the severe acute respiratory syndrome coronavirus (SARS-CoV), human coronavirus NL63 (which causes paediatric disease) and infectious bronchitis virus (IBV), which is a respiratory pathogen and is the major disease of farmed poultry in the UK. IBV induces a reduction in cellular proliferation and a G2/M phase arrest a complete ablation of cyclin D1 in all infected cells. The functional consequence for this is that viral RNA and protein synthesis is up-regulated in the G2/M phase which leads to an increased production and release of progeny virus. This was the first description for coronaviruses showing a direct link between cell cycle control and virus biology. Further, using quantitative RT-PCR (TaqMan) we showed that down-regulation of cyclin D1 occurred post-transcription and the use of metabolic inhibitors demonstrated that down-regulation occurred via a virus-mediated pathway. Fluorescent recovery after photo-bleaching (FRAP) and fluorescent loss in photo-bleaching (FLIP) coupled to the arrest of cells in different stages of the cell cycle was used to show that the trafficking of IBV nucleocapsid (N) protein to a dynamic sub-nuclear structure called the nucleolus was cell cycle-dependent; with most nucleolar localisation occurring in the G2/M phase of the cell cycle, due to the increased mobility of this protein in the nucleus/nucleolus.

We delineated both nuclear import and export signals in IBV N protein and defined a novel nucleolar localisation signal, composed of eight amino acids, that is both necessary and sufficient to direct N protein to the nucleolus and a CRM-1 independent nuclear export signal (NES). Apart from our studies with IBV N protein, we also have studied the trafficking of SARS-CoV N protein and its relationship with the nucleolus, and have recently mapped a novel NES. Together this research has contributed a shift in the way the interaction of many positive strand RNA viruses with the host cell nucleus is viewed.

Collaborators

Gavin Brooks, University of Reading, UK and Pete Kaiser, Institute for Animal Health, UK.

Publications

Hiscox, J.A. RNA viruses: hijacking the dynamic nucleolus. (2007). *Nature Reviews Microbiology* **5**, 119-127.

Cawood, R., Harrison, S.M., Dove, B.K., Reed, M.L. & Hiscox, J.A. (2007). Cell cycle dependent nucleolar localization of the coronavirus nucleocapsid protein. *Cell Cycle* **7**, 863-867.

Reed, M.L., Howell, G. Harrison, S.M., Spencer, K.A. & Hiscox, J.A. (2007). Characterization of the nuclear export signal in the coronavirus infectious bronchitis virus nucleocapsid protein. *Journal of Virology* **81**, 4298-4304.

Harrison, S.M., Dove, B.K., Rothwell, L., Kaiser, P., Tarpey, I., Brooks, G. & Hiscox, J.A**.** (2007). Characterisation of cyclin D1 down-regulation in coronavirus infected cells. *FEBS Letters* **581,** 1275-1286.

You, J.H., Reed, M.L. & Hiscox, J.A. (2007). Trafficking motifs in the SARS-coronavirus nucleocapsid protein. *Biochemical and Biophysical Research Communications* **358**, 1015-1020.

Funding

This work was supported by the BBSRC, Yorkshire Cancer Research and Intervet Ltd.

The role of phosphorylation in the coronavirus nucleocapsid protein

Julian A. Hiscox

Introduction

Coronaviruses cause diseases relevant to both animal and human health. Examples of coronaviruses range from the severe acute respiratory syndrome coronavirus (SARS-CoV), human coronavirus NL63 (which causes paediatric disease) and infectious bronchitis virus (IBV), which is a respiratory pathogen and is the major disease of farmed poultry in the UK. Coronaviruses are a group of enveloped positive strand RNA viruses which replicate in the cytoplasm of an infected cell. Crucial to the successful biology of the virus is the virus encoded nucleocapsid (N) protein. N protein is one of the most abundant proteins produced during virus infection, is immunogenic and can be used as part of diagnostic reagents to detect virus infection. N protein functions to associate with the viral RNA forming a ribonucleoprotein complex and hence encapsidate the viral RNA for packaging into newly synthesized virus particles. Previously we mapped the post-translational modifications of IBV N protein using mass spectrometry. Only four sites were occupied by phosphate groups and these located to two distinct clusters, amino acids Ser^{190} and Ser^{192} in the central region and Thr^{378} and Ser^{379} in the C-terminal region. Using surface plasmon resonance (SPR) for a kinetic binding analysis we found that phosphorylation of N protein was responsible for discriminating between viral and non-viral RNA. Recombinant phosphorylation N protein mutants were then generated in which appropriate Ser or Thr sites had been substituted for alanine. SPR was again utilised to conduct a kinetic binding analysis with viral and non-viral RNA targets. The C-terminal phosphorylation cluster (Thr^{378} and Ser^{379}) was found to confer high affinity binding of N protein onto viral RNA.

To evaluate how the differentially phosphorylated N proteins affect virus biology we utilised the finding that the rescue of infectious coronavirus full length clones is more efficient if N protein is provided *in trans* through expression from an appropriate plasmid. In the case of rescuing an IBV full length clone using a variety of different methodologies, providing N protein in trans is an absolute requirement for rescue. We have shown that wild type N protein (fully phosphorylated) and a mutant N protein which was phosphorylated at Thr^{378} and Ser^{379} (and with Ser^{190} and Ser^{192} substituted for Ala), were more efficient at rescuing recombinant IBV than mutant N proteins which were phosphorylated at Ser^{190} and Ser^{192} (with Thr^{378} and Ser^{379} substituted for Ala) or where all four sites were substituted for Ala, pointing to a role of phosphorylated N protein in virus biology.

Collaborators

Ferdinand Osorio, University of Nebraska (Lincoln) and Paul Britton, Institute for Animal Health (UK).

Publications

Spencer, K.A., Dee, M., Britton, P. & Hiscox**,** J.A. **(**2008). Role of phosphorylation clusters in the biology of the coronavirus infectious bronchitis virus nucleocapsid protein. Virology. **370**, 373-381.

Spencer, K.A., Osorio, F.A. & Hiscox**,** J.A. (2007). Recombinant viral proteins for use in diagnostic ELISAs to detect virus infection. Vaccine **25**, 5653-5659.

Funding

This work was supported by the BBSRC , National Pork Board (USA) and Guildhay Ltd.

Understanding the driving forces behind molecular affinity in model protein systems

Neil Syme, Caitríona Dennis, Simon Phillips and Steve Homans

Introduction

A better understanding of the factors that determine the affinity for ligand-protein interactions remains an important goal in biophysical and medicinal chemistry. Three-dimensional structures reveal a significant amount of information about a complex, but this represents only part of the picture. Affinities are governed not only by the energetics of an interaction, concerning the spatial disposition of interacting groups, but also by the dynamics of these groups. Proteins undergo motions on a wide range of time-scales in order to perform their functions. Thus, to more accurately predict the affinity of a protein for a ligand, it is essential to understand both the enthalpic and entropic contributions to binding. However, these components are enormously complex, and involve contributions from new ligand-protein interactions, solvent rearrangement and changes in protein and ligand degrees of freedom. We employ isothermal titration calorimetry (ITC), NMR techniques and X-ray crystallography to study the thermodynamics of ligand-protein interactions.

In recent years we have made a great deal of progress understanding the interactions of the model hydrophobic system MUP (mouse major urinary protein) with various ligands. It is useful therefore to compare the thermodynamics of hydrophobic versus hydrophilic interactions, to understand further the nature of biomolecular associations.

HBP2 as a hydrophilic model system

Histamine-binding protein 2 (HBP2) from the tick *Rhipicephalus appendiculatus* is, like MUP, a member of the lipocalin protein superfamily and also binds a range of structurally related molecules. Ticks secrete HBP2 during feeding to sequester histamine and prevent an immune response. Unusually for a lipocalin, HBP2 binds hydrophilic ligands and has two binding sites (Figure 1) which differ in their affinity for histamine. In addition to histamine, HBP2 binds tyramine, dopamine, tryptamine, and serotonin. The interaction with histamine involves a number of charge interactions, notably between the amino group of histamine and aspartate residues in the two binding sites.

Figure 1. Histamine-binding protein 2. The apo protein is coloured in raspberry, while the histamine-bound complex is coloured in wheat. Small conformational changes can be seen in the loop regions of the protein. The low affinity binding site is located at the top of the molecule, as shown, and the high affinity site at the bottom.

Binding thermodynamics

Ligand binding to HBP2 gives the expected thermodynamic signature for an interaction of this type, that is an enthalpy driven interaction, with an unfavourable entropic term. Histamine interacts with both binding sites with nanomolar affinity. ITC studies on the other

ligands reveal that they bind with micromolar affinity and appear only to be capable of binding to the low affinity site. Interestingly, the affinity of these larger ligands appears to depend more on the presence of hydroxyl groups than their size.

NMR relaxation studies of protein and ligand dynamics

NMR relaxation experiments are being used to study the dynamics of HBP2 which contribute to the entropy of binding. Studies examining the backbone amide dynamics of apo HBP2 and the HBP2-histamine complex, reveal that there is a slight increase in backbone dynamics upon ligand binding. While this finding is counterintuitive, recent studies on a number of other systems (including MUP) have revealed this phenomenon.

We also know that the modified amino acid histidine methyl ester binds to HBP2. Using an isotopically labelled form of this ligand we intend to probe the dynamics of the ligand in the bound state, of which little is currently known.

X-ray crystallography

In order to gain a complete picture of the interaction between a protein and its ligand, it is vital to have three-dimensional structures of the various states under study so that measured thermodynamic changes can be interpreted in terms of a physical picture. We have solved the structure of the apo protein so that it can be compared with the existing holo structure of HBP2. Small conformational changes can be seen in the loop regions of the protein (Figure 1) and a more significant change can be seen in the high affinity binding site (Figure 2a). A comparison of the two structures also reveals the number of water molecules displaced by the ligand (Figure 2b), which is important to understand the solvation contribution to binding.

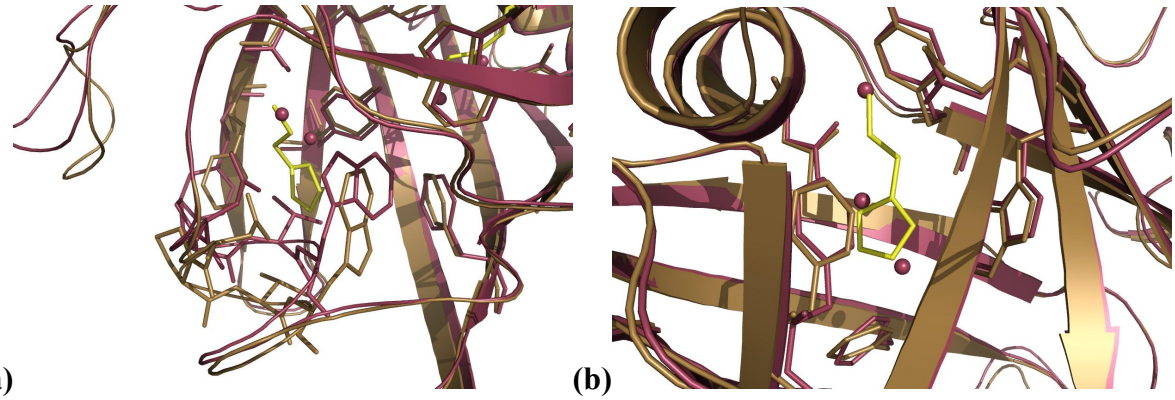

Figure 2. Close up of the high affinity binding site in apo (raspberry) and holo (wheat) HBP2. In (a) it can be seen that W42 flips round in order to accommodate the incoming histamine molecule. In (b) the water molecules (spheres) in the apo protein can be seen occupying the same positions as the nitrogen atoms of the histamine molecule in the complex.

Collaborators

Dr. Guido Paesen, CEH Oxford

Publications

Syme N.R., Dennis C., Phillips S.E.V. and Homans S.W. (2007) Origin of heat capacity changes in a “nonclassical” hydrophobic interaction. *ChemBioChem* 8:1509-1511

Funding

This work is funded by the BBSRC and The Wellcome Trust.

Role of the prion protein in Alzheimer's disease

Isobel Morten, Heledd Griffiths, Nicole Watt, Tony Turner and Nigel Hooper

Introduction

Alzheimer's disease (AD) is the commonest neurodegenerative disease of old age. Currently, there are no drugs available to halt or slow the progression of this devastating disease which is placing a huge burden on patients and carers. AD is characterised by the deposition in the brain of senile plaques that are composed of the amyloid-β peptide (Aβ) (Fig. 1). Through mechanisms that are poorly understood, Aβ oligomers, fibrils and/or aggregates are toxic to nerve cells. Aβ is derived from the larger transmembrane amyloid precursor protein (APP) through proteolytic cleavage by the β- and γ-secretases. The β-secretase (BACE1) cleaves within the APP sequence at the N-terminus of the Aβ peptide, with the γ-secretase complex cleaving the resulting membrane-bound stub at the C-terminus of the Aβ sequence. Inhibition of both the β- and γ-secretases are being considered as potential therapeutic approaches to combat AD.

The prion protein is probably best known for its role in the transmissible spongiform encephalopathies or prion diseases, such as Creutzfeldt-Jakob disease in humans and bovine spongiform encephalopathy in cattle. In these diseases the normal cellular for of the prion protein (PrP^{C}) undergoes a conformational conversion to the infectious form, PrP^{Sc}. PrP^{C} appears to have roles in the cellular resistance to oxidative stress, in cellular copper and zinc homeostasis and in cell signalling. In addition, we have shown that PrP^{C} inhibits the β-secretase cleavage of APP, lowering the amount of Aβ produced and, therefore, potentially protecting against AD (Fig. 1). In both cell models and mice, reduction of PrP^{C} levels resulted in an increase in Aβ production. BACE1 co-immunoprecipitated with PrP^{C} and recombinant BACE1 has been shown to interact directly with recombinant PrP^{C} in an ELISA format. This inhibitory effect of PrP^{C} on the BACE1 cleavage of APP was lost when PrP^{C} contained insertion or point mutations associated with human prion diseases or when the protein was converted to the infectious form PrP^{Sc}, raising the possibility that Aβ contributes to prion disease pathogenesis.

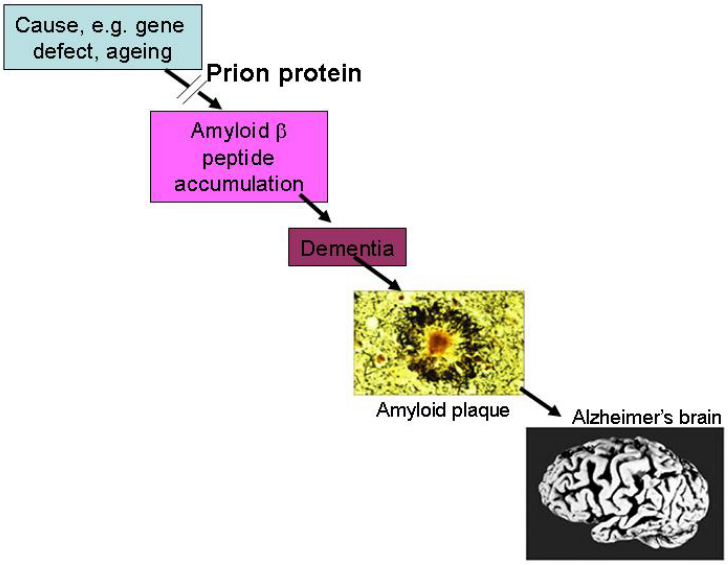

Figure 1. The role of the prion protein in Alzheimer's disease prevention.
In the amyloid cascade hypothesis of AD, a genetic mutation, ageing or some other environmental trigger causes an accumulation of the neurotoxic Aβ peptide that aggregates to form the characteristic amyloid plaques found post-mortem in the brains of AD patients. The normal cellular form of the prion protein, PrP^{C}, through inhibiting the production of the Aβ peptide, may prevent the development of AD.

These observations raise the following questions which we are actively pursuing: (i) Could mimicking the mechanism by which PrP^C inhibits Aβ peptide formation be a potential therapeutic treatment for AD? (ii) Could small reductions in PrP^C levels in individuals affect the proteolytic processing of APP in a subtle way over decades to affect long-term Aβ production that, in turn, would accelerate the onset of AD? (iii) Does Aβ contribute to the pathogenesis of prion diseases? (iv) Is depletion of PrP^C a sound approach for the treatment of prion diseases?

Publications

Parkin, E.T., Watt, N.T., Hussain, I., Eckman, E.A., Eckman, C.B., Manson, J.C., Baybutt, H.N., Turner, A.J. & Hooper, N.M. (2007) Cellular prion protein regulates β-secretase cleavage of the Alzheimer's amyloid precursor protein. *Proc. Natl. Acad. Sci USA* **104**, 11062-11067.

Hooper, N.M. & Turner, A.J. (2008) A new take on prions: preventing Alzheimer's disease. *Trends Biochem. Sci.* **33**, 151-155.

Funding

This work was funded by the MRC and BBSRC.

Biomolecular modeling and structural bioinformatics

Nicholas Burgoyne, James Dalton, John Davies, Karine Deville, Jonathan Fuller, Nicola Gold, Sarah Kinnings, Sally Mardikian, Monika Rella, and Richard Jackson

Binding site similarity analysis for the functional classification of proteins

We have continued the development of our binding site structural similarity database, SitesBase, adding a more statistically robust measure of site similarity using the Poisson index in collaboration with the School of Maths. This work has also continued in looking at an all-against-all similarity comparison across the whole of protein space and currently, we are undertaking a large-scale comparison of protein kinase ATP-binding sites. The analysis is allowing us to discover binding site similarity in different sub-families of protein kinase that are not evident from sequence similarity alone. It is also enabling us to quantify the effect of how different drug molecules bind to the same binding site and influence the local binding site conformation. We aim to propose a relevant classification of the protein kinase family based on the similarity of their binding sites. Not only will this classification highlight features that are important for the potency and selectivity of kinase inhibitors, but it will also be able to predict possible cross-reactivities among the protein kinases.

Protein binding site prediction

Q-SiteFinder locates ligand binding sites by clustering favourable regions for van der Waals (CH_3) probes on the protein surface. Q-SiteFinder and has been made available online (www.bioinformatics.leeds.ac.uk/qsitefinder) and it is already widely used and cited. Work has continued in characterising binding sites in a wide range of different protein interactions (protein-protein, protein-ligand, protein-drug, as well as protein-small molecule inhibitors of protein-protein interactions). We have utilised an energy based definition for the volume envelope of favourable van der Waals interaction to define 'active pockets' on the protein surface. Analysis of these active pockets has shown that there are significant differences between different classes of interaction which might be exploited in the design of effective new drugs and in the prediction of protein-protein complexes.

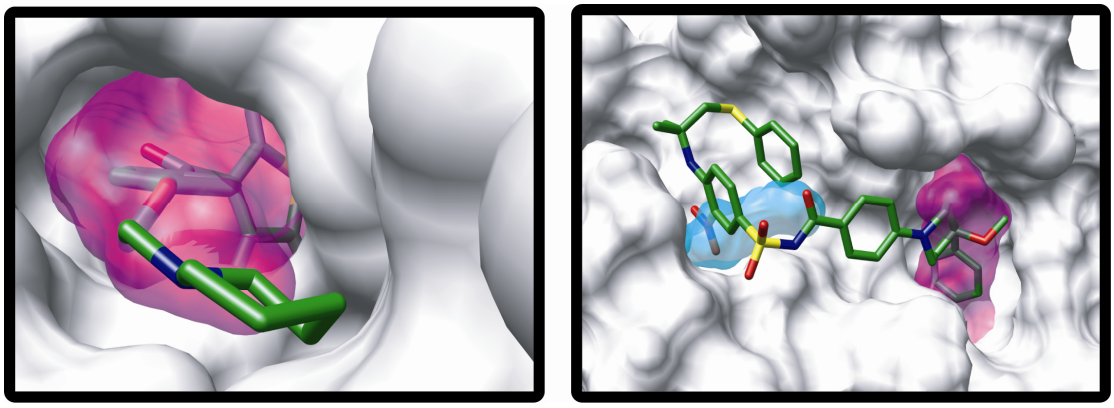

A typical protein-drug interaction occurring in a single high volume site: Human Estrogen Receptor complexed with Raloxifene. PDB Code: 1err, site 1: volume 509Å3. A typical small-molecule protein-protein interaction inhibitor occurring in several low volume sites: Anti-apoptosis protein Bcl-2 complexed with an acyl sulfonamide ligand. PDB Code: 2o2f, site 2: volume 217Å3, site 3: volume 286Å3.

Modelling protein interactions and docking

We continue to develop a homology modeling method for the prediction of protein-ligand interactions. We are developing a novel and fully automated computational method capable of protein-ligand homology modeling that brings together new and existing ideas. The method is based on the 'induced' fit concept where there is flexibility in both residue side-chains and ligand. This is implemented by generating a broad range of possible

conformations for all side-chains and ligand, which are then refined with a mean field optimisation calculation, resulting in the lowest available energetic state of the binding-site.

In collaboration with the group of Prof. Goody (Max Plank Institute, Dortmund) we have developed a novel knowledge-based scoring function that uses information theory to predict the binding affinity of ligands to proteins for use in structure-based inhibitor design.

In collaboration with the group of Prof. Brito (University of Coimbra, Portugal) we are currently using molecular docking and pharmacophore modelling to develop novel inhibitors to prevent amyloid fibril formation in familial amyloidotic polyneuropathy. In this disease, single point mutations encode for less stable variants of transthyretin (TTR), which undergo tetramer dissociation and monomer unfolding. The initial tetramer dissociation is thought to be the rate limiting step in the process, and some success has been achieved through inhibition of this process using small molecule thyroxine mimetics. The aim is to design and synthesise inhibitors that prevent fibril formation.

In collaboration with the group of Dr. Baldo Oliva (University of Pompeu Fabra, Barcelona) we have developed a novel method that uses structural models to reduce a large number of *in silico* predictions of protein-protein interactions to a high confidence subset that is amenable to experimental validation. Due to the limitations in experimental methods for determining binary interactions and structure determination of protein complexes, the need exists for computational models to fill the increasing gap between genome sequence information and protein annotation.

In collaboration with the groups of Prof. Hooper and Prof. Turner we have identified and characterised a novel mammalian homologue of ACE gene called Angiotensin Converting Enzyme-3 (ACE3), using a combined bioinformatics and experimental study.

Collaborators
Prof. David Westhead (University of Leeds)
Prof. Anthony Turner (University of Leeds)
Prof. Nigel Hooper (University of Leeds)
Prof. Kanti Mardia (School of Maths, University of Leeds)
Prof. Charles Taylor (School of Maths, University of Leeds)
Dr. Val Gillet (University of Sheffield, UK)
Prof. Rui Brito (University of Coimbra, Portugal)
Prof. Roger Goody (Max Plank Institute, Dortmund, Germany)
Dr. Baldo Oliva (University of Pompeu Fabra, Barcelona, Spain)

Visiting Researchers
Mr. Mahesh Kulharia (Max Plank Institute, Dortmund, Germany)
Mr. Carlos Simoes (University of Coimbra, Portugal)

Publications
Davies J.R, **Jackson R.M,** Mardia K.V, Taylor C.C. (2007) The Poisson Index: a new probabilistic model for protein ligand binding site similarity. *Bioinformatics* **23**: 3001-3008.

Dalton, J.A.R. & **Jackson, R.M.** (2007) An evaluation of automated homology modelling methods at low target template sequence similarity. *Bioinformatics* **23**: 1901-1908.

Rella, M., Elliot, J.L., Revett, T.J., Lanfear, J., Phelan, A., **Jackson, R.M.**, Turner, A.J. & Hooper, N.M. (2007) Identification and characterisation of the angiotensin converting enzyme-3 (ACE3) gene: a novel mammalian homologue of ACE. *BMC Genomics* **8**: 194.

Gold N.D., Deville K., & **Jackson, R.M.** (2007) New opportunities for protease ligand-binding site comparisons using SitesBase. *Biochem Soc Trans.* **35**: 561-565.

Cockell, S.J., Oliva, B., & **Jackson, R.M.** (2007) Structure-based evaluation of *in silico* predictions of protein-protein interactions using comparative docking. *Bioinformatics* **23**: 573-581.

Funding
These projects were funded by the BBSRC, MRC, EPSRC, University of Leeds and The Wellcome Trust.

Electrodes for redox-active membrane proteins

Andreas Erbe, Sophie Weiss, Nikolaos Daskalakis, Steve Evans, Richard Bushby, Simon Connell, Peter Henderson and Lars Jeuken

Introduction

Redox proteins, which are estimated to account for a quarter of all proteins, perform a myriad of functions in biology. They shuttle electrons and catalyse redox reactions in many vital processes, including photosynthesis and metabolism. Dynamic electrochemical techniques have proven to be powerful tools to study these proteins. The thermodynamics and kinetics can be studied in detail if they are electrochemically connected or 'wired' to the electrode surface. The main challenge is to adsorb proteins in their native state on the electrode while efficiently exchanging electrons. Because membrane proteins are more difficult to manipulate experimentally than globular proteins, less work has been reported on the electrochemistry of these proteins. Here, we report a novel approach to link membrane proteins to an electrode surface.

Cholesterol tethers to 'wire' membranes

We have prepared electrode surfaces which enables the characterisation of redox-active membrane enzymes in a native-like environment. For this, we have used the methodology of tethered bilayer lipid membranes (tBLM), in which the lipid bilayer is attached to the electrode surface via special chemical anchors that are bound to the surface on one side and insert into a bilayer leaflet at the other (Figure 1). Cholesterol derivatives have been synthesised, which, via a hydrophilic linker, are connected to a thiol group that form self-assembled monolayers (SAMs) on gold electrodes. These cholesterol-lipids have been mixed with small thiols to provide space for transmembrane proteins. The surfaces of these mixed SAMs have been characterised in detail by friction AFM and shown to exhibit a complex pattern of phase separation, confirming the demixing of the two thiols schematically shown in Figure 1.

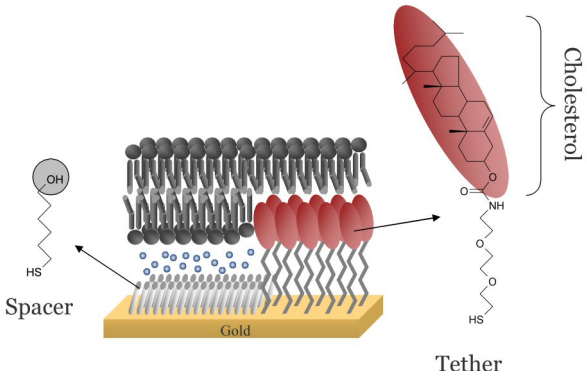

Figure 1: Chemical structures of 6-mercaptohexanol (spacer) and the cholesterol tether molecule used to form tBLMs.

Spectroscopic studies

The formation of tBLMs from lipid vesicles via self-assembly has been studied in detail with attenuated total reflectance infrared spectroscopy combined with impedance spectroscopy. This novel combination of spectroscopies was made possible by the design of a new experimental setup and the results indicate that the structure of the tBLM varies with varying the mixed SAM composition. On SAMs with a high content of cholesterol tether, tBLMs with reduced fluidity were formed. For SAMs with low content, the results are consistent with the adsorption of flattened vesicles, while spherical vesicles have been found in a small range of surface compositions.

Electric field effects

The tBLMs on gold also provide an excellent platform to study the effects electric fields have on the structure of lipid membranes. Electric-field induced changes in structure and conductivity of the tBLM have been studied at submicroscopic resolution using atomic force microscopy (AFM) and electrochemical impedance spectroscopy. At electric fields of ≤ 0.45 V across the membrane, it was found that the conductance of the membrane starts to increase

and membrane areas of less than 150 nm in size are found to elevate from the surface up to 15 nm in height. The latter observation suggests that pockets of solvent appear or are formed beneath the membrane. These results increase our understanding of electroporation phenomena.

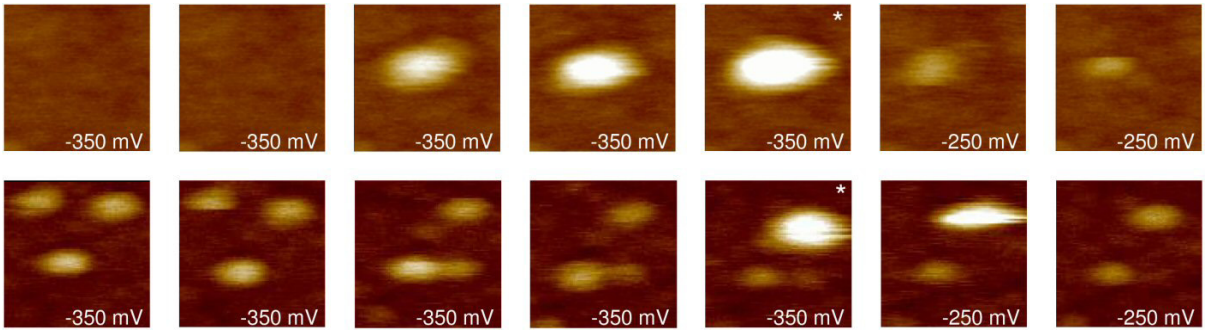

Figure 2: Two selected areas of consecutive AFM images of a tBLM at varying DC potentials (the electric field experienced by the lipid membrane is about 200 mV larger than the applied potential). The size of the selected areas is 200×200 nm and the height scale 18 nm.

Electrochemistry

Quinones (also known as Coenzyme-Q) are important electron mediators in biology and function by transporting electrons between membrane enzymes. The electron transfer properties of quinones are closely coupled its protonation and biology has utilised this to build up a proton motive force (*pmf*) across the membrane, which is the key feature in the generation of energy in all living organisms. We have used the tBLM system to study the quinone redox properties and have found that the protonation can only occur at the membrane-solution interface as protons are not able to penetrate the membranes. Importantly, however, it was shown that quinones can also accept protons in the membrane directly from commonly-used proton uncouples like CCCP, which shows an previously unknown action of this class of compounds that are often used to disrupt *pmf* in experimental systems.

tBLM from bacterial membrane extracts

New protocols have been developed to prepare tBLMs from inner membranes extract from *E.*

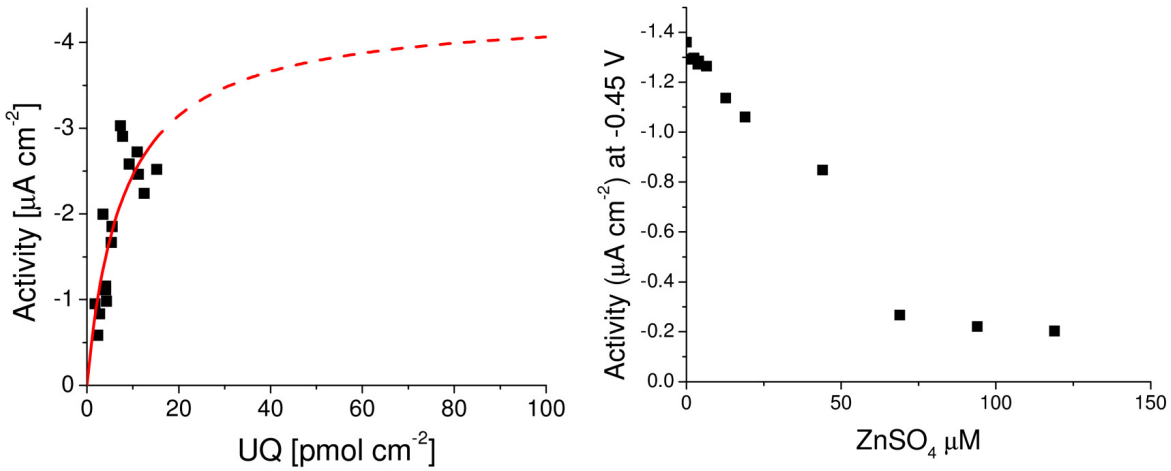

Figure 3: Examples of enzymatic data obtained for cytochrome bo_3 using the tBLM system prepared from inner membrane extracts from cyt bo_3. (Left) The maximum oxygen reduction activity of inner membranes (1:9 mixed with *E. coli* lipid extract) as a function of ubiquinol-10 present in the membrane. A Michaelis Menten curve is fitted to illustrate it is not possible to incorporate enough ubiquinone-10 in the membrane to determine a K_m as too much ubiquinone-1 destabilise a lipid membrane. (Right) A typical example of the inhibitoon effect of Zn^{2+} on the activity of cytochrome bo_3

coli. In contrast to the systems prepared previously with purified membrane proteins, these systems are easier to prepare and more robust in nature. The quinones in these tBLM system still acts a substrate for quinone enzymes that are located in the inner membrane. Using this novel membrane system, the activity of an ubiquinol oxidase from *Escherichia coli*, cytochrome bo_3 (cbo_3) is studied using voltammetry techniques. This allows the accurate and controlled characterisation of interaction between UQ and cbo_3, which has previously only been studied using soluble analogues of UQ or by means which resulted in a large amount of variability in obtained data.

Future directions

We aim to continue to study the enzyme mechanics of cbo_3 and other quinone enzymes with particular focus on properties that made UQ a special substrate when compared to aqueous solutes. Properties like UQ diffusion through the membrane and oxygen solubility in the membrane are considered. In a second project, intact vesicles with fluorescent pH indicators are adsorbed on the surface in order to monitor simultaneously the electron and proton transfer properties of the redox enzymes of interest.

Collaborators and Funding

We thank Prof. Robert B. Gennis (University of Illinois, Urbana, USA) for his help with cbo_3 and providing several *E. coli* strains. This work was funded by the BBSRC, EPSRC, Royal Society and Philips.

Publications

Jeuken, L.J.C., Bushby, R.J., Evans, S.D. (2007) Proton transport into a tethered bilayer lipid membrane, *Electrochem. Comm.*, **9**, 610-614.

Jeuken, L.J.C., Daskalakis, N.N., Han, X., Sheikh, K. Erbe, E., Bushby, R.J. Evans, S.D. (2007) Phase separation in mixed self-assembled monolayers and its effect on biomimetic membranes, *Sensors and Actuators B: Chemical*, **124**, 501-509.

Erbe, A., Bushby, R.J., Evans, S.D., Jeuken, L.J.C. (2007) Tethered bilayer lipid membranes studied by simultaneous attenuated total reflectance infrared spectroscopy and electrochemical impedance spectroscopy, *J. Phys. Chem. B*, **111**, 3515-3524.

Wijma, H.J., Jeuken, L.J.C., Verbeet, M.P., Armstrong, F.A., Canters, G.W. (2007) Protein Film Voltammetry of Copper-containing Nitrite Reductase reveals Reversible Inactivation, *J. Am. Chem. Soc.*, **129**, 8557-8565.

Dodd, C.E., Johnson, B.R.G., Jeuken, L.J.C., Bugg, T.D.H., Bushby, R.J., Evans, S.D. (2008) Native *E. coli* inner membrane incorporation in solid supported lipid bilayer membranes, *Biointerphases*, **in press.**

Jeuken, L. J. C. (2008) AFM study on the electric-field effects on supported bilayer lipid membranes, *Biophys. J.*, **in press.**

Structure of switched-off smooth muscle myosin

Stan A. Burgess, Shuizi Yu, Rhoda J. Hawkins and Peter J. Knight

Introduction

The muscles that drive movement in the gut, contraction of the uterus and that maintain tone in the walls of arteries are all smooth muscles. They lack the highly organised structure seen in the striated muscles of the heart and skeleton, but still use a system of myosin and actin filaments to produce contractile force, albeit the myosin filaments have a different architecture. Myosin filaments can be depolymerised by high salt concentrations, and myosin is then seen to comprise two 16 nm heads attached to one end of a ~160nm tail. The heads are the motors of contraction, containing the ATPase and actin-binding sites, while the tail, a canonical α-helical coiled coil, binds to other tails to hold many myosin molecules together and it transmits the forces generated by the heads.

Smooth muscle contraction is regulated by phosphorylation of a regulatory light chain in each head by a specific kinase, which switches on contraction. Relaxation follows dephosphorylation by protein phosphatase. It has been known since the 1980s that *in vitro* the active smooth muscle myosin filaments depolymerise into individual molecules when dephosphorylated. Moreover, unlike myosin in high salt, the tail of these molecules is folded up, roughly into thirds, so that a distal part of the tail is associated with the heads. In this state the ATPase of myosin is essentially zero, and the molecule does not bind to actin. Folded myosin may therefore be able to diffuse or be carried in the cell to allow remodelling of the contractile apparatus in the quiescent muscle. Evidence is accumulating that *in vivo* a significant pool of this monomeric myosin is present, although many myosin filaments persist.

Structure of switched-off myosin

Considering the significance of the folded molecule, surprisingly little detailed work has been done on its structure. We have redressed this by using electron microscopy of single folded molecules from turkey gizzard muscle in negative-stained specimens, followed by single particle image processing (Fig. 1). We have studied both whole myosin and a proteolytic fragment (heavy meromyosin, HMM) that lacks most of the tail, but is still regulated.

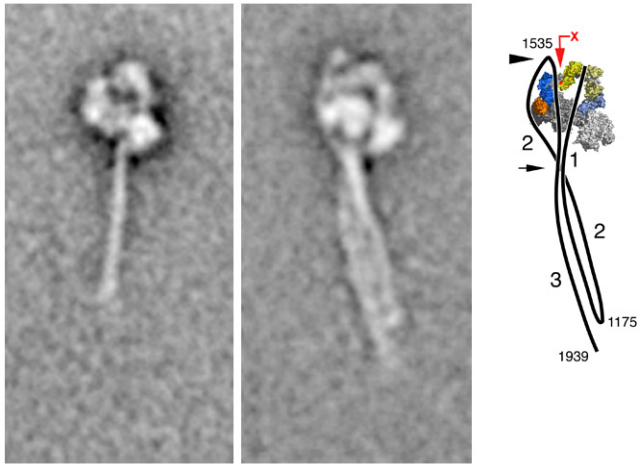

Fig. 1 Conformation of switched off smooth muscle myosin as seen by electron microscopy and image processing. Left panel is the HMM fragment that lacks ~2/3 of the tail; centre panel the intact myosin molecule. The right panel is a diagram of the folded molecule in which the heads derive from an atomic model, with various parts coloured and a black line represents the path of the folded tail. The three segments of the tail are labelled, as are the estimated amino acid sequence positions of the bends. The black arrowhead marks the second bend visible as a pale spot in the image, the arrow highlights where the tail segments are especially close, and the red arrow points at a site on the left head that had previously been shown to be close to the tail.

In both myosin and HMM the two heads are arranged in a very specific and asymmetric way, in contrast to the free movement of the heads around the head-tail junction seen in high salt concentrations. The arrangement is strikingly similar to a structure found in an earlier study when the HMM formed 2-dimensional crystals on a lipid monolayer, and shows that that structure was not an artefact. We have found that the folded molecule is more compact than previously thought. The three segments of the tail are grouped together, and interact in a very specific way with just one of the two heads. We further found that the interaction of the folded tail with the heads stabilised the specific conformation of the heads, and this probably accounts for the very low ATPase of myosin compared to HMM, where these interactions are absent.

Quantifying flexibility of the myosin tail

We have also analysed the structure of the tail. The lengths of the three segments are precise, which implies that the sites of bending in the tail are also precise (Fig. 1). It is not yet clear why the tail bends at these points rather than elsewhere. We have used image processing to examine the variation in the shape of the tail between molecules. For HMM, the single tail curves to a variable degree along its length. On the assumption that this appearance is due to the Brownian forces we have estimated the Young's modulus of the coiled coil tail to be 0.5 GPa. This is close to an earlier value obtained by light scattering from myosin in solution. The folded tail of the intact molecule appears less flexible, as expected if the three segments interact to counter thermal perturbation. This analysis shows that our electron microscopy method can be used to explore the thermally-induced flexibility within macromolecules.

Collaborator

Joseph Chalovich, East Carolina University, NC, USA

Publications

Burgess, S. A., Yu, S., Walker, M. L., Hawkins, R. J., Chalovich, J. M. & Knight, P. J. (2007). Structures of smooth muscle myosin and heavy meromyosin in the folded, shutdown state. *J. Mol. Biol*. **372**, 1165-1178.

Funding

This work was funded by BBSRC and NIH.

Load-dependent mechanism of nonmuscle myosin 2

Kavitha Thirumurugan and Peter J. Knight

Loads on molecular motors regulate and coordinate their function. It would be attractive for energy economy in the living cell if a motor that was stalled by a high load also had low fuel consumption. It has been difficult to investigate such effects of load using solution biochemistry because the molecules are then free in solution. Nonmuscle myosin 2 (NM2) is a motor protein that is a key player in such processes as cell division, where it drives the constriction of the cleavage furrow, and tonic tension maintenance in smooth muscle. We have taken advantage of the two-headed structure of this myosin to generate internal load within its heads when both heads bind to the same actin filament (Fig. 1A). The internal strain pulls one head towards the direction of movement, while the other head is pulled back. This allowed us to compare the effects on ATPase kinetics of both forward and reverse strain. Nonmuscle myosin 2 is especially useful in this regard because its complex with ADP binds tightly to actin, allowing the kinetics of ADP release and ATP binding to be explored.

We used a truncated fragment of NM2 that lacks the filament forming part of the tail, and which therefore remains two-headed but monomeric in solution. Electron microscopy showed that the two heads were indeed both bound to single actin filaments (rather than each binding a different filament (Fig. 1D). Image processing further showed that the heads were attached to adjacent subunits in the actin polymer. Since the helical structure of actin is well established, this allowed the strains in the doubly-attached molecules to be calculated.

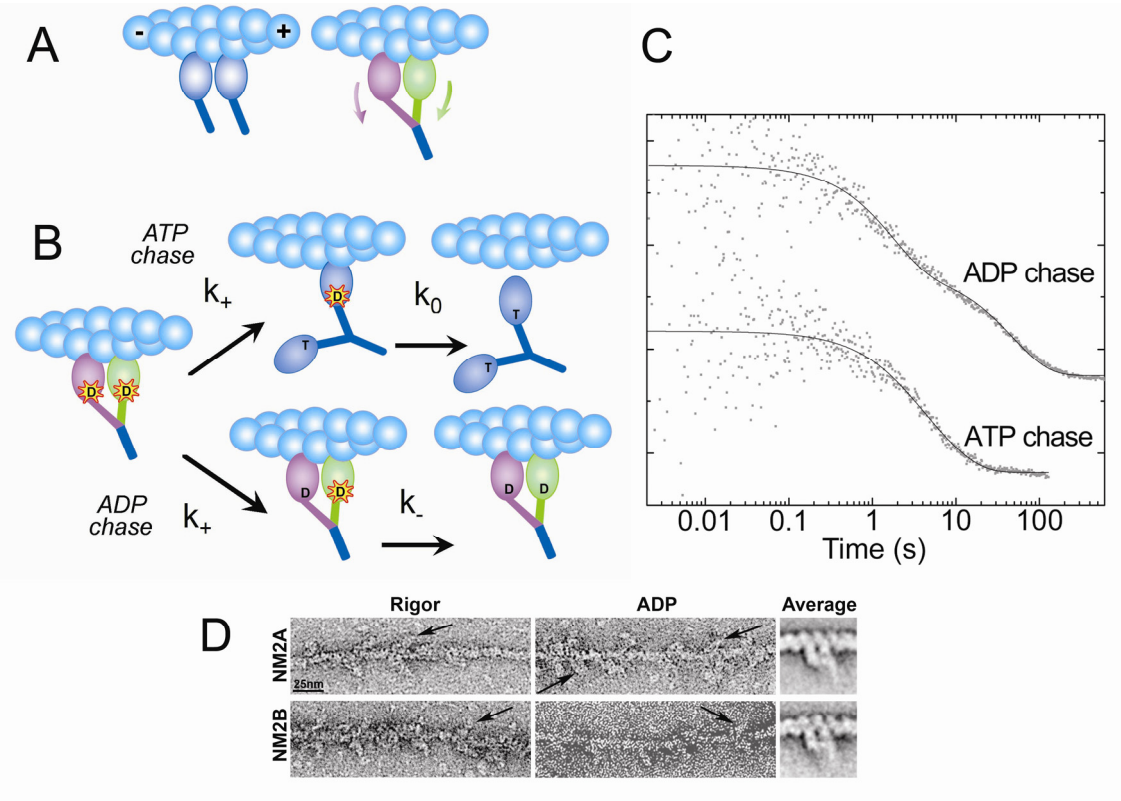

Fig. 1. Using the two heads of myosin to allow measurements of the effects of strain on kinetics.
A: Uniting the bases of two heads at a common head-tail junction distorts both of them. B: A molecule loaded with a fluorescent ADP analogue will show different dissociation kinetics if chased with unlabelled ATP (which releases the heads) or ADP (which maintains them attached). C: Stopped flow kinetics data for NM2A on actin. ATP chases show both k_+ and k_0 are fast; ADP chases show large difference between k_+ and k_-; the ADP trace is shifted upscale for clarity of display. D: Electron micrographs of NM2A and NM2B (two isoforms of NM2) binding by both heads to actin, both in the absence and presence of ADP. At right image processing reveals the subunits of the actin filament and the NM2 heads on adjacent subunits, 5.5nm apart.

The kinetic data indeed reveal large effects on ADP release kinetics (Fig. 1C). Forward strain enhances ADP release, which may function to reduce the drag this myosin would otherwise produce if a faster motor was also active in the cell, such as in smooth muscle. Rearward strain produced marked reductions in rate, such that the ATPase cycle time could be extended to minutes rather than seconds. This would allow resistive load to stall this myosin in a strong binding state, converting the molecule into a tension-producing tether. NM2B shows particularly marked effects of load; NM2A while perturbed by loads, is not kinetically-tuned to act as a tether. These differences between isoforms are presumably part of their adaptations to fulfil distinct roles in the cell.

Collaborators

Mihaly Kovács, Eötvös University, Budapest, Hungary
James Sellers, National Heart, Lung and Blood Institute, NIH, MD, USA

Publications

Kovács, M., Thirumurugan, K., Knight, P. J. & Sellers, J. R. (2007). Load-dependent mechanism of nonmuscle myosin 2. *Proc. Natl. Acad. Sci. USA*, **104**, 9994-9999.

Funding

This work was funded by Wellcome Trust, NIH and EMBO-Howard Hughes Medical Institute.

Structural studies of innate immune signalling proteins

Tom Burnley, Jennifer Ly, Arwen Pearson, Thomas Edwards and Andrew Macdonald

Introduction

The innate immune response is a highly conserved early defence mechanism against microbial pathogens including viruses. The success of this defence against virus invasion depends on the capacity of the host cell to detect the invader and rapidly induce a programme of gene expression that leads to the production and dissemination of interferons (IFNs), which convert the host environment into one that is hostile to viruses. The innate immune response relies on an array of pattern recognition receptors that detect microbial metabolic products including the nucleic acids of viruses. These receptors, which include the RNA helicases RIG-I and Mda-5, act as an early warning system in the defence against invasion. They function by transmitting signals to critical protein kinases, including TBK1, which phosphorylate transcription factors such as IRF3/7 and NFκB that bind to specific promoter elements and up-regulate the transcription of anti-viral genes including IFNβ.

Studies on the RNA helicases RIG-I and Mda-5

Despite great recent interest, the molecular mechanism of nucleotide recognition and signalling of RIG-I and Mda-5 is unknown. Hence, we have initiated studies with the aim of producing high-resolution structures primarily using X-ray diffraction methods. Homology mapping predicts RIG-I and Mda5 to be composed of a C-terminal helicase domain. Nucleic acid binding assays demonstrate that the helicase of RIG-I binds with high affinity to single stranded RNA with a five prime tri-phosphate (ssRNA), whilst the helicase of Mda-5 has a greater preference for double-stranded RNA (dsRNA). The helicases of these proteins are coupled to two amino-terminal caspase recruitment (CARD) domains, which are necessary for transmitting the appropriate anti-viral signal via protein-protein interactions with other CARD containing proteins. Several constructs comprising different combinations of the domains (Fig 1, top) have been successfully cloned into pGEX GST-fusion vectors and recombinant protein over-expression has been achieved in *E.coli* (Fig 1, bottom). This has enabled the efficient production of high-levels of pure protein for either full-length protein or specific domains (e.g. ~50 mg from 4L culture for RIGI CARD1/2) using glutathione affinity chromatography. In addition, the use of luciferase reporter technology has demonstrated that the CARD fusion proteins are able to efficiently transduce an anti-viral signal to the IFNβ promoter (data not shown). High-throughput crystallization trails are in progress using the in-house robotic facilities present in the Astbury Centre. It is expected that the first 3D structures of these important proteins will solved in Leeds within the next 12 months.

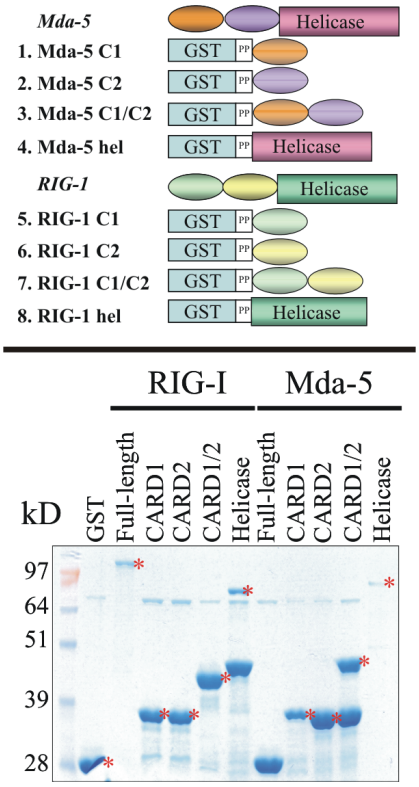

Fig 1. *Top*. Domain organisation of RIG-I and Mda-5 constructs. *Bottom,* Denaturing SDS-PAGE image showing levels of recombinant protein expression in *E.coli*. Expected position of GST-fusion construct is denoted by (*).

Studies on regulators of the innate immune response

Studies from our laboratory have identified the protein optineurin as a critical regulator of the anti-viral response. The mechanism by which optineurin regulates the anti-viral response is currently unknown, although it may require an interaction with the protein kinase TBK1 and upstream signalling proteins that are ubiquitylated. Optineurin is a member of the AHD-family of ubiquitin binding proteins. This family includes the well characterised regulator of NFκB, NEMO. NEMO forms a trimer in response to various stimuli and this higher molecular weight form of the protein is critical for correct functioning. Preliminary experiments have determined that optineurin also forms a higher molecular weight oligomeric structure in response to viral nucleic acids (Fig. 2). We are currently funded by the Royal Society to analyse the structural and molecular biology of optineurin in greater detail, with the eventual aim of solving the three dimensional structure of this critical mediator of signalling.

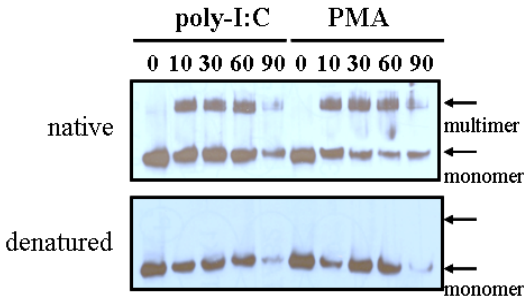

Fig 2. Formation of higher order structures by optineurin. Cells expressing Optineurin were stimulated with the viral dsRNA mimic poly-I:C or treated with the mitogen PMA and lysed at the indicated time-point. Lysates were analysed either by non-denaturing native electrophoresis (top) or by denaturing electrophoresis (bottom).

Publications

Kaiser M., Wiggin, G., Lightfoot, K., Arthur J.S.C., & Macdonald, A. (2007). MSK regulate TCR-induced CREB phosphorylation but not immediate early gene transcription. *European Journal of Immunology* **37**, 2583-2595.

McCoy, C.E., Macdonald, A., Morris, N.A., Campbell, D.G., Deak, M., Toth, R., Mcilrath, J. & Arthur, J.S.C. (2007). Identification of novel phosphorylation sites in MSK1 by precursor ion scanning Mass Spectrometry. *Biochemical Journal.* ***402,*** 491-501.

MacDonald, A., Campbell, D.G., Toth, R., McLauchlan H.J., Hastie, C.J., & Arthur, J.S.C. (2006). Pim kinases phosphorylate multiple sites on Bad and promote 14-3-3 binding and dissociation from Bcl-X-L *BMC Cell Biology* **7**, 1.

Funding

This work is funded by Research Council UK, Yorkshire Cancer Research, The Royal Society and the University of Leeds.

High-dimensional models of protein folding

Supreecha Rimratchada, Sheena Radford and Tom McLeish

Introduction

Most theoretical treatments of protein folding suffer from an unreasonably large "dimensional reduction" from the hundreds of degrees of freedom explored by real polypeptide chains as they undergo collapse to simple 1- or 2- dimensional landscapes. In this project we are exploring the consequences of retaining a significant number of degrees of freedom in a series of well-studied types of fold. Within this view, the Levinthal paradox is overcome by designing the sequence of important degrees of freedom to contain "hypergutters", subspaces of the overall search space at lower energy than the larger spaces, and which restrict the search for the native state to subspaces of lower and lower dimension. Although this all sounds rather abstract, it does hold the promise of predicting in advance experimental measures of protein folding kinetics such as the behaviour as a function of denaturant ("chevron plots") or phi-values.

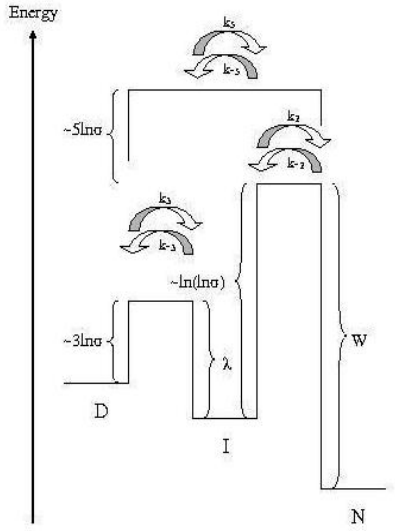

3-helix bundle proteins

The model system we have concentrated on so far is the 3-helix bundle. If the helices are partially formed at an early stage, the rest of the folding can be coarse-grained naturally into a diffusive search in a 5-dimensional space. Furthermore, if the two outer helices possess hydrophobic stripes, then the intermediate but non-native burying of these residues can divide the dimensional reduction into a sequence of 2 and 3 dimensional searches. This is much faster than the full 5 dimensional search, and offers one explanation of why folding through intermediates can be faster than 2-state folding. Expressions for the rates of transition between the various subspaces (see figure) can be derived from the dimensions of the searches.

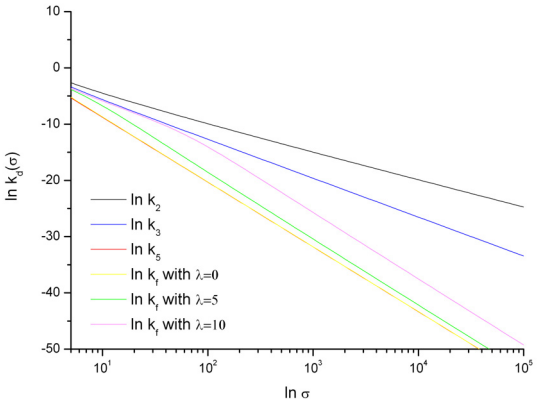

Chevron plots

The 3-helix hypergutter model contains only 3 parameters: the size of the dimensional reduction from denatured to native state (σ), the stabilizing hydrophobic energy of the dynamic intermediate (λ), and the stabilization energy of the native state (W). By coupling the first two to the concentration of denaturant we are exploring the space of possible chevron plots (see figure). As the hydrophobic interaction is increased so a "roll-over" sets in, indicating the activity of the intermediate state (boarder of green and purple regions in the plot).

Currently we are exploring the unfolding branch of the chevron plots, and attempting to parameterize the model for the bacterial immunity proteins using experimental data from stopped flow analysis.

Funding and Acknowledgements

This work was funded by the Thai Government, and EPSRC *via* the White Rose DTC.

Dynamic allostery in proteins

Hedvika Toncrova, Peter Stockley and Tom McLeish

Introduction

Allosteric proteins constitute a great puzzle. Classically it is believed that the communication between distant sites proceeds via a series of conformational changes. Recently allosteric proteins without substantial conformational change have been observed. This cannot be accounted for with the classical theory and therefore we have built a model that explains the long distance signaling in such cases. We believe that the signaling proceeds via a change in dynamic behavior of the protein and we illustrate the feasibility of such explanation on a few examples. Our most recent calculations involve allosteric signaling in Catabolite Activator Protein (CAP) and DNA.

Dynamical allostery of CAP

The CAP dimer displays a negative cooperativity without conformational change upon binding two CAMp ligands (one in each monomer). The binding is accompanied by dramatic changes in the protein dynamics as has been observed in detailed NMR experiments. Our coarse-grained model shows that the negative cooperativity can have a purely entropic origin. This is achieved by finely tuning the coupling between the monomers of the CAP dimmer. The allosteric free energy ($\Delta\Delta F$) landscape is shown in Figure 1. The plane $\Delta\Delta F = 0$ is shown to highlight the area of negative cooperativity area ($\Delta\Delta F > 0$).

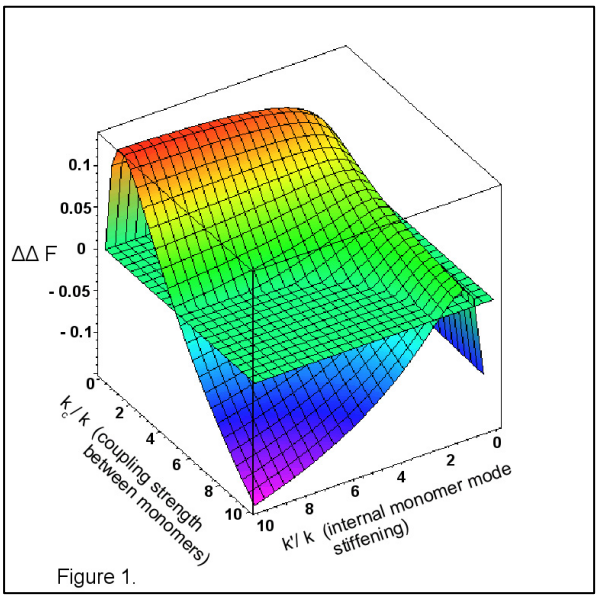

Figure 1.

Dynamical allostery in DNA

A second example constitutes a very popular DNA dye (HOECHST 33258) binding cooperatively to DNA (Fig. 2). Experiments (NMR and calorimetry) and computer simulations observe very strong positive cooperativity ($\Delta\Delta F \approx -10kT$). Many drugs and regulatory proteins bind cooperatively to DNA and therefore our model could serve as a paradigm for other drug-DNA and protein-DNA complexes. We coarse-grained the DNA as a rod with bending and twisting stiffness locally changing upon the dye binding. Our results give reasonable qualitative predictions, but fail to recover the cooperativity strength. This is probably due to excessive coarse-graining.

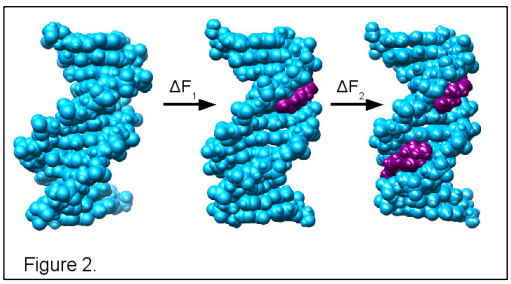

Figure 2.

Funding and Acknowledgements

This work was funded by the EPSRC. We acknowledge useful discussions with Dr. Sarah Harris.

Recombinant production of self-assembling and therapeutic peptides in biological expression systems

Kier James, Stephen Parsons, Stuart Kyle, Jessica Riley and Mike McPherson

In the area of bionanoscience, some of the most promising biomaterials are based on short peptides capable of hierarchical self-assembly into macromolecular structures such as micelles, fibrils and fibres. Such materials offer inherent advantages over current materials, including biodegradability and the ability to tailor make 'smart' materials with specific surface, mechanical, and responsive properties.

A major problem is achieving high yield production of such peptides. Solid or liquid phase chemical synthesis have several limitations including low yields and high cost, prohibiting industrial scale use. Our alternative approach is high yield recombinant production of self-assembling peptides rationally designed by the Centre for Self Organising Molecular systems (SOMS). These peptides form β-sheets that hierarchically self-assemble into helical tapes, twisted ribbons (double tapes) fibrils (twisted stacks of ribbons) and fibres (entwined fibrils) with increasing concentration, and/or in response to environmental cues such as pH or temperature. Proposed uses include matrices for tissue engineering, lubricants and various surface coatings.

Our initial research has used the bacterium *Escherichia coli* in which yields of 0.6 g/L of peptide have been achieved. We are also exploring yeast and plant expression hosts, *Pichia pastoris* and *Nicotiana tabacum* (tobacco). A range of synthetic gene constructs are being tested with different numbers of peptide repeats, various fusion proteins, purification tags and cleavage sequences. The resulting peptides are characterised by biophysical methods including TEM, AFM, CD and FT-IR. Mammalian cell tissue culture experiments of the suitability of self-assembling peptide hydrogels as tissue engineering matrices are underway. We are also exploiting our expression systems to express therapeutic, bioactive peptides.

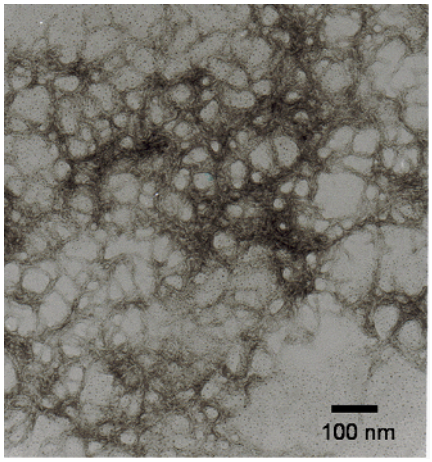

Figure 1. Transmission electron micrograph of a porous peptide network produced by a recombinant self-assembling peptide. The peptide comprises four tandem repeat units.

Collaborators: Amalia Aggeli, Centre of Self Organising Molecular Systems (SOMS); Eileen Ingham, IMCB, University of Leeds; Rudi Koopmans, Dow Chemicals.

Funding: We acknowledge studentship funding from BBSRC, The Wellcome Trust, Dow Chemical Company and the University of Leeds Institute of Bionanosciences.

Peripheral calcium influences cofactor biogenesis in *E. coli* amine oxidase

Pascale Pirrat, Mark Smith, Peter Knowles, Simon Phillips and Mike McPherson

Escherichia coli copper amine oxidase (ECAO) is a 160 kDa homodimer protein containing one copper ion and a post-translationally modified tyrosine cofactor; 2,4,5-trihydroxyphenylalanine quinone (TPQ) per subunit. TPQ biogenesis is an autocatalytic event requiring copper and oxygen. The enzyme therefore catalyses two reactions, first the single turnover formation of TPQ, and second the multiple turnover oxidation of substrate amines. Amine oxidation occurs by a ping-pong mechanism with reductive and oxidative half reactions. The reoxidation of reduced TPQ is couple to the reduction of O_2 to H_2O_2. The role of the TPQ and the copper in the oxidative half cycle remain unclear. Previous studies have suggested either a redox or a non-redox role for copper during amine turnover. Our studies, which have involved exploring the role of calcium in ECAO, have provided definitive evidence for a non-redox role for copper in ECAO. To explore the roles of the two peripheral calcium ions in ECAO we have undertaken structural, biochemical and mutagenesis studies.

One calcium lies at the ends of a 2 anti-parallel β-strand feature whose other end carries two of the three histidine ligands to the active site copper ion. Mutagenesis of this site indicates the calcium is important for initial folding and stability of the enzyme. The second calcium site is more peripheral, lies some 30Å from the active site and can be replaced by a wide range of mono- and di-valent metals. Surprisingly this calcium site influences TPQ biogenesis. Structural studies of two mutations of ligands to this calcium reveal conformational restriction of the active site pocket and the presence of precursor tyrosine close to the copper, rather than TPQ in an off-copper conformation; we speculate that this is due to oxygen entry and positioning being compromised. Further mutagenesis studies of residues around the active site have failed to compensate for this long-range structural effect of the calcium ligand. Further structural, spectroscopic and biochemical analyses are under way.

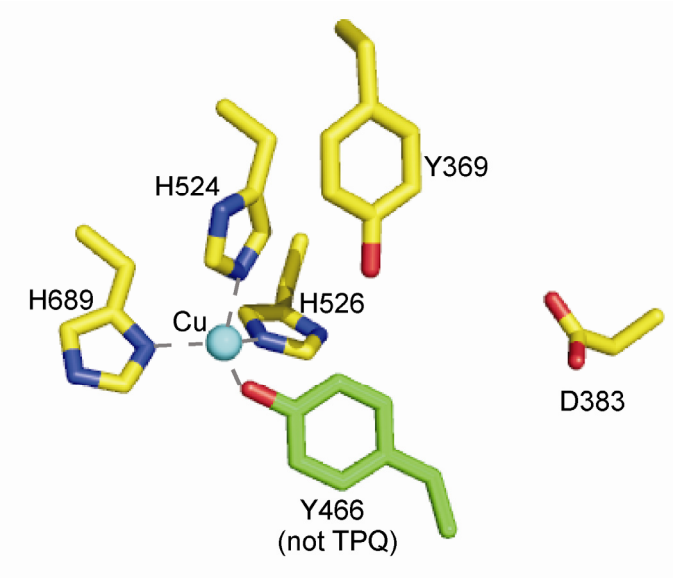

Figure 1: Active site structure of E573Q mutant of ECAO. The precursor Tyr466 is shown in an "on-copper" conformation. Long-range conformational restriction of the active site by the mutation has prevented TPQ biogenesis.

Acknowledgements
This work is supported by funding from BBSRC and the Wellcome Trust PhD programme.

The diversity-oriented synthesis of natural product-like molecules of unprecedented scaffold diversity

Christopher Cordier, Stuart Leach, Gordon McKiernan, Daniel Morton,
Catherine O'Leary-Steele, Thomas Woodhall, Stuart Warriner and Adam Nelson

Introduction

Synthetic organic chemistry is an immensely powerful tool for Chemical Biology, which we exploit in a wide range of biological problems: from the directed evolution of enzymes for use in synthetic chemistry (using biology to control synthetic chemistry), to chemical genetic studies (using chemistry to control biology). A list of the papers accepted for publication in 2007 is provided. You might like to browse our group webpages at www.asn.leeds.ac.uk to find out more about what we do!

The diversity-oriented synthesis of natural product-like molecules

The field of Chemical Genetics is founded on the premise that small molecules may be used to perturb the cellular functions of specific biological macromolecules. A key challenge in chemical biology, therefore, is to design and synthesise libraries which span large tracts of biologically-relevant chemical space. This challenge has spawned a new field in synthetic chemistry – diversity-oriented synthesis (DOS) – in which chemical libraries with high substitutional, stereochemical and/or scaffold diversity are prepared. The synthesis of libraries with high scaffold diversity is particularly challenging, though synthetic innovations have been devised to allow the parallel synthesis of libraries based on *ca.* ten scaffolds.

Here, we describe an iterative approach to the diversity-oriented synthesis of molecules with natural product-like features. Natural product families are large libraries of pre-validated, functionally diverse compounds which selectively modulate unrelated macromolecular targets. Our synthetic approach has yielded molecules which retain many of the broad structural features found in natural products which are needed to recognise macromolecules. We have used the approach to prepare a library of natural product-like compounds with unprecedented scaffold diversity.

Our synthetic approach is described in Scheme 1 with four illustrative examples of natural product-like final compounds. In an initial phase, building blocks are attached iteratively to a fluorous-tagged linker that we have developed. Then, alkene metathesis cascade reactions are used to 'reprogramme' the molecular scaffolds to yield final compounds. In the illustrative examples in Scheme 1, four skeletally diverse compounds were obtained from two building blocks through variation of the order and nature of the attachments.

The skeletal diversity of the final compounds may be assessed in terms of an hierarchical scaffold classification. We have prepared over one hundred natural product-like skeletons: thus, our approach yields libraries with unprecedented scaffold diversity. Representative examples of final compounds based on twenty alternative primary scaffolds are shown in Scheme 2.

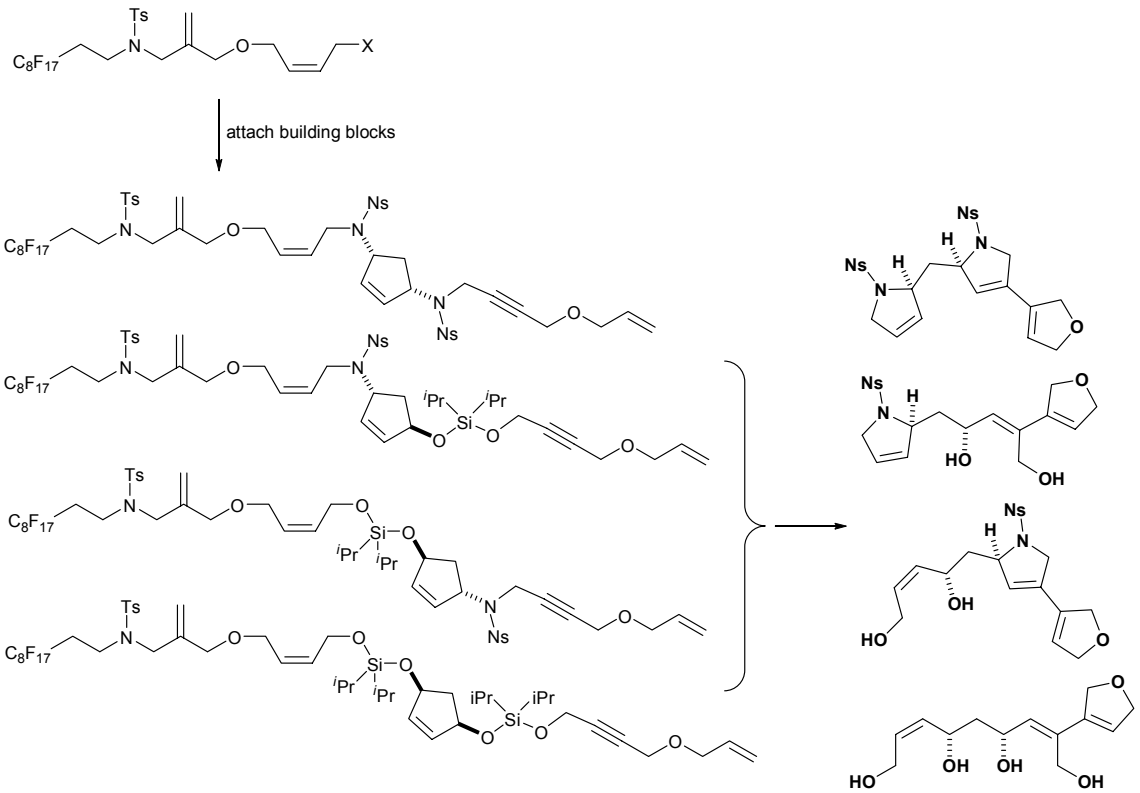

Scheme 1: Iterative attachment of building blocks to a fluorous-tagged linker yields alternative substrates for metathesis cascade reactions. The cascade reactions 'reprogramme' the molecular scaffolds to yield skeletally diverse final compounds. The scaffold of each final compound is determined by the nature of the attachment reactions, and the order of the building blocks.

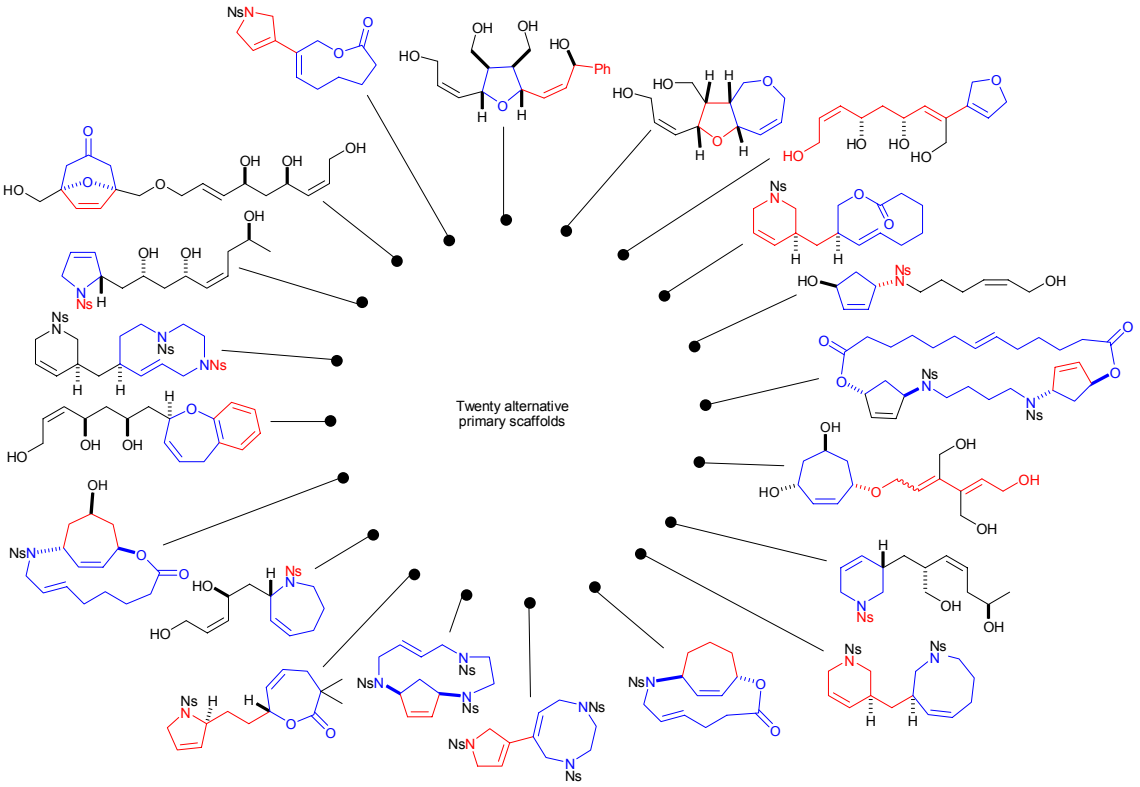

Scheme 2: Representative examples of final compounds prepared using our diversity-oriented synthetic approach. The approach has yielded compounds with over one hundred distinct skeltons in which twenty primary scaffolds are represented. Here, the primary (blue) and secondary (red) scaffolds are highlighted.

Summary
A diversity-oriented synthetic approach has been developed which yields skeletally diverse natural product-like compounds. Final compounds with over one hundred distinct scaffolds have been prepared. A wide range of future developments are envisaged: the extension of the approach to macrocyclic natural product-like compounds; the development of an automated approach to diversity-oriented synthesis; and the application of the approach to fragment-based ligand discovery.

Acknowledgements
ASN holds an EPSRC Advanced Research Fellowship (2004-2009). We thank EPSRC, BBSRC, the Wellcome Trust and GSK for funding.

Publications

M. P. Storm, H. K. Bone, C. G. Beck, P.-Y. Bourillot, V. Schreiber, T. Damiano, A. Nelson, P. Savatier and M. J. Welham, "Regulation of Nanog expression by phosphoinositide 3-kinase-dependent signalling in murine embryonic stem cells", *J. Biol. Chem.* 2007, **282**, 6265-6273.

A. Ironmonger, B. Whittaker, A. J. Baron, B. Clique, C. J. Adams, A. E. Ashcroft, P. G. Stockley and A. Nelson, "Scanning conformational space with a library of stereo- and regiochemically diverse aminoglycoside derivatives: The discovery of new ligands for RNA hairpin sequences", *Org. Biomol. Chem.* 2007, **5**, 1081-1086.

R. Hodgson, A. Kennedy, A. Nelson and A. Perry, "Synthesis of 3-sulfonyloxypyridines: Oxidative ring expansion of α-furylsulfonamides and *N→O* sulfonyl transfer", *Synlett* 2007, 1043-1046.

K. Dodd, D. Morton, S. Worden, R. Narquizian and A. Nelson, "Desymmetrisation of a Centrosymmetric Molecule by Carbon–Carbon Bond Formation: Asymmetric Aldol Reactions of a Centrosymmetric Dialdehyde", *Chem. Eur. J.* 2007, **13**, 5857-5861.

C. Cordier, S. Leach and A. Nelson, "1,3-Dioxetanes and 1,3-Dioxolanes", ed. S. Warriner, in *Science of Synthesis*, vol. 29, Stuttgart Thieme, (2007), 407-486.

T. Damiano, D. Morton and A. Nelson, "Photochemical transformations of pyridinium salts: mechanistic studies and applications in synthesis", *Org. Biomol. Chem.* 2007, **5**, 2735-2752.

A. Bolt, A. Berry and A. Nelson, "Directed evolution of aldolases for exploitation in synthetic organic chemistry", *Arch. Biochem. Biophys*. 2008, in press.

S. G. Leach, C. J. Cordier, D. Morton, G. J. McKiernan, S. Warriner and A. Nelson, "A fluorous-tagged linker from which small molecules are released by ring-closing metathesis", *J. Org. Chem.* 2008, 73, in press

Protein folding landscapes from computer simulations

Lucy Allen, Zu ThurYew and Emanuele Paci

Protein folding is a crucial reaction in biology (because most proteins function only in their folded conformation) but elusive and difficult to characterize experimentally. In theory, with a perfectly accurate model and infinite computation time, molecular dynamics simulations could solve the problem completely by allowing each stage of the folding process to be followed at an atomic level of detail. However, such models do not yet exist, and available computation power is limited. These problems can be addressed in several different ways, for example by the development of new sampling methods and more accurate models, or by the use of simpler, computationally more efficient models. Alternatively, useful information may be obtained using experimental data as restraints in simulations. The availability of high spatial and temporal resolution experimental data is providing better defined questions which simulation may help to answer and information which is in turn valuable to improve theoretical models and make them fully predictive.

Sampling is perhaps the most constraining issue in protein folding simulation: the most accurate models are computationally expensive and simulations cannot be run for enough time for folding to occur *ab initio*. One way of overcoming this is to use simple models; these may be less accurate but can sample at equilibrium and in many cases show features which are characteristic of real proteins. A good example is that of the immunity proteins Im7 and Im9. These small, four-helical proteins have the same fold and are 60% identical in sequence, however they fold by different kinetic mechanisms; Im9 two-state and Im7 three-state. Structure-based models, which are designed so that the native state is the global energy minimum, reproduce this difference in behaviour, showing that small differences in the energy function can have a large effect on the folding mechanism.

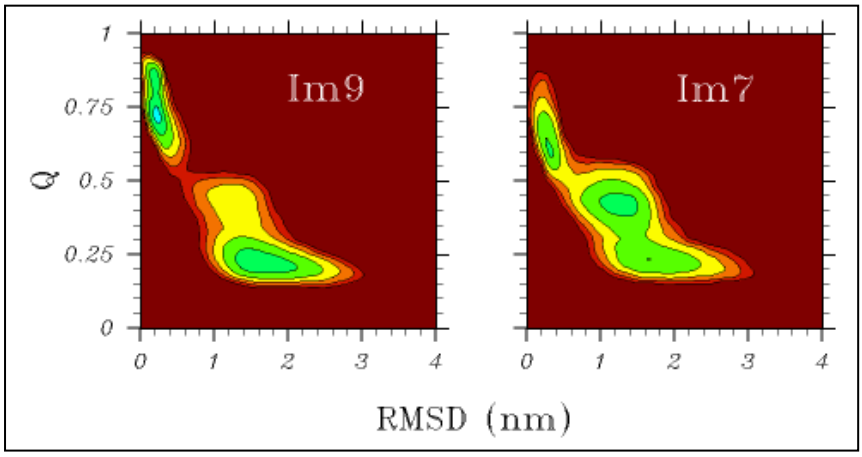

Another way of overcoming sampling problems is to use experimental values as restraints in simulation. This method has been used to look at the transition state ensembles of the Im proteins; sets of experimental φ-values were used to constrain the simulations to regions of conformation space where they were satisfied. Significant differences were found between the two proteins: the Im9 ensemble was much more heterogeneous than the Im7 ensemble. This result indicates that, in this case, the role of the intermediate is to channel flux towards the native state. The restraints method is useful for calculating and visualizing structures compatible with experimental data, or at least a structural interpretation of the data, but should be used with caution: it assumes a large number of approximations. In fact we have shown that, in the case of transition state ensembles, the calculated structures resemble, but are not the same as, true transition states.

The development of new sampling techniques such as replica-exchange MD means that even detailed protein models can now be simulated for hundreds of microseconds; this should allow fast folding events to occur. The FBP 28 WW domain has a very fast folding time, of the order of 10 μs, which makes it a good system for an attempt to fold a protein *in silico*.

Using models with various degrees of coarse graining, atomistic with explicit treatment of the solvent, coarse-grained or structure based we used conventional and replica exchange MD to explore the native and denatured states. We found that, whilst all the force-fields represented certain regions of the energy landscape accurately, they also all had weaknesses. This indicates that running simulations with a single force-field may provide misleading results; a multi-method approach and comparison with experimental data is preferable. New experimental techniques which give more detailed information on the different states in folding pathways will undoubtedly be valuable in the development of more accurate force-fields.

Using a model protein, filamin, we have also begun to investigate the relationship between the energy landscapes of proteins in the absence and presence of an applied force. It is commonly assumed that properties of the protein (e.g. kinetic mechanism and nature of the states) in the presence of mechanical load - even under non-equilibrium conditions - are representative of the energy landscape of the protein in the absence of the applied force. However, given that the force specifically stabilizes transitions that elongate the protein along the force vector, it is not clear if this assumption is generally valid.

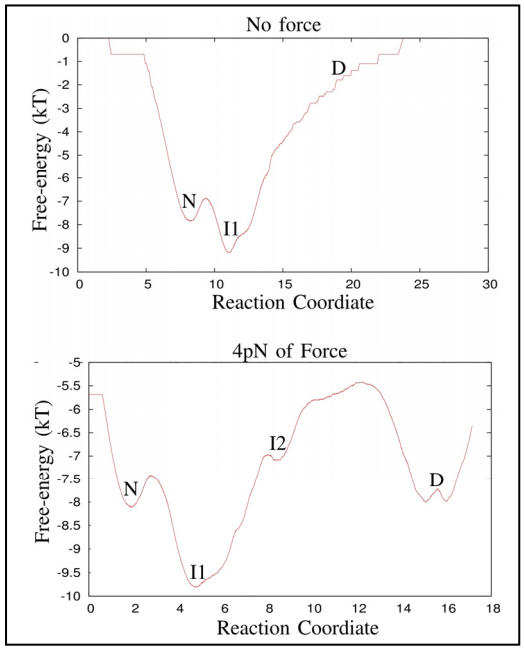

On the 1D free-energy landscapes of filamin at zero and 4pN applied force (left) N and D denote the native and denatured states respectively while I1 and I2 denote two distinct intermediate states**.** With a simple Cα model, we have been able to simulate the dynamics of filamin at equilibrium. In addition, using a sophisticated method, we are also able to project the energy landscape of the protein onto a 1D reaction coordinate that reproduces the kinetics of the system. Our simulations indicate that in the absence of a force, the kinetic mechanism of filamin is likely to be 2-state while in the presence of a force; it is at least 3-state. Furthermore, we also found that the various equilibrium intermediates are not only different at different forces, but are also distinct from the major unfolding intermediate encountered when we mechanically unfolded the protein under non-equilibrium conditions. Therefore, our results imply that care should be taken when trying to relate properties of a protein under force to those in the absence of force.

Publications

Allen L and Paci E., Transition state for protein folding using molecular dynamics and experimental restraints, *J. of Phys. Cond. Matt.,* 2007, 19,285221

Morton V, Friel C, Allen L, Paci E, Radford, SE, Increasing the stability of an intermediate influences the subsequent transition state ensemble in the folding of the bacterial immunity protein Im9, *J. Mol. Biol.* 2007, 371, 554-568

Funding

This work was funded by the EPSRC, INTAS, and the Wellcome Trust. We acknowledge useful discussions with Sheena Radford, David Brockwell, Tom McLeish and Peter Olmsted.

Chaperone-assisted pilus assembly revealed in atomic detail by molecular dynamics

Emanuele Paci, Rebecca J. Rose, Sheena E. Radford and Alison E. Ashcroft

Adhesive multi-subunit fibres are assembled on the surface of many pathogenic bacteria *via* the chaperone-usher pathway. In the periplasm, a chaperone donates a β-strand to a pilus subunit to complement its incomplete immunoglobulin-like fold. At the outer membrane, this is replaced with a β-strand formed from the N-terminal extension (Nte) of an incoming pilus subunit by a donor-strand exchange (DSE) mechanism.

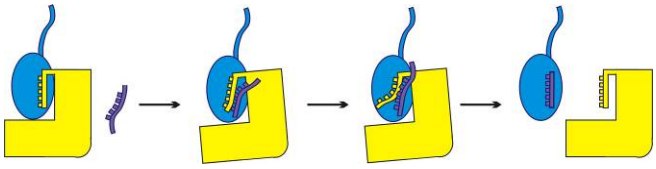

Schematic representation of the DSE mechanism. Simulations show that the first step on the left is triggered by spontaneous fluctuations on one residue in and out of it binding pocket.

This reaction has been shown to proceed *via* a concerted mechanism, in which the Nte interacts with the chaperone:subunit complex before the chaperone has been displaced, forming a ternary intermediate (see in this report Rose *et al.*, Subunit specificity in P pilus assembly studied by mass spectrometry). Thereafter, the pilus and chaperone β-strands have been postulated to undergo a strand swap by a 'zip-in-zip-out' mechanism, whereby the chaperone strand zips out, residue by residue, as the Nte simultaneously zips in**.**

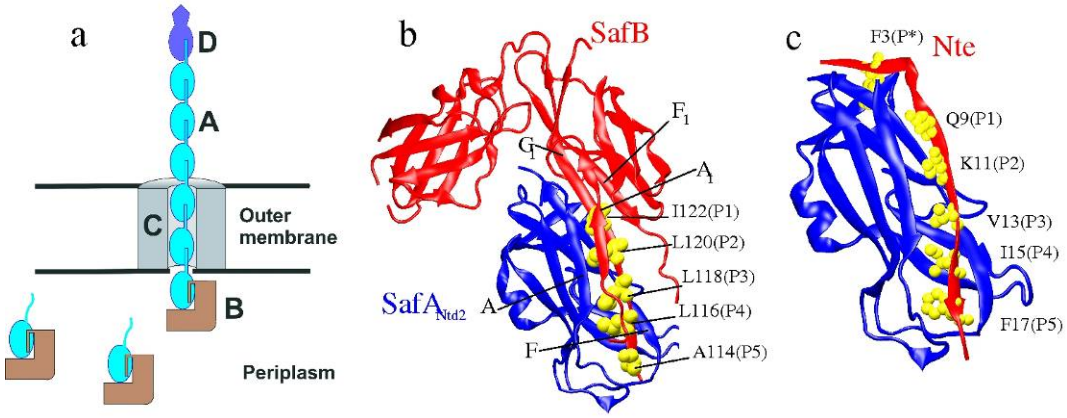

a) Saf pilus biogenesis at outer membrane. Chaperone:subunit complexes in periplasm are targeted to the usher assembly platform at the outer membrane. Subunits polymerise by donation of their Nte to an adjacent subunit at the usher pore, which extrudes the growing pilus. For the Saf pili that are the focus of this manuscript, the major pilus subunit SafA is shown in blue; the chaperone, SafB, in brown; the usher, SafC, in grey; and distal adhesin, SafD, in purple b) Crystal structure of $SafA_{Ntd2}$ (blue) in complex with SafB (red) Indicated are the A_1, F_1 and G_1 β-strands of SafB while the F_1-G_1 loop is not resolved. Also shown are the highly conserved hydrophobic residues P1-P5 of the chaperone that insert into the hydrophobic binding pockets of $SafA_{Ntd2}$. c) Crystal structure of $SafA_{Ntd2}$ (blue) in complex with the Nte peptide (red) (2CO4). The highly conserved hydrophobic residues P1-P5 of the Nte are shown, as is the P* binding residue.

Molecular dynamics simulations allow the direct investigation of the zip-in-zip-out hypothesis at an atomic level. Simulations been used to probe the DSE mechanism during formation of the *Salmonella enterica* Saf pilus and the uropathogenic *E. coli* P pilus. The simulations provide an explanation of how the incoming Nte is able to dock and initiate DSE due to inherent dynamic fluctuations within the chaperone:subunit complex. The chaperone donor-strand unbinds from the pilus subunit residue by residue, in direct support of the zip-in-zip-out hypothesis. Simulations showed that the unbinding of the subunit from the

chaperone is initiated by spontaneous fluctuations of a specific amino acid (see figure below) in and out of its binding pocket, thereby enabling entry of the incoming subunit that triggers DSE. This phenomenon is illustrated below for the Saf pilus which only involves one type of subunit. For the P pilus, which also undergoes assembly by a DSE mechanism but is formed of six different subunit types assembled in a specific order, MS shows that dynamics at the key site is also important. Very interestingly in this case the different affinities between subunits revealed by mass spectrometry (see in this report Rose *et al*., Subunit specificity in P pilus assembly studied by mass spectrometry) can be related to different dynamics at the key site. Such fluctuations make the DSE reaction possible despite the fact that the chaperone binds the subunit very strongly. On the other hand, the binding of the two subunits is essentially irreversible; this is due to additional strong interactions which are not present in the chaperone:subunit pair. The unbinding of two subunits (or of a subunit:Nte peptide complex) can be studied by simulation by adding an external force. Such simulations in the saf:Nte complex show that an additional binding pocket, named P* seen in the crystal structure of the subunit:Nte complex, effectively caps the reaction and plays an important role in preventing the reaction to regress (i.e., the pilus to dissociate).

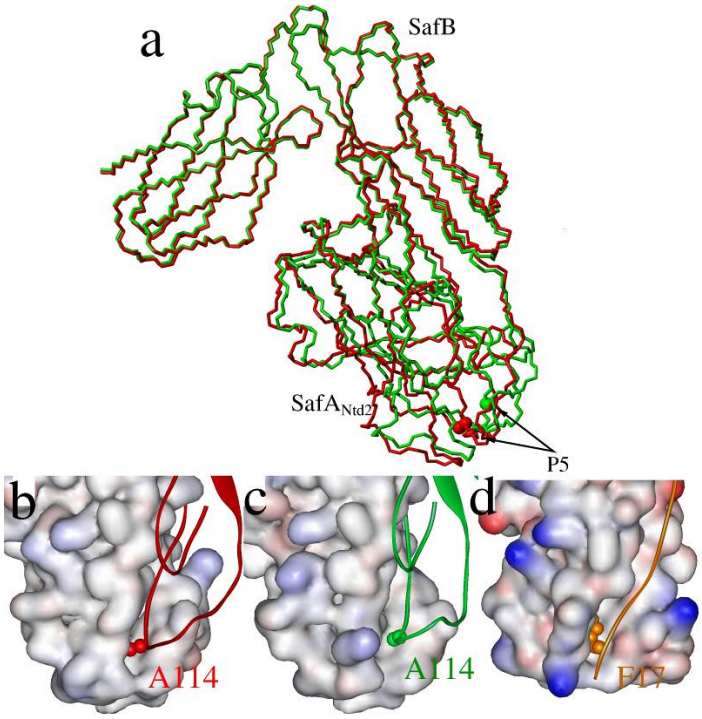

Superposition of the SafB:SafA$_{Ntd2}$ complex in the two different states. The conformation of the complex in which A114 (indicated as P5) is closest to SafA$_{Ntd2}$ strand A is shown in red. The conformation in which A114 is closest to SafA$_{Ntd2}$ strand F is shown in green. A114 moves 2.6Å between the two structures. (b,c,d) Enlargement around the P5 pocket where SafA$_{Ntd2}$ is represented as solvent accessible surface: SafA$_{Ntd2}$ in complex with (b) SafB (red) in the conformation in which A114 is close to SafA$_{Ntd2}$ A strand, (c) SafB (green) in the conformation in which A114 is closest to SafA$_{Ntd2}$ F strand, and (d) the Nte peptide. A114 and F17 are shown in ball and stick representation.

Publications

Rose, R. J., Welsh, T., Waksman, G., Ashcroft, A.E., Radford, S. E. and Paci, E. (2008) Donor-strand exchange in chaperone-assisted pilus assembly revealed in atomic detail by molecular dynamics. *J. Mol. Biol.*, **375,** 908-919.

Funding

This work was funded by the BBSRC, the Wellcome Trust, and Waters Corp. We acknowledge useful discussions with Gabriel Waksman and his group at the Institute of Structural Molecular Biology & School of Crystallography, Birkbeck College, London.

Exploring the effect of mechanical forces on biopolymers through theory, models and novel experimental techniques

Igor Neelov, Simon Connell, Zu-Thur Yew, Bhavin Khatri, Neal Crampton, Sheena Radford, David Brockwell, Peter Olmsted, Emanuele Paci and Tom McLeish

In the past 10 years mechanical experiments on single proteins has not only revealed how proteins unfold when extended, but has also addressed key questions on the initial stages of protein folding. Within the Astbury Centre, mechanical unfolding and mechanical properties of biopolymers in general have been extensively studied using innovative experimental and theoretical approaches.

On the experimental side we have developed a technique where, in addition to the force that is applied to the protein by retracting the AFM cantilever, a small periodical perturbation force is added. We have also perfected our novel low noise AFM force spectroscopy apparatus, with damping of thermal noise on a very soft AFM cantilever down to an effective temperature of 3 Kelvin (in a 300 K buffer solution). Recent results using the system in a force-clamp mode have shown a second unfolding event in the mechanical unfolding of protein L for the first time.

A theoretical framework based on viscoelastic models with internal friction and two- and three-state models has been developed to interpret the fluctuations of the distance between the two ends of a tethered protein. This provides the elasticity, relaxation times and internal frictions and has been tested on polysaccharides (cellulose, dextran, pectin). We are currently using this approach to investigate peptides and proteins. Computer simulation on increasingly complex systems was used to test the theory: starting from a freely jointed chain, we then simulated polysaccharides (dextran and pectin) and we have recently simulated short peptides of different structure (α-helical, β-hairpin and a flexible structureless peptide). Even in these more complicated cases where the free energy landscape has multiple minima, the spectrum of the fluctuations can be interpreted in terms of the simple models mentioned above. These simulations provide a proof of principle of the possibility of extracting more information from single molecule mechanical experiments than the force of unfolding and distance to the transition state (xu) obtainable using force velocity and force clamp experiments.

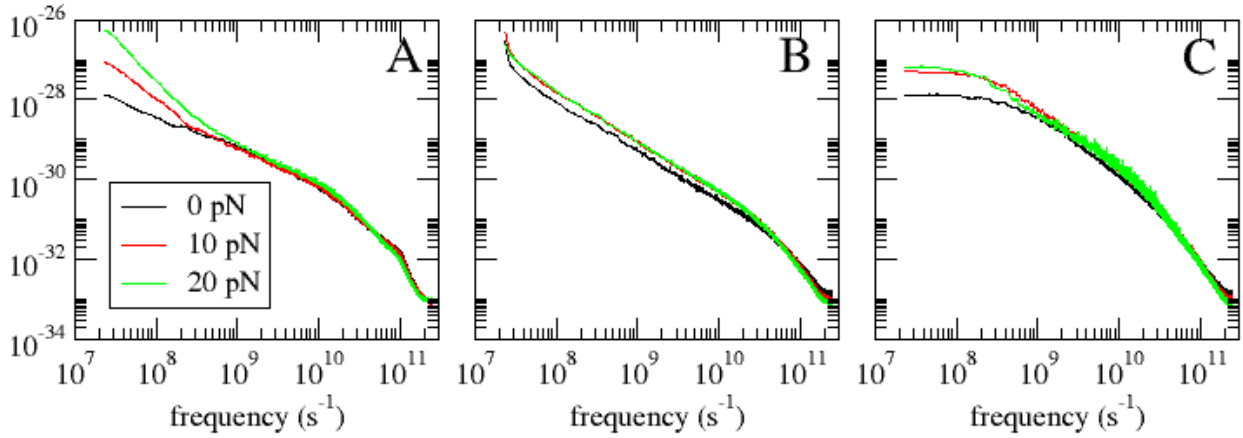

Power Spectral Density (PSD) of the fluctuations of end-to-end distance for three peptides with different secondary structural propensity: A) α-helical (Ala12), B) β-hairpin and C)3- flexible (Gly10) peptides. The PSD is the Fourier transform of the time correlation function of the end-to-end distance of peptide and thus defines some characteristic time τ (or times τ_i) for system. This function can be measured by single molecule AFM and is related to the energy dissipation spectral density $D(\omega)= \zeta\, \omega PSD(\omega)$ at given frequency ω (where ζ is the friction). In the case of a simple dynamical process with characteristic time τ (or friction coefficient ζ) and elasticity coefficient K it has a plateau at low frequencies and linear decay at higher ones in log-log scale. If

there are more processes each of these corresponds to a plateau and a linear decay in log-log scale. The frequency at which PSD decreases to half of its plateau value is equal to reciprocal characteristic time τ of process. The plateau value of PSD is a function of both elasticity coefficient K and characteristic time τ. Such fitting at different forces F applied to the end of peptide in single molecule AFM have been used to obtain the dependence of $K(F)$ and $\tau(F)$ on force. Thus PSD(ω) provides a dynamical fingerprint of the peptides.

Force clamp and constant velocity experiments have traditionally used a Bell-type model to exctract thermodynamic information about the unfolding (or unbinding) properties of a protein (see Using force to investigate the stability of proteins and their complexes Eleanore Hann, Jim Pullen, David Sadler, Sheena Radford and David Brockwell in these reports). Improved methods to treat the experimental data still have the drawback of involving the projection of the free-energy landscape on a single variable. We have recently analysed the distribution of unfolding times while a constant force is applied to a protein, which are measurable with force-clamp technology. This provides the model-free estimation of parameters which characterise the free energy landscape and the dynamics, but it still assumes a projection onto a one-dimensional variable. Ongoing work to improve this theory includes devising and modelling simple potentials for unfolding, which can be generalized systematically by adding more degrees of freedom. This will provide additional physical mechanisms that can contribute to the effective 1D parameters, and provide guidance for new experiments to probe the directional dependence of mechanical resistance, as well as how the control of noise can, perhaps unexpectedly, be a valuable probe of the shape of the energy landscape.

Publications

Khatri, B. S., and T. C. B. McLeish. 2007. Rouse model with internal friction: A coarse grained framework for single biopolymer dynamics. *Macromolecules* **40**, 6770-6777.

Khatri, B. S., K. Byrne, M. Kawakami, D. J. Brockwell, D. A. Smith, S. E. Radford, and T. C. B. McLeish. 2008. Internal Friction of Polypeptide Chains at High Stretch. *Faraday Discuss*. **139**, 1–18.

Neelov, I., D. Adolf, and T. McLeish. 2007. Molecular dynamics of pectin extension. *Macromolecular Symposia* **252**, 140-148.

Best, R. B., E. Paci, G. Hummer, and O. Dudko. 2008. Pulling direction as a reaction coordinate for the mechanical unfolding of single molecules. *J. Phys. Chem. B* In press.

Funding

This work was funded by the EPSRC, INTAS, and the Wellcome Trust.

Photo-induced cross-linking studies of amyloid

David P. Smith, Jon Anderson, Jeffrey Plante, Alison E. Ashcroft, Sheena E. Radford, Andrew J. Wilson and Martin J. Parker

Introduction

Amyloid formation is associated with a number of severe diseases, including Alzheimer's, Parkinson's and the prion diseases. Despite over a decade of intense research we still have little understanding of what amyloid is, what it looks like, and how its formation leads to disease. Recent studies suggest that toxicity is largely associated not with the mature amyloid fibrils themselves, but with small soluble oligomers. These non-covalent assemblies are highly dynamic, meta-stable and heterogeneous, making it very difficult to isolate individual forms and carry out detailed structural and biochemical analyses. Such studies are vital for rationalising their toxic properties and for therapeutic strategies which target them.

Introducing photo-induced cross-linking (PIC) groups site specifically into proteins provides a means of trapping transient protein-protein interactions, enabling 'snapshots' of assembly reactions to be taken and otherwise meta-stable intermediates to be isolated for further studies. Analysis of the cross-links formed, moreover, generates valuable structural information in the form of spatial restraints. To serve as an effective probe the PIC group must be non-invasive, non-toxic and photolyse relatively quickly at non-damaging wavelengths to generate a highly reactive intermediate, enabling irreversible cross-linking with stable groups. The products formed must also be stable enough to enable isolation, purification and analysis. Trifluoromethyldiazirine (tfmd) (Fig. 1(a)) satisfies these criteria, photolysing rapidly at 350 nm to generate a singlet carbene, which is highly reactive, even towards relatively stable aliphatic CH bonds.

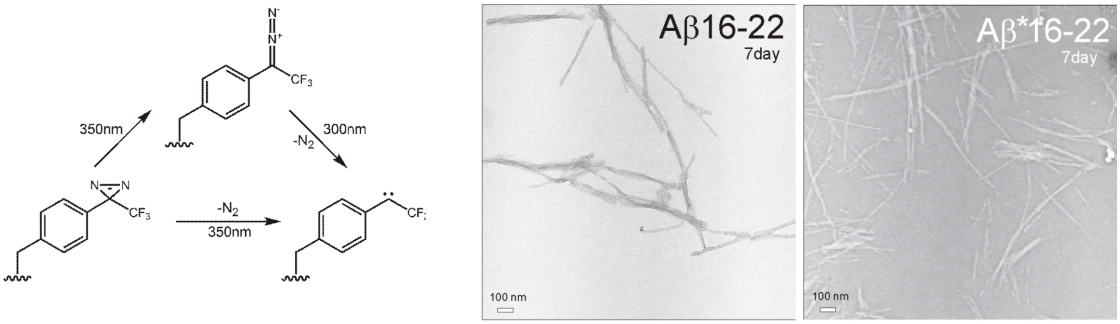

Figure 1. (a) (LHS) Photo-chemistry of tfmd-phe. (b) (RHS) Negative stain electron microscopy images of amyloid fibrils formed by Aβ16-22 and Aβ*16-22.

Results

We synthesized pure tfmd-phenylalanine (tfmd-phe; Fig. 1(a)) to high yield. To test its capacity to probe inter-molecular interactions in amyloid we incorporated tfmd-phe at the fourth position in a seven-residue fragment of the Alzheimer's peptide (Aβ) using standard Fmoc-based chemistry (Aβ*16-22; N-acetyl-KLV[tfmd-F]FAE-NH_2). Residues 16-22 constitute the central hydrophobic cluster of Aβ and are critical for amyloid formation. The synthetic unmodified peptide (Aβ16-22; N-acetyl-KLVFFAE-NH_2) itself forms cross-β amyloid fibrils, with an anti-parallel organisation of β-strands aligned perpendicular to the fibril axis. We grew fibrils for Aβ16-22 and Aβ*16-22 under identical conditions. Both formed apparently identical fibrils on the same timescale (~1 wk), as assessed by negative stain electron microscopy (Fig. 1(b)). These results demonstrate that the introduction of tfmd does not perturb amyloid formation significantly. Given the high degrees of structural order observed in cross-β amyloid fibrils, this is a very encouraging result.

The Aβ*16-22 fibrils were irradiated with light of ~350 nm. The insoluble cross-linked fibrils were then pelleted, fully dissociated and analysed using a cutting-edge mass spectrometry method: electrospray ionisation ion mobility spectrometry mass spectrometry (ESI-IMS-MS). The resulting spectrum is shown in Figure 2(a). The peaks observed are consistent with the formation of monomers and dimers only.

To locate the position of the inter-peptide cross-link the two dimers (species B & C, Fig. 2(a)) were separated by IMS and fragmented via collision induced dissociation (ESI-IMS-MS/MS). The resulting m/z spectra of peptide fragments (not shown) demonstrate conclusively that the inter-peptide cross-links in both occur exclusively between the two (tfmd)-phe side chains, indicating that these are in close contact in the fibril.

Conclusions

Tfmd-phe residue pairs in an in-register anti-parallel β-sheet occur at two distinct sites: one with two backbone H-bonds ($\beta_{A,HB}$), and one with no H-bonds ($\beta_{A,NHB}$) (Fig. 4). Analyses of χ_1-χ_1 distributions show that most aromatic-aromatic pairs at $\beta_{A,HB}$ sites adopt g^-t or g^-g^+ conformations, where the face or edge of one aromatic ring interacts with the C_β atom of its partner. Most aromatic-aromatic pairs at $\beta_{A,NHB}$ sites, by contrast, adopt tg^+ conformations, where archetypical off-set stacking of the aromatic rings is achieved (Fig. 2(b)). Our findings are consistent with the latter case, where inter-peptide cross-links would be expected to form exclusively between pairs of tfmd-phe residues at $\beta_{A,NHB}$ sites. The former case would be expected to give rise to larger species (trimers, tetramers, etc) via cross-strand and cross-sheet cross-links (i.e., the t conformation at the $\beta_{A,HB}$ site in Fig. 2(b) points tfmd towards groups in the adjacent sheet).

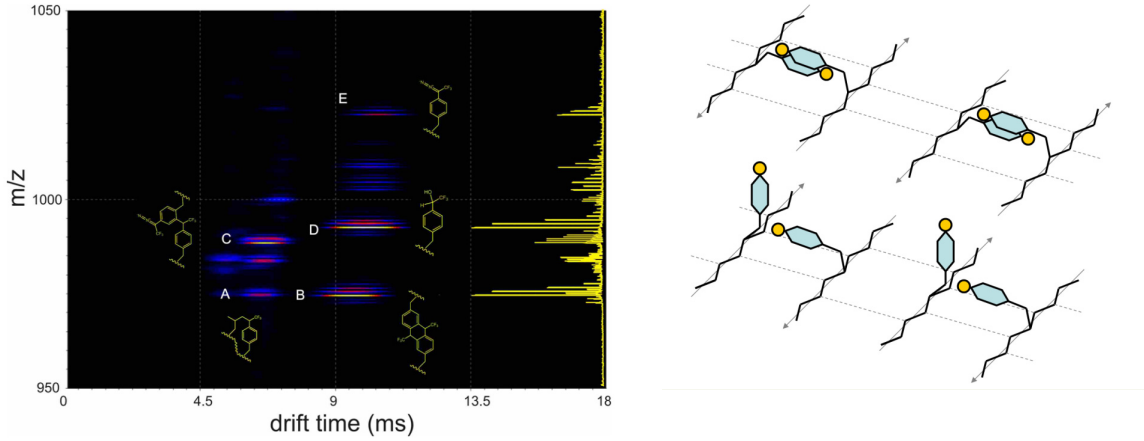

Figure 2. (a) (LHS) ESI-IMS-MS spectrum of cross-linked Aβ*16-22 fibrils: **A**, monomer resulting from intra-peptide cross-link; **B**, dimer resulting from two inter-peptide cross-links; **C**, dimer resulting from one inter-peptide cross-link; **D**, monomer (water adduct); **E**, monomer, where tfmd-phe has isomerised to unreactive diazo (see Fig. 1(a)). Hypothetical cross-links are shown. Wiggly lines represent peptide backbones. (b) (RHS) Tfmd-phe residue pair conformations: top, tg^+ at $\beta_{A,NHB}$ sites; bottom, g^-t at $\beta_{A,HB}$ sites. H-bonds (dashed lines) are parallel to fibril axis.

In summary, we have demonstrated that tfmd is a suitable non-invasive probe for site-specific PIC studies of amyloid, and shown how combining this technique with the separating and analytical power of MS can provide valuable insights on the structural organisation in these assemblies. This bodes well for potential PIC studies of transient pre-fibrillar oligomers, which will require, among other things, the development of suitable optics to maximize cross-linking yield and time resolution.

Funding

We thank the BBSRC and University of Leeds for financial support.

Developing new single crystal spectrophotometers for structural biology

Kasia M. Tych, John E. Cunningham, Giles Davies,
Edmund Linfield and Arwen R. Pearson

Introduction

To fully understand biological processes a knowledge of the structure of the macromolecules involved is vital. The most common method of structure determination is X-ray crystallography, and the many protein and DNA structures already determined have provided incredible insights into the molecular underpinnings of life. However, most X-ray crystal structures are static average snapshots of a molecule and only yield information about a single state of a complex reaction.

In order to address this we, and other groups, have combined single crystal spectroscopy and X-ray crystallography, taking advantage of the many enzymes which retain their catalytic activity when crystalline. These studies have focused on proteins whose chemistry can be easily followed, since they contain functional groups that change colour during the chemical reaction, making the process of catalysis easy to observe by UV/Vis single crystal spectroscopy. Intermediates observed spectroscopically can then be trapped by flash freezing at 100K for structure determination.

On-line and off-line UV/Vis/Raman multimode spectrophotometers

Unfortunately, only a small subset of proteins involved in disease have functional groups amenable to UV/Vis single crystal spectroscopy, thus alternate ways of tracking changes in the protein are required. One possibility being explored is the use of Raman single crystal spectroscopy; this has the advantage that it does not require any coloured functional groups and so opens the door to study of a much wider range of proteins. Recent work by other groups has shown that single crystal Raman spectroscopy is feasible and have reported its use to study a variety of proteins and biochemical processess, including ligand binding, catalysis and confirmational change.

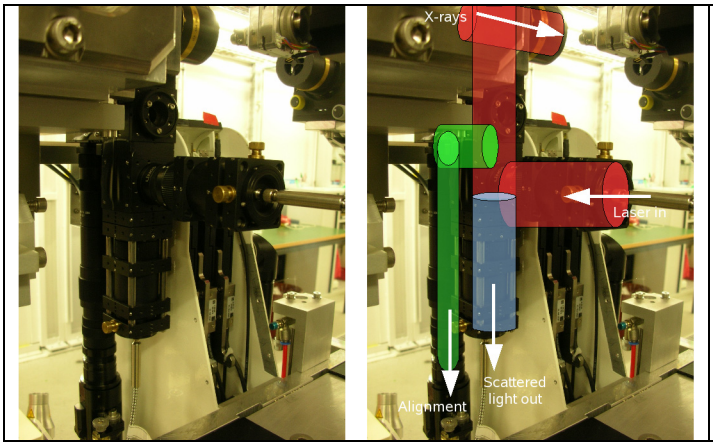

Figure 1: Left: The SLS multimode spectrophotometer mounted at beamline X10SA. Right: Schematic showing the light flow through the system for Raman spectroscopy during X-ray data collection.

A multi-mode spectrometer capable of both UV/Vis and Raman single crystal spectroscopy is currently in an advanced stage of construction/design at the Swiss Light Source (SLS, Paul Scherrer Institut, Villigen, Switzerland) (Figure 1). The instrument is unique in its use of an on-axis geometry that allows accurate and unambiguous intersection of both probing visible light (focal spot size <10um diameter) and the X-ray beam (focal spot size 50x15um to 150x150um). A motorised illumination optic is available for UV/Vis studies. As well as avoiding the crowding issues associated with other synchrotron based single crystal spectroscopy systems, this design allows permanent installation of the spectrometer at the beamline, avoiding the long setup times associated with existing designs.

In parallel with this, a portable UV/Vis Raman multimode spectrophotometer is under construction in the Astbury Centre. This instrument builds on a commercially available chassis to yield a small, easily movable instrument for off-line and on-line measurements. Once commissioning and benchmarking is completed, the Swiss Light Source instrument will be available as a general user facility. The Leeds instrument will be an available resource for the UK structural biology community.

On-chip terahertz time-domain spectroscopy of single crystal proteins

The dynamics of proteins relevant to biology span a wide range of time-scales. As well as the extremely fast atomic bond vibrations that are probed by Raman and Infra-red spectroscopy, there are also much slower motions of entire protein domains that are associated with breathing and conformational change. We are exploring the use of terahertz time-domain spectroscopy (THz-TDS) to probe slower (pico-second to nano-second, of GHz to THz) functionally related protein dynamics.

Over the past decade, THz-TDS has become routine for the investigation of low-frequency inter-molecular vibrations in polycrystalline small organic molecular systems. By contrast, protein THz-TDS experimental studies to date have concentrated on proteins in full solution, where vibrational absorption modes associated with the motion of groups of atoms are not observed or on dried films, whose relevance to the state of proteins *in vivo* is dubious. Despite an expanding literature predicting the existence of normal modes in proteins in the terahertz frequency range THz-TDS has not yet been demonstrated to access specific protein vibrational modes.

We are using a combination of established and developmental terahertz systems to investigate the utility of THz-TDS to study protein dynamics in single crystals. A promising general approach, tailored to the study of small microscopic objects, has recently been developed at the University of Leeds; this approach, which uses on-chip terahertz waveguides, will be suitable for studying almost any size of protein crystal (from 30 μm^2 upwards). By lithographically defining such waveguides in an on-chip terahertz system (comprising terahertz emitter and detector), we have very recently verified that terahertz spectral absorption resonances can be recorded in crystalline materials over a sampling area of just a few tens of square microns (Fig. 2).

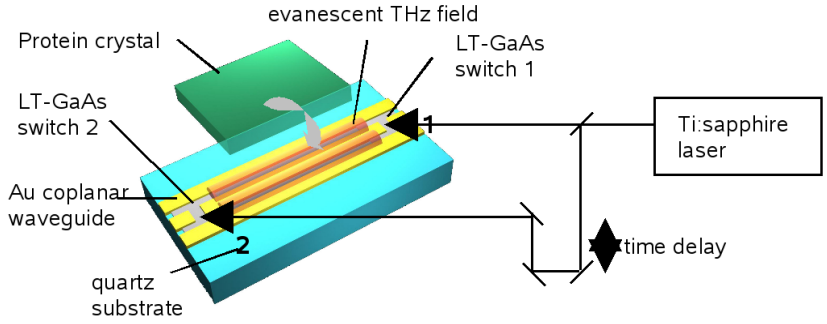

Figure 2: Schematic of the guided-wave evanescent-field THz technique to be developed for investigation of protein crystals.

Collaborators

The development of the SLS UV/Vis/Raman multimode instrument is being carried out in collaboration with Robin L. Owen and Clemens Schulze-Briese, SLS, PSI Villigen.

Funding

The development of the UV/Vis/Raman multimode instruments is supported by funding from the European Union and the Swiss Light Source. The on-chip THz spectroscopy project is supported by funding from the Leverhulme Trust.

The crystal structure of bacteriophage T7 endonuclease I resolving a Holliday Junction

Jonathan M. Hadden, Stephen B Carr and Simon E.V. Phillips

The rearrangement, or recombination, of DNA is an ancient and ubiquitous biological process. Recombination is central to many biological processes such as the generation of genetic variation (and therefore evolution) and the incorporation of viral DNA into host DNA, resulting in successful infection. The process of DNA recombination occurs in distinct stages (Figure 1), and the formation of a four-way (Holliday) junction is a central step in this process. For recombination to proceed, the Holliday junction must be cleaved to yield two linear duplexes. This is regulated by a junction resolving enzyme that cleaves the Holliday junction, resulting in rearranged DNA strands. Bacteriophage T7 encodes a protein, endonuclease I, which has been shown to act as a Holliday junction resolving enzyme.

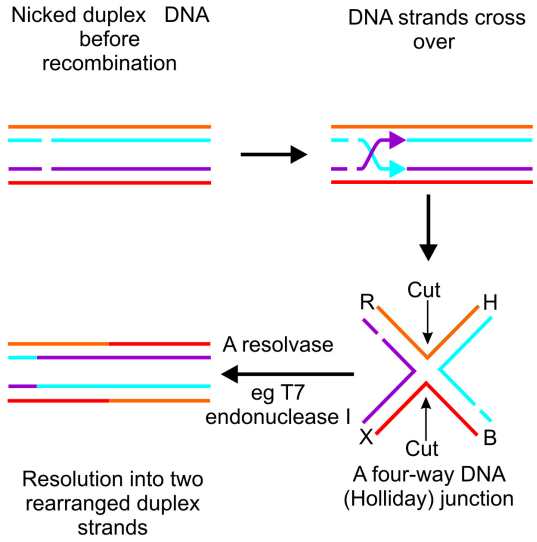

Figure 1: The process of recombination.

To understand the mechanism by which endonuclease I binds and cleaves Holliday junctions, we have solved the structure of a complex of endonuclease I and a synthetic four-way DNA junction using X-ray crystallography. In order to obtain high quality X-ray diffraction data we had to purify 17 different Holliday Junction complexes, setup 25,000 crystallisation trials and collect data from approximately 200 crystals using station ID23-2 at the European Synchrotron Radiation Facility (ESRF). Our best data extended to 3.1Å resolution and the structure of the complex was solved by molecular replacement using the structure of DNA-free endonuclease I as the search model.

The overall structure of the complex (Figure 2) is in excellent agreement with our earlier model. The pairs of DNA helical arms are essentially stacked on top of one another (R stacked on H and X stacked on B) to form two pseudo-continuous duplexes with an angle between them of -80°. This represents an alteration of ~ 130°, from the right-handed stacked X-structure of the free Holliday junction in solution (interaxial angle ~ +50°) and is consistent with studies of the structure of the Endonuclease I - Holliday Junction complex in solution. The observed conformation creates an almost continuous deep groove across the major groove face of the junction which forms the principal binding site for the protein.

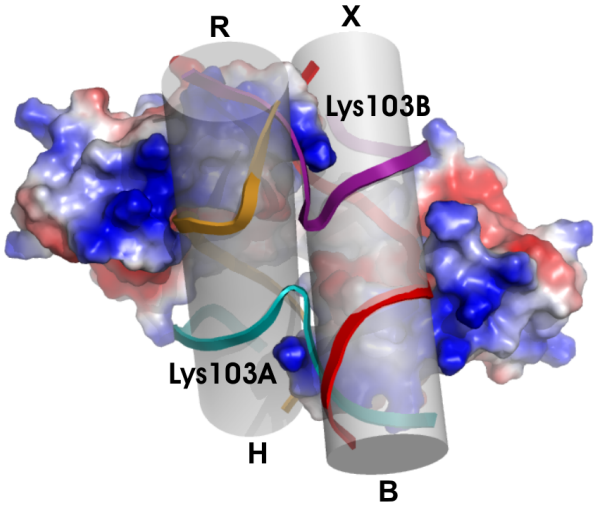

Figure 2: Overall structure of the Holliday Junction - Endonuclease I complex.

Significant induced fit occurs in the interaction, with changes in the structure of both the protein and the junction. The enzyme is a dimer of identical subunits and presents two equivalent binding channels that contact the backbones of the junction's helical arms over 7

nucleotides. These interactions effectively measure the relative orientations and positions of the arms of the junction, thereby ensuring that binding is selective for branched DNA that can achieve this geometry.

Endonuclease I binding results in significant distortion of the structure of the junction, both globally (discussed above) and locally. The DNA backbones of the exchanging strands make tight turns at the centre of the junction, in order to pass from one duplex to the other. The adjacent phosphate groups around these turns come within ~ 6 Å of one another and the positively charged side chain of Lys103 is inserted between these two groups (Figure 2) to reduce the electrostatic repulsion.

The structure of the complex of Endonuclease I bound to a Holliday junction shows how the geometry of this branched structure can be recognized, while at the same time being distorted by the enzyme. The recognition process exploits the dynamic character of the junction, allowing it to be 'moulded' onto the large binding surface of the protein.

Publications

Jonathan M. Hadden, Anne-Cécile Déclais, Stephen B. Carr, David M. J. Lilley and Simon E. V. Phillips. *Nature*, **449**, 621-624 (2007).

Collaborators

Anne-Cécile Déclais and David M. J. Lilley. CRC Nucleic Acid Structure Research Group, University of Dundee, UK.

Acknowledgements

This work was supported by funds from the Wellcome Trust, BBSRC and Cancer Research UK.

X-ray structures of two manganese superoxide dismutases from *Caenorhabditis elegans*

Chi H. Trinh, Emma E. Stewart and Simon E. V. Phillips

Introduction

The free-living nematode, *Caenorhabditis elegans* expresses five superoxide dismutases (SOD) that are necessary to protect cellular components against the detrimental effects of reactive oxygen species. Three of these SODs contain copper and zinc and protect cytosolic and extracellular components, while the other two contain manganese (MnSOD) and are targeted to the mitochondria.

In reactions that proceed near diffusion-controlled rates, SOD catalyzes the dismutation of superoxide anions (O_2^-) into hydrogen peroxide and oxygen. During catalysis, the manganese ion cycles between Mn^{2+} and Mn^{3+} oxidation states in a two-step process. The first step oxidises a substrate molecule to dioxygen, while the second reduces a substrate molecule to hydrogen peroxide (hence, a dismutation). The precise pathway of proton transfer is still under investigation.

Structures of the manganese superoxide dismutases

We have determined the crystal structure of the two MnSODs of C.*elegans* (MnSOD-2 and MnSOD-3) to a resolution of 1.7Å. X-ray diffraction data were collected on station I03 at the Diamond Light Source facility. As mitochondrial enzymes, we expressed them in *E.coli* without their N-terminal transit peptides, in which state they are each around 22 kDa and contain 197 or 194 amino acids (MnSOD-2 and MnSOD-3 respectively). No purification tags were used, though, like recombinant human MnSOD, the proteins retained N-terminal methionine residues.

The structures reveal that they are not only very closely related but typical of all mononuclear SODs, that also include iron-containing SOD (found in prokaryotes and plants) and show greatest homology to human MnSOD. Each subunit of the tetrameric SOD binds one atom of manganese in a site formed from four residues, between two domains. Two manganese-binding residues are derived from the N (α-helical) domain (His26 and His75) and another two from the C (α/β) domain (Asp156 and His160). A fifth ligand is also visible in the structure and is presumably a hydroxyl group derived from a solvent molecule. This puts the Mn(III) and its ligands into a roughly trigonal bipyramidal configuration. The Mn(III) imparts the protein and its crystals with a bright, pink colour. The dimer interface is important for SOD activity, one residue in particular, Glu159, makes a salt bridge to the metal ligand His160 of the other subunit, linking the two active sites together. The dimer interface also forms the substrate funnel with many solvent molecules revealed in the structure. The hydrogen bonding network formed in the second coordination shell as well as the substrate funnel, is now considered to help to fine tune the redox potential of the protein-bound metal. Substitution of the manganese for iron, for example, produces an inactive protein. Which residues may be responsible for this is now under active investigation.

Views of the structure of MnSOD-3 from *C. elegans* are shown on the next page with subunits coloured red, green, blue and orange and with manganese ions shown as pink spheres (Figure 1). Residues responsible for metal binding are shown in pink, while those from the second subunit of the dimer are shown in red. The presumed OH bound to the metal is a large red sphere and solvent is shown as red spheres (Figure 2).

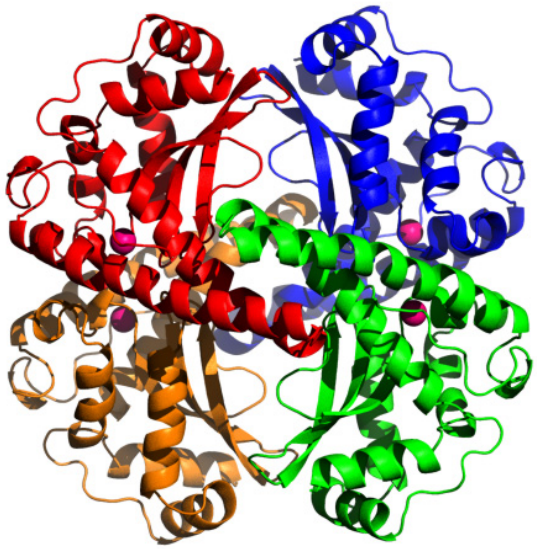

Figure 1. The tetrameric interface is formed from 2 4-helix bundles in the centre of this image.

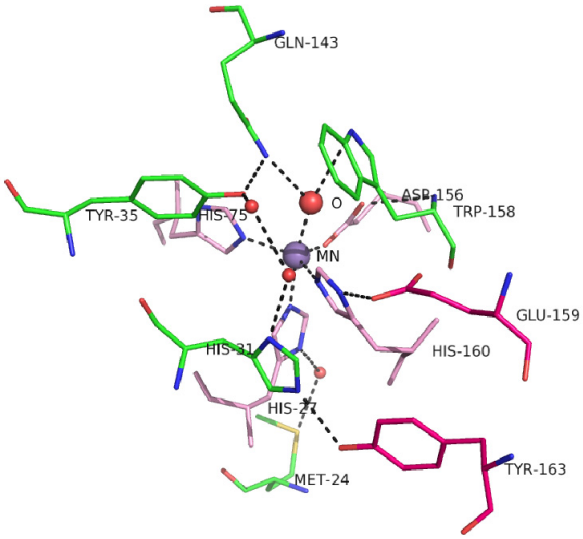

Figure 2. The hydrogen bonding network around the active site involves residues from an adjacent subunit of the dimer.

Collaborators

This work was carried out in collaboration with Dr Gary J. Hunter and Dr Therese Hunter from the University of Malta.

Funding

This work is partially funded by the University of Malta.

A systems approach for investigating bacterial signal sensing mechanisms: expression, purification and activities of the entire family of sensor kinases of *Enterococcus faecalis*

Pikyee Ma, Hayley M. Yuille, Victor Blessie, Nadine Göhring, Zsófia Iglói,
Peter J. F. Henderson and Mary K. Phillips-Jones

Two-component signal transduction systems are the main mechanism by which bacteria sense and respond to their environment, and their membrane-located histidine protein kinases generally constitute the sensory components of these systems. Relatively little is known about their fundamental mechanisms, three-dimensional structures and even the precise nature of the molecular signals sensed, because of the technical challenges of producing sufficient quantities of these hydrophobic membrane proteins. However, previous work by our group established that these challenges can be overcome and we were the first to demonstrate the successful heterologous overexpression and purification of any intact membrane sensor kinase. Using *in vitro* phosphorylation assays, we also demonstrated that the resulting purified protein was active and responsive to 'signals' that stimulated its phosphorylation signalling state. To determine how widely applicable such an approach might be, and to learn more about the roles of such kinases in processes such as virulence and antibiotic resistance, we evaluated the successes of expressing and purifying the full genome complement of membrane sensor kinases of *Enterococcus faecalis*, an important agent of hospital-acquired infection in the UK.

Following the systematic cloning of the genes for each of the sixteen intact proteins into the membrane protein expression vector pTTQ18His, all but one sensor was expressed successfully in *E. coli* inner membranes (Fig. 1). In a screen involving twenty-three detergents, fourteen intact proteins were successfully solubilised. Purification of the hexa-histidine 'tagged' recombinant proteins was achieved for thirteen of the intact kinases, and all but one of these were successfully verified as intact by electrospray ionisation mass spectrometry and/or *N*-terminal sequencing and Western blotting. Thirteen intact kinases possessed autophosphorylation activity in the absence of added signal when assayed in membrane vesicles or as purified proteins. Signal testing using one of the functionally-characterised kinases of this bacterium, VicK, with twelve candidate signals successfully identified glutathione and possibly redox potential as direct modulators of VicK activity *in vitro*, examplifying the potential use of *in vitro* activity assays using intact proteins for routine or systematic signal identification (Fig. 2). By using VicK with its purified downstream partner response regulator VicR, the impact of DTT on VicK phosphorylation resulted in increased levels of VicR-P, thereby confirming the

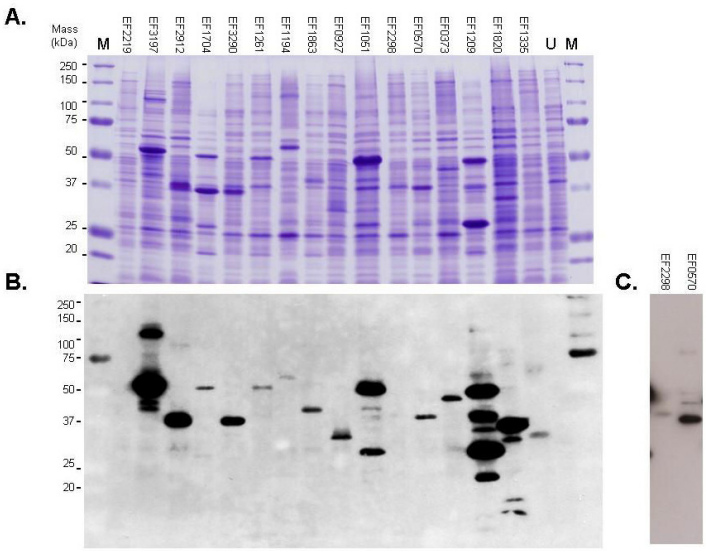

Figure 1. Expression of the sixteen intact membrane sensor kinases of *E. faecalis* in *E. coli* BL21 (DE3). (A) SDS-PAGE of *E.coli* mixed membranes using Coomassie blue staining (upper panel); (B) and (C), Western blotting to detect the engineered hexa-histidine tag at the C-terminus of each protein using an INDIA^{TM} His probe.

potential of this *in vitro* approach for future studies to investigate modulator effects on the entire signal transduction process of two-component systems.

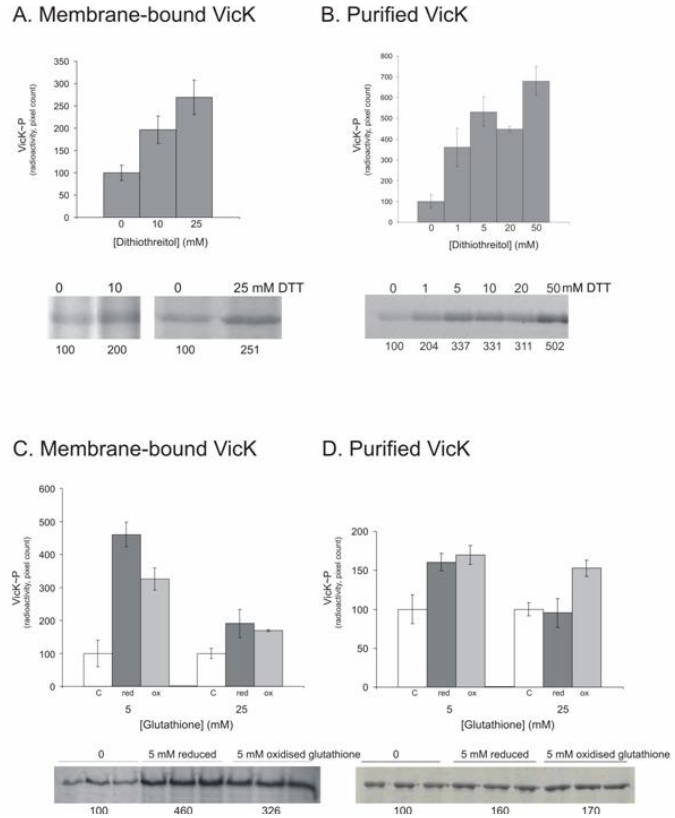

Figure 2. Effects of dithiothreitol (DTT) and reduced and oxidised glutathione on autophosphorylation activity of intact VicK.

Publications

Potter, C.A., Jeong, E-L., Williamson, M.P., Henderson, P.J.F. & Phillips-Jones, M.K. (2006) Redox-responsive *in vitro* modulation of the signalling state of the isolated PrrB sensor kinase of *Rhodobacter sphaeroides* NCIB 8253. *FEBS Lett*. **580**, 3206-3210.

Funding

This work was funded by the BBSRC and the European Membrane Protein consortium, EMeP

Exploring the folding energy landscape for immunity proteins

Lucy Allen, Alice Bartlett, Claire Friel, Dan Lund, Gareth Morgan, Victoria Morton, Emanuele Paci, Clare Pashley and Sheena Radford

Introduction

Determining the molecular details of how a protein folds to its native state requires detailed structural information on all of the states that are populated, in order to describe the energy landscape for the folding reaction. Although the native states of proteins are accessible to conventional structural techniques at high resolution, rare, transiently populated or conformationally flexible states can only be studied indirectly, using biophysical methods to build up a complete picture. In particular, kinetic methods are crucial for obtaining information on transition states, which cannot be observed at equilibrium. We are investigating the folding landscapes of the closely related colicin immunity proteins, Im7 and Im9. We have previously shown that these four-helical proteins fold to their native states *via* distinct kinetic mechanisms at neutral pH: Im7 transiently populates a compact, on-pathway, but misfolded intermediate, while Im9 does not. The folding intermediate of Im7 is composed of three of its four native helices, docked in a non-native manner and stabilised by both native and non-native interactions. Helix 3, which is not formed in the intermediate state, only docks onto the native structure after the protein has crossed the rate-limiting transition state for folding, which divides the intermediate and native states.

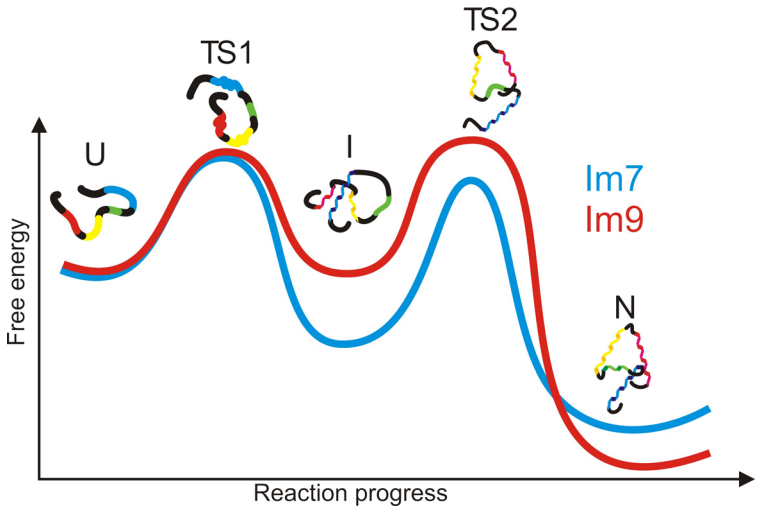

Figure: Energy land-scapes for the folding of Im7 (blue) and Im9 (red). Although both proteins can access the misfolded, three-helical intermediate state (I) within the first millisecond of folding, this species is populated to a detectable degree only by Im7. Helix 3, in green, is only formed after the second transition state (TS2). Populating I also alters the pathway through TS2 for Im7, which is shown by the differing widths of the TS2 barrier for Im7 and Im9

The first folding transition state ensemble

When refolding of Im7 is initiated, the protein populates its intermediate state by traversing a transition state ensemble (TS1 in Figure) within the first millisecond of the reaction. The molecular details of these very early events are crucial for understanding folding. Using ultra-rapid mixing and stopped-flow kinetic techniques on a series of Im7 mutants, combined with molecular dynamics simulations, we have been able to characterise TS1 at the level of individual residues, and have identified a core of three key residues that initiate the folding process. Together with our previous studies of I and TS2, this work provides one of the most complete descriptions of the folding landscape for a protein that populates an intermediate that has been described to date, as well as the earliest state on a folding pathway to be characterized to date.

The effect of native and non-native interactions on the folding intermediate

Although Im9 is closely related to Im7 and folds to the same native structure, it does not visibly populate an intermediate during folding. By mutating two residues in helix 2 of Im9, creating a variant that we have called SIm9, an intermediate that is closely analogous to that

of Im7 becomes populated during its folding. SIm9 has proved to be valuable for examining the roles played by native and non-native interactions in shaping the folding energy landscape of these proteins. We have been able to show that the rate-limiting transition state for folding involves reorganisation of the non-native interactions, and that this region of the energy landscape consists of multiple parallel pathways through which the protein can fold. Perturbing the stability of different interactions by mutation or changing solvent conditions alters the balance of flux through these pathways. Although the intermediate state is misfolded, the non-native interactions guide the protein through a subset of pathways to the native state. This suggests that the intermediate has specifically evolved to maximise folding efficiency by allowing only certain non-native interactions to form and reducing the likelihood of aggregation-prone intermediates. The binding of the immunity proteins to their target proteins is also important in their evolution: helix 3, which initiates binding, is conserved, while other residues, which determine the specificity of the interaction, can mutate to form new interactions to evolve in parallel with their targets.

Current work

Although we have determined the order of many events and interactions on the folding landscape of Im7, there are still many details to uncover. To gain insights into the molecular mechanisms by which Im7 forms its hydrophobic core, we are investigating a series of mutants in which polar groups or aromatic moieties are inserted into the protein, which will allow us to track both the hydration and packing of Im7's core at all stages of the folding pathway. We are also investigating the unfolded state from which the folding process begins, and which is visited by the protein at equilibrium. Having already characterized the unfolded state of Im7 in denaturant, we are now investigating the unfolded state which is visited by the protein at equilibrium under native conditions. We are creating mutants in which key native contacts are disrupted in order to prevent the protein from reaching the intermediate or native states. We hope to understand the dynamics of the unfolded chain, and how this determines the initial events in folding. We are also refining computational methods based on restrained molecular simulations to interpret experiments in structural terms, focusing particularly on the microscopic interpretation of macroscopic experimental parameters such as φ values.

Publications

Brockwell, D.J., and Radford, S.E. (2007) Intermediates: ubiquitous species on folding energy landscapes? *Curr. Opin. Struct. Biol.* **17**, 30-37.

Morton, V.L., Friel, C.T., Allen, L.R., Paci, E., and Radford, S.E. (2007) The effect of increasing the stability of non-native interactions on the folding landscape of the bacterial immunity protein Im9. *J. Mol. Biol.* **371**, 554-568.

Allen L and Paci E. (2007) Transition state for protein folding using molecular dynamics and experimental restraints, *J. of Phys. Cond. Matt.***19**, 285221.

Funding and acknowledgments

This work is funded by the BBSRC and The Wellcome Trust. We thank Keith Ainley and Anne Holland for technical support.

Collaborators

Joerg Gsponer & Michele Vendruscolo (University of Cambridge), Jim Bardwell (University of Michigan, USA)

Fibril growth kinetics of β_2-microglobulin

Geoffrey Platt, Katy Routledge, Timo Eichner, Andrew Hellewell, John Hodkinson, Carol Ladner, David Smith, Nathalie Valette, John White, Wei-Feng Xue and Sheena Radford

Introduction

There are more than twenty proteins with unrelated amino acid sequences and native structures that aggregate to form highly ordered amyloid fibrils *in vivo* and result in amyloid disease. More recently, several of these proteins, and some that are not disease-related, have been shown to form amyloid *in vitro* by manipulation of solution conditions. In all cases the normally soluble proteins deposit as insoluble amyloid-like fibres with characteristic cross-β structure. Our research aims to elucidate the molecular and structural mechanisms of fibril formation for human β_2-microglobulin (β_2m) which causes haemodialysis related amyloidosis in all patients with chronic renal failure.

Fibril growth kinetics reveal a region important for nucleation and elongation of aggregation

Amyloid is a highly ordered form of aggregate comprised of long, straight and unbranched proteinaceous fibrils that are formed with characteristic nucleation-dependent kinetics *in vitro*. Currently, the structural molecular mechanism of fibril nucleation and elongation is poorly understood. We have investigated the role of sequence and structure of the initial monomeric precursor in determining the rates of nucleation and elongation of human β_2m. We have studied the kinetics of seeded and spontaneous (unseeded) fibril growth of wild-type β_2m and twelve variants at pH 2.5, targeting specifically an aromatic-rich region of the polypeptide chain (residues 62-70) that has been predicted to be highly amyloidogenic (Figure 1a). Kinetics were monitored using fluorescence of the amyloid-specific dye, thioflavin-T, and the end-products were visualised by electron microscopy (Figures 1b, c). The results reveal the importance of aromatic residues in this part of the β_2m sequence in fibril formation under the conditions examined. The data show that this region of the polypeptide chain is involved in both the nucleation and elongation phases of fibril formation, because the rates of these processes are specifically sensitive to mutation of this region of the protein.

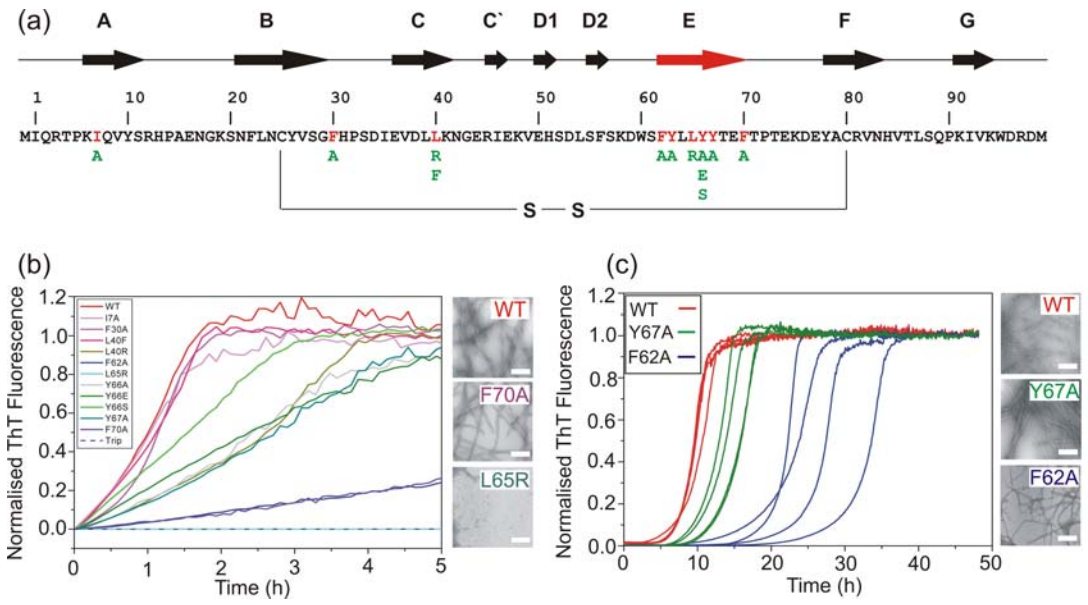

Figure 1. (a) Sequence of β_2m indicating the amino acid changes made in this study and the positions of the disulphide bridge and secondary structure in the native state. (b) Average kinetics of seeded β_2m fibril formation with example images of the final fibrillar product shown by EM. (c) Example kinetic traces of unseeded fibril grows (including a lag phase), with EM images of the final fibrillar products.

Structural analysis of the conformational properties of the unfolded monomer for each variant using NMR relaxation methods revealed that all variants contain significant non-random structure involving two hydrophobic clusters comprising regions 29-51 and 58-79, the extent of which is critically dependent on the sequence (Figure 2). No direct correlation was observed, however, between the extent of non-random structure in the unfolded state and the rates of fibril nucleation and elongation, suggesting that the early stages of aggregation involve significant conformational changes from the initial unfolded state. Together, the data suggest a model for β_2m aggregation in which structurally specific interactions involving the highly hydrophobic and aromatic-rich region comprising residues 62-70 provides a complementary interface that is key to the generation of amyloid fibrils for this protein.

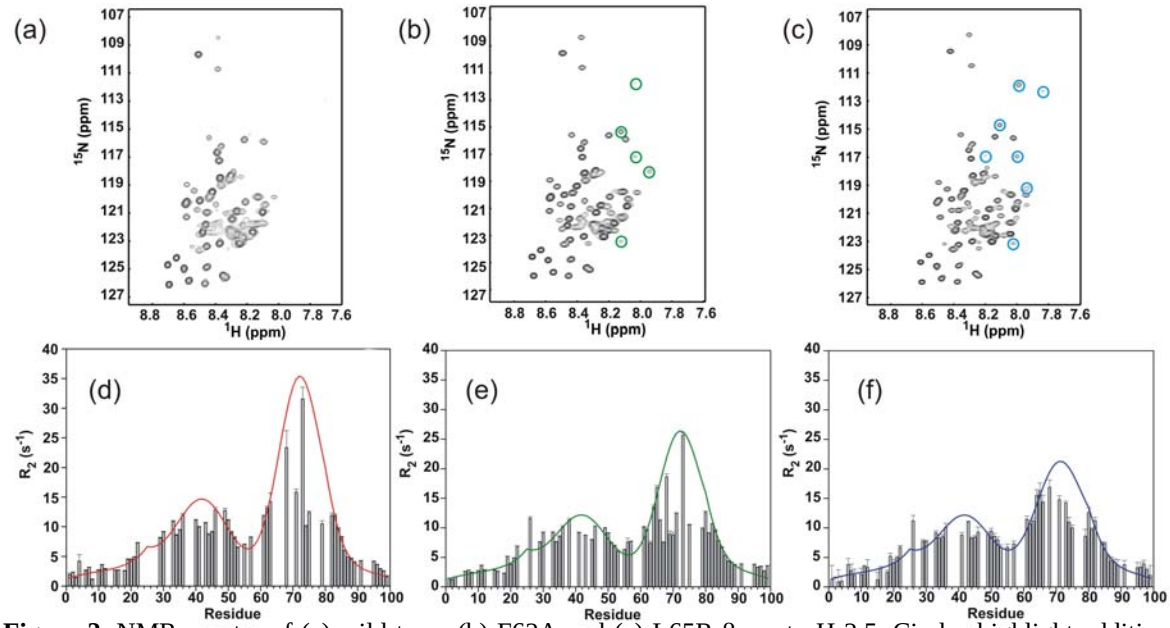

Figure 2. NMR spectra of (a) wild-type, (b) F62A and (c) L65R β_2m at pH 2.5. Circles highlight additional peaks not observed in the wild-type spectrum. T_2 relaxation rates (R_2) of (d) wild-type, (e) F62A and (f) L65R β_2m indicate the presence of non-native hydrophobic clusters under these conditions, especially in the aromatic rich region of the protein. Lines are a model fit to two hydrophobic clusters and a disulphide bridge.

Structural and molecular nature of β_2m fibril formation

Mutagenesis experiments have been extended throughout the protein sequence to ascertain whether other regions (outside residues 62-70) also have a large impact on the kinetics of fibril formation. The data from these studies are being used alongside information obtained from algorithms that predict fibril formation rates from random coil states to infer the importance of structure in the early stages of this process. Furthermore, other experimental methods, such as size-exclusion chromatography and analytical ultracentrifugation, used in conjunction with NMR spectroscopy, are being used to better understand the structural mechanisms of the early stages of fibril formation by β_2m. Finally, a battery of biophysical techniques is being used to gain an insight into the structure of the amyloid-like fibrils that are formed by β_2m.

Publications

Platt, G.W., Routledge, K.E., Homans, S.W. & Radford, S.E. (2008) Fibril growth kinetics reveal a region of β_2-microglobulin important for nucleation and elongation of aggregation. *J. Mol. Biol.* (in press)

Funding

We gratefully acknowledge the University of Leeds, BBSRC and The Wellcome Trust for financial support.

The nucleation-dependent self-assembly mechanism of β_2-microglobulin

Wei-Feng Xue, Timo Eichner, Andrew Hellewell, John Hodkinson, Carol Ladner, Geoffrey Platt, Katy Routledge, David Smith, Nathalie Valette, John White and Sheena E. Radford

Introduction

Self-assembly of misfolded forms of normally soluble and functional proteins or peptides into amyloid fibrils results in numerous human diseases. Understanding how amyloid self-assembly occurs, therefore, is of paramount importance for a molecular interpretation of amyloidosis, as well as for the rational development of therapies against amyloid disease. Over the past decade, advances have been made toward a more complete description of amyoid fibril formation, including the determination of increasingly refined models of fibril structures, as well as the identification of amyloid precursors and oligomeric states, one or more of which could be the culprits of cytotoxicity associated with several amyloid diseases. However, the molecular events occurring during the self-assembly process itself remain obscure because of the heterogeneity and the complexity of the early association events. We are currently working on the mechanism of nucleated self-assembly, which is essential in delineating the origins of amyloid disease, such as the identity and concentration of cytotoxic species and the rate of increase in the fibril load, and in developing therapeutic agents able to control the causative characteristics of amyloid diseases.

Systematic analysis of nucleation-dependent polymerisation

In order to better our understanding of the kinetic, thermodynamic and structural molecular mechanism of amyloid self-assembly, we have been developing a new experimental and theoretical approach for the analysis of the mechanism of amyloid fibril formation. Using this novel approach, we have been studying the assembly of β_2-microglobulin (β_2m) into amyloid fibrils (Figure 1). From this study, we are able to dissect the assembly mechanism of β_2m in the context of both structural and thermodynamic aspects of nucleated amyloid assembly, providing new information on nucleated mechanisms and secondary processes that speed up fibril formation, as well as predicting the presence of oligomeric populations that have been experimentally and independently verified. Efforts are now focused on the nature of these oligomers and their specific roles in fibril assembly under physiological conditions.

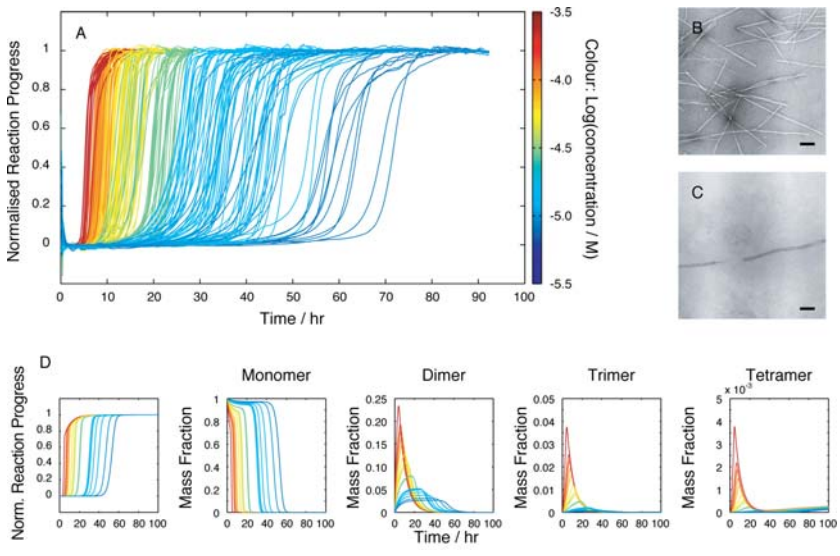

Figure 1: Systematic analysis of the nucleated assembly of β_2m fibrils. (A) Reaction progress curves monitored by ThT fluorescence. A total of 235 traces are shown at 20 different protein concentrations ranging from 8 to 244 μM (colour-bar on the right). (B)-(C) Negative stain EM images of samples after the reaction reached completion obtained at a protein concentration of 244 μM (B) or 8 μM (C). Bars denote 100 nm. (D) Model prediction of the reaction progress and the populations of 1-4:mers during the course of the reaction.

Effect of surfaces on amyloid self-assembly

Nucleated amyloid fibril assembly *in vivo* is modified by the presence of different surfaces, natural as well as artificial. Nanomaterals, considered likely to revolutionize many arenas,

including information technology and biomedical industries in the coming decades, present a significant source of artificial surfaces where many nanoparticles are small enough to access all parts of the body, including the brain. We have been studying the potential for nanoparticles to promote protein assembly into amyloid fibrils *in vitro* by assisting the nucleation process. Through detailed kinetic studies, we found that nanoparticles with different surface properties increase the rate of protein fibril nucleation of β_2m dramatically in the absence of preformed specific seeds (Figure 2), by interacting with the particle surface and providing a locally increased protein concentration promoting oligomer formation.

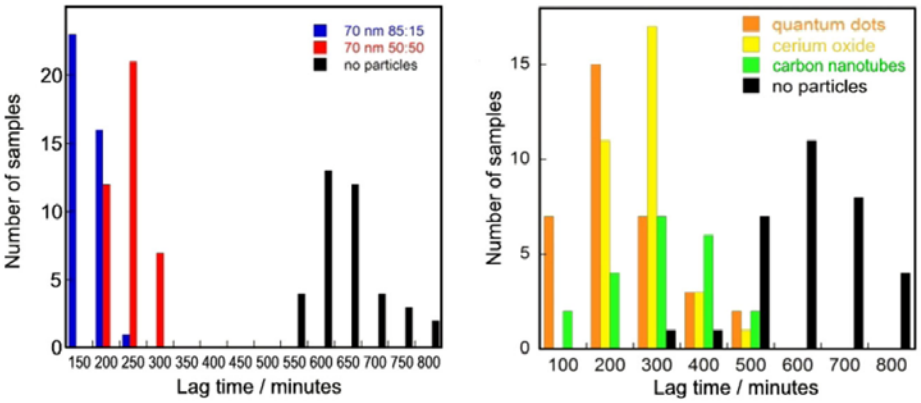

Figure 2: β_2m fibril assembly promoted by the presence of nano particles shown as histograms of observed lag times. Colour coding of histograms: blue (0.01 mg/ml 70-nm 85:15 NIPAM/BAM particles), red (0.01 mg/ml 70-nm 50:50 N-isopropyl acryl-amide / N-tert-butyl-acrylamide particles), orange (100 nM 16-nm quantum dots), green (0.01 mg/ml 6-nm-diameter multiwalled carbon nanotubes), yellow (0.01 mg/ml 16-nm cerium oxide particles), and black (samples without particles).

Interaction between biological membranes and species populated during different stages of amyloid assembly present another important aspect of biologically relevant surface mediated processes important to amyloid assembly. Membrane disruption has also been suggested to be a mechanism by which amyloid formation is linked to cytotoxic responses of amyloid diseases. We are currently conducting kinetic studies using model liposome membrane systems to probe the interactions between β_2m and membrane surfaces in order to further understand the role of biological membranes in amyloid disease.

Collaborators

This project is in collaboration with Alison Ashcroft, Eric Hewitt, Steve Homans and Stuart Warriner of the Astbury Centre. The study of β_2m self-assembly in the presence of nano-particle surfaces is in collaboration with Prof. Sara Linse and Prof. Kenneth A. Dawson from School of Chemistry and Chemical Biology, and Conway Institute, University College Dublin.

Publications

Linse, S., Cabaleiro-Lago, C., Xue, W.-F., Lynch, I., Lindman, S., Thulin, E., Radford, S.E., and Dawson, K.A. (2007) Nucleation of protein fibrillation by nanoparticles. *Proc. Natl. Acad. Sciences. USA.* **104**, 8691– 8696.

Xue, W.-F., Homans, S.W., Radford, S.E. (2008) Systematic analysis of nucleation-dependent polymerisation reveals new insights into the mechanism of amyloid self-assembly. *Proc. Natl. Acad. Sciences. USA.* in press.

Funding

We are grateful to the University of Leeds, BBSRC and The Wellcome Trust for financial support.

Electron microscopy studies of yeast prion Ure2p fibrils

Ngai Shing Mok and Neil Ranson

Introduction

Prions are protein molecules that can assume a stable misfolded conformation, which can autocatalytically induce the misfolding of the normal conformation of the protein. These misfolded forms are prone to aggregation, and typically an amyloid-like aggregate results. The mammalian protein PrP is the causative agent for neurodegenerative disorders such as Creutzfeldt-Jakob Disease (and its variants) in humans, Bovine Spongiform Encephalopathy (BSE) in cattle, and Scrapie in sheep. However the prion phenomenon is not confined to higher organisms, and several prion proteins are found in yeast. Direct studies of PrP are exceptionally difficult owing to the long incubation period of the disease, and the risk of iatrogenic infections. Yeast prions are harmless to humans and therefore easier to handle, and so make ideal model systems to study the prion phenomenon. One such yeast prion, Ure2p, forms ordered, twisted fibrils, which are thought to contain an amyloid-like structure. However, only low-resolution, 2-D structural data is currently available to support this model.

Current work

Low-resolution CCD images of unstained Ure2p fibrils in ice have been collected on a Tecnai F20 microscope in the Astbury Centre. Image averages of aligned fibril segments show that twisted Ure2p fibrils have a distinct punctate appearance and rather poor helical order. We are currently implementing an improved alignment scheme and assessing polarity of the segments before generating a preliminary 3-D model. We are also collecting a much larger, higher resolution dataset on film to extend the resolution of these preliminary 3-D models.

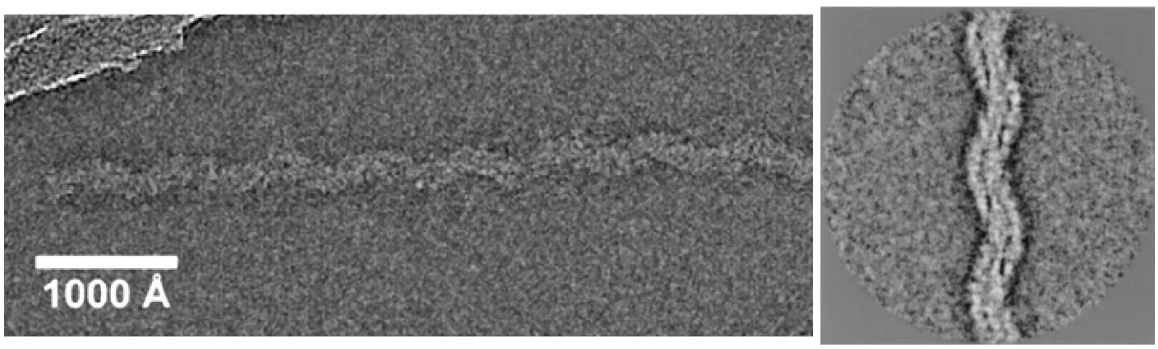

Figure 1. On the left, a raw cryo-EM image of an unstained, twisted Ure2p fibril embedded in vitreous ice. The fibril was grown from wild-type, full length Ure2p at physiological pH and ionic strength. On the right, an average of ~100 aligned Ure2p fibril segments shows the twisted, punctate appearance of the Ure2p fibril in greater detail.

Publications

Ranson, N., Stromer, T., Bousset, L., Melki, R. and Serpell, L. C. (2006). Insights into the architecture of the Ure2p yeast protein assemblies from helical twisted fibrils. *Protein Sci.* **15**, 2481-2487.

Funding

This work was supported by the BBSRC. NAR is a University of Leeds Research Fellow

Acknowledgements

This work is in collaboration Drs. Ronald Melki and Luc Bousset at the Laboratoire d'Enzymologie et Biochimie Structurales, CNRS, Gif-sur-Yvette, France.

RNA packaging and capsid assembly in bacteriophage MS2

Katerina Toropova, Óttar Rolfsson, Gabriella Basnak, Peter G. Stockley and Neil A. Ranson

The *T*=3 bacteriophage MS2 provides a model system to investigate how genomic RNA is packaged during capsid assembly in single stranded RNA (ssRNA) viruses. *In vitro*, MS2 capsids can be reassembled by incubation of recombinant coat protein dimers (CP_2) with a short (19 nucleotides) RNA sequence that encompasses the start codon of the viral replicase gene. This sequence (TR) forms a stem loop structure and acts as a specific assembly initiation sequence *in vivo*. Using cryo-electron microscopy, we have obtained low-resolution reconstructions of recombinant MS2 capsids reassembled with two synthetic oligonucleotides; TR and S2 (TR with a 12 nt, 5' extension). The TR-MS2 map is strikingly similar to published crystallographic models, indicating that cryo-EM reconstructions of reassembled MS2 capsids accurately reflect their structure. The S2-MS2 map shows additional density consistent with the longer RNA used, and suggesting that sequences flanking TR interact with the CP as the additional density interacts with the inside of the capsid.

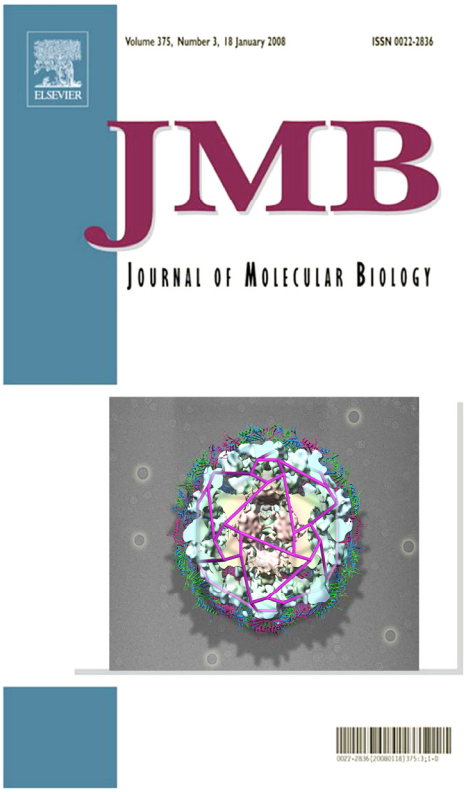

Figure 1. A view of the rear half of a bacteriophage MS2 virion. The crystal structure for the capsid protein (fitted into EM density which is not shown) is in a cartoon representation, and the A, B & C quasi-equivalent conformers are coloured blue, green and red respectively. Cryo-EM density for encapsidated RNA is shown as a radially-coloured density, and a polyhedron describing how RNA binds to the inner surface of the capsid is overlayed (magenta). From the cover of the Journal of Molecular Biology, Volume 375(3).

To investigate the structure of the packaged genomic RNA we determined the structure of the wild-type virus at ~ 9 Å resolution. This map showed the genomic RNA, in unprecedented detail, as adopting a novel arrangement consisting of two concentric shells connected at each five-fold vertex. The outermost shell lies directly beneath the CP layer, and maps to the known RNA binding sites. This strongly implies that upon packaging, sequences in the genome assume stem-loop structures that are capable of binding CP_2 in a non-sequence specific manner. The connections to the inner shell of density are approximately the correct size to accommodate an RNA duplex. We estimate that ~85% of the genomic RNA is resolved in our map.

This work is now continuing with a further investigation of the effects of RNA length and sequence on both the efficiency of MS2 capsid assembly, and on the structure of the packaged RNA, using large sub-genomic RNA fragments.

Publications:

Toropova, K., Basnak, G., Twarock, R., Stockley, P.G. and Ranson, N.A. (2008). The three-dimensional structure of genomic RNA in bacteriophage MS2: implications for assembly. *J. Mol. Biol.* **375**, 824-836.

Acknowledgements: wt MS2 virions were a gift from Prof. D. Peabody, University of New Mexico. This work is in collaboration with Drs. R. Twarock and T. Keef at the University of York, and was funded by the LUII in Bionanosciences and The Wellcome Trust. NAR is a Leeds University Research Fellow.

Picornavirus cell entry: genome-release and membrane penetration

Tobias J. Tuthill, Matthew P. Davis and David J. Rowlands

Introduction

A fundamental step in the process of viral infection is the delivery of the virus genome across the hydrophobic barrier of the host cell membrane. This is conceptually straightforward for the enveloped viruses (such as HIV), which can transfer their genetic material directly into the cytoplasm via a mechanism of membrane fusion. However, non-enveloped viruses lack a membrane and must employ alternative mechanisms to infect cells.

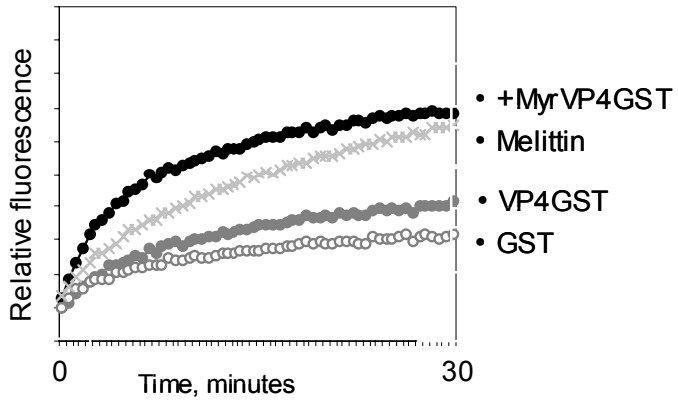

Figure 1. Liposome membrane permeability induced by myristylated (+MyrVP4GST) or unmyristylated VP4GST, GST and the pore forming peptide melittin.

The picornavirus family of non-enveloped viruses includes a number of important human and animal pathogens, e.g. poliovirus (PV), human rhinovirus (HRV, common cold) and foot-and-mouth disease virus (FMDV). They have icosahedral capsids that enclose a single-stranded positive sense RNA genome. Cell entry involves receptor binding, uptake by various endocytic pathways followed by release of the genome from the capsid (uncoating) and delivery of the genome across the endosome membrane into the cytoplasm. The mechanisms for genome release and membrane penetration remain elusive. However it is known for PV & HRV that the capsid remains intact during the uncoating process while the small N-terminally myristylated protein VP4 is released from the particle and becomes associated with the membrane. A key question is: does VP4 form a channel through which the viral RNA penetrates the membrane?

Recombinant VP4 induces permeability in model membranes

VP4 from HRV16 was expressed in *E. coli* as a soluble VP4GST fusion. VP4GST was produced either unmyristylated or myristylated by the co-expression of N-myristyl transferase. VP4GST associated with liposomes in lipid floatation assays while GST did not. In carboxyfluorescein release-unquenching assays, VP4GST induced a myristylation dependent permeability in liposomes (Figure 1).

Permeabilized liposomes remain intact

Liposomes were analyzed by flow cytometry. By immunostaining with anti-GST antibody, two populations of intact liposomes were identified, those that had bound VP4GST and lost the majority of internal carboxyfluorescein (Figure 2, purple) and those with little protein bound and which retained their internal carboxyfluorescein (Figure 2, orange). The presence of permeabilized but intact liposomes strongly suggests that VP4GST induces pore-formation without causing vesicle disruption.

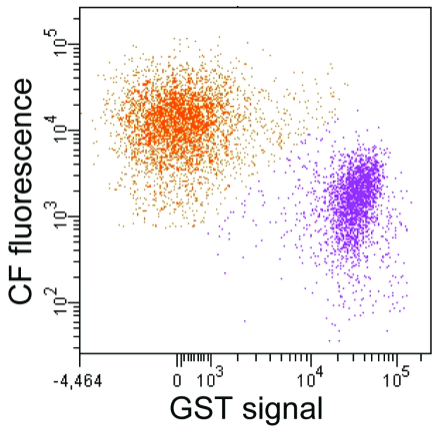

Figure 2. Flow cytometry showing VP4GST mediated permeability in intact liposomes.

Publications

Davis, M.P., Bottley, G., Beales, L.P., Killington, R.A., Rowlands, D.J. & Tuthill, T.J. (2008) Recombinant VP4 of human rhinovirus induces permeability in model membranes. *J Virol*. **82**, 4169-74.

Funding

This work was funded by the MRC and Wellcome Trust.

Aphthovirus cell entry: characterization of equine rhinitis A virus and its low pH derived empty particle

Tobias J. Tuthill and David J. Rowlands

Introduction

The picornavirus family of non-enveloped viruses includes a number of important human and animal pathogens, e.g. poliovirus (PV), human rhinovirus (HRV,) and foot-and-mouth disease virus (FMDV). They have icosahedral capsids enclosing a single-stranded positive sense RNA genome. Studies with PV and HRV have led to models for infection by these viruses in which the virus interacts with a cell membrane during the uncoating process to coordinate delivery of the RNA genome from within the particle, across the membrane, into the cytoplasm. Key to this model is genome delivery from within an *intact* particle so that the RNA is not exposed to the hostile environment within the endosome.

In contrast, the FMDV capsid is known to dissociate at the mild acid pH of the early endosome into protein subunits and released RNA. However, we have no explanation of how the naked RNA is protected within the endosome nor how its delivery to the cytoplasm is coordinated.

Equine rhinitis A virus (ERAV) is also a member of the aphthovirus genus but is not subject to the strict biocontainment required for FMDV. We are, therefore, using ERAV to study the mechanism of infection by these viruses.

ERAV dissociates at low pH via a transient empty particle

Picornavirus virions, empty particles and dissociated subviral particles may be distinguished by their sedimentation in density gradient ultracentrifugation. Figure 1 shows the acid induced formation of transient empty ERAV particles prior to dissociation. This observation may reconcile the apparent conflict between existing entry models for PV/HRV and FMDV/aphthoviruses.

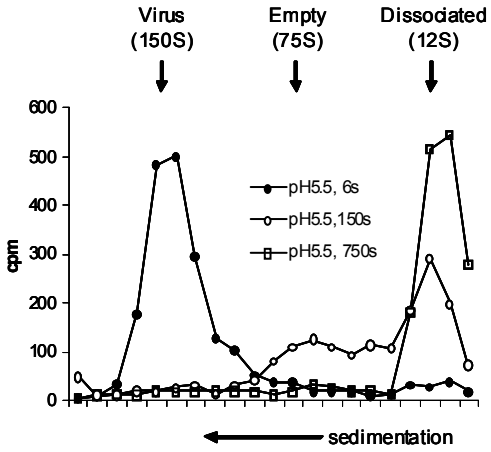

Figure 1. Transient empty particles by time-course of acid exposure

Crystal structures of ERAV and the low pH derived empty particle

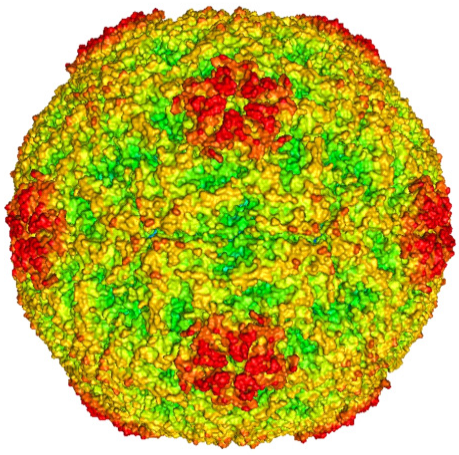

Figure 2. Crystal structure of ERAV

ERAV was purified and crystallized at neutral and acidic pH and X-ray data collected to 3Å at ESRF, Grenoble. Structure determination (E. Fry) was by molecular replacement using existing FMDV coordinates. The structure of ERAV (figure 2) is broadly similar to FMDV with some similarities with other related picornaviruses. The structure derived from acid crystallization has reduced contacts between capsid subunit interfaces, consistent with a particle in a 'pre-dissociation' state.

Collaborators
Tom Walter, Karl Harlos, Elizabeth E. Fry and David I. Stuart, Division of Structural Biology and Oxford Protein Production Facility, The Henry Wellcome Building for Genomic Medicine, Roosevelt Drive, Headington, Oxford OX3 7BN, UK.
Nick Knowles, Institute for Animal Health, Pirbright Laboratory, Ash Road, Pirbright, Surrey, GU24 0NF, UK**.**

Funding
This work was funded by the MRC and BBSRC.

Determining a molecular pathway for formation of a *T*=3 viral capsid using ESI-MS and ESI-IMS-MS

Victoria L. Morton, Ottar Rolfsson, Gabby Basnak, Nicola J. Stonehouse,
Alison E. Ashcroft and Peter G. Stockley.

Introduction

The detailed molecular mechanisms underlying the *in vitro* self-assembly reactions of viruses have been difficult to investigate because intermediates on the assembly pathways are both present in limited amounts and transient. In order to study the detailed molecular mechanism(s) of ssRNA virus assembly, we have been using bacteriophage MS2, whose reassembly into a *T*=3 capsid shell can be initiated by a sequence-specific non-covalent coat protein-RNA stem-loop (TR) interaction. We are examining the effects of changing sequences/structure of RNA stem loops used to initiate self-assembly of dissociated coat protein dimers, and look at the effects of local genomic sequences outside the 19 nucleotide consensus TR sequence on the kinetics and efficiency of capsid assembly.

Using nanoESI-MS we have studied the assembly of MS2 capsids, which contain 180 identical coat protein subunits that form 90 non-covalent dimers that pack into a *T*=3 shell. Reassembly from coat protein dimers is initiated by addition of various RNA sequences, with and without the natural packaging TR sequence. Assembly with TR alone at a molar ratio of 1:2 with coat protein dimers (CP_2) results in the formation of an initial [CP_2:TR] com-plex accompanied by higher order species and capsid production (Fig. 1a).

RNA aptamer stem-loops known to bind to the MS2 coat protein have been studied. All form the initiation complex but not all lead to capsid formation; others form capsid rapidly. RNAs with 5' (S2) or 3' (S4) extensions of genomic sequence at either side of the TR initiator stem loop have also been examined. We have been able to quantitate the appearance and subsequent disappearance of the assembly initiation complex [CP_2+RNA] and show that capsid formation is comparable with that of the consensus TR for S2, but slower for S4, consistent with a direct role for local sequences in assisting quasi-equivalent conformer switching during assembly.

Future experiments aim to characterise on-pathway virus assembly intermediates using ESI-MS(/MS) and ESI-TWIMS-MS (Figure 1 (b) and (c)), to compare their cross-sectional areas and their relative stabilities.

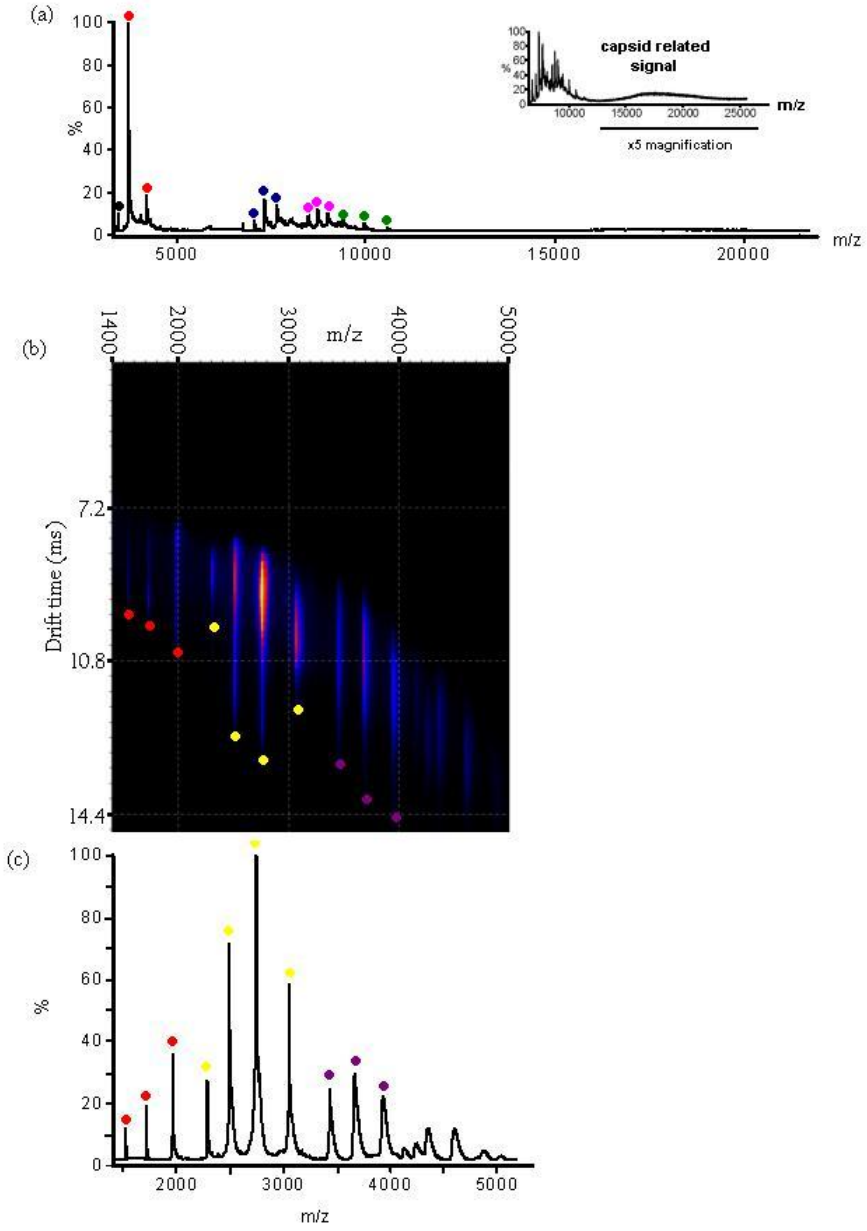

Figure 1. Mass spectrometric assay of MS2 reassembly.
The spectra were acquired over the range m/z 500-30000, for samples in ammonium acetate (40 mM) at pH 5.2-5.7 (a) Virus reassembly reaction in the ratio 2:1 CP_2:TR after 30 minutes. The observed intermediates are labelled as follows: Black spots = CP; red spots = CP_2:TR; blue spots = 182.7 kDa, assigned as [3(CP_2:TR)+3CP_2], green spots = 169.2 kDa species assigned as [3(CP_2:TR)+2CP_2+CP], and pink spots = 304.8 kDa, assigned as [5(CP_2:TR)+5CP_2]. Inset shows the signals that match those observed when *T*=3 capsids are sprayed. (b) ESI-IMS-MS Driftscope plot showing drift time (y axis) versus *m/z* (x axis) for the analysis of dissociated coat protein showing red spots CP; yellow spots CP_2 and purple spots $2CP_2$ (c) Spectrum of the dissociated coat protein showing the same species as in (b).

Publications

Stockley, P. G., Rolfsson, O., Thompson, G. S., Basnak, G., Francese, S., Stonehouse, N. J., Homans, S. W. & Ashcroft, A. E., 2007, A simple, RNA-mediated allosteric switch controls the pathway to formation of a T=3 viral capsid, *Journal of Molecular Biology*, **369**(2), 541-552.

Toropova, K., Basnak, G., Twarock, R., Stockley, P. G. & Ranson, N. A., 2008, The three dimensional structure of genomic RNA in bacteriophage MS2: Implications for assembly, *Journal of Molecular Biology*, **375**(3), 824-836.

RNA aptamers against disease related proteins.

David H. J. Bunka, Stuart E. Knowling, Andrew J. Baron, Benjamin J. Mantle, Sheena E. Radford and Peter G. Stockley.

Aptamers are DNA or RNA molecules specifically selected for their ability to bind to (and in some cases inhibit the function(s) of) a given bio-molecular target. They are isolated from combinatorial starting libraries of ~10^{15} oligonucleotide sequences, through repeated cycles of amplification and competitive isolation; in a process known as SELEX (**S**ystematic **E**volution of **L**igands by **Ex**ponential Enrichment).

This process can take anywhere from a few weeks to several months to isolate a pool of tight binding species, suitable for further characterisation. We have successfully automated this process allowing high throughput isolation of aptamers against several targets, simultaneously. This set up has allowed us to isolate aptamers against over one hundred different targets (or targets under different conditions) to date. Our progress on two of these projects will be described here.

In collaboration with our colleagues at the Leeds Institute of Molecular Medicine (Dr. Jenny L. Barton & Prof. Constanze Bonifer), we have isolated RNA aptamers against the Runt Homology Domain (RHD) of the transcription factor RUNX-1, bound to the core binding factor beta subunit (CBFβ). The RUNX-1/CBFβ complex is highly conserved throughout evolution and is one of the most important regulators of hematopoietic specific genes. As well as its role in the regulation of normal hematopoiesis, the RUNX1 gene is also associated with several acute leukemias. Translocations involving the RUNX-1/CBFβ complex result in the creation of onco-proteins that alter gene regulation in blood cells and hence cause disease.

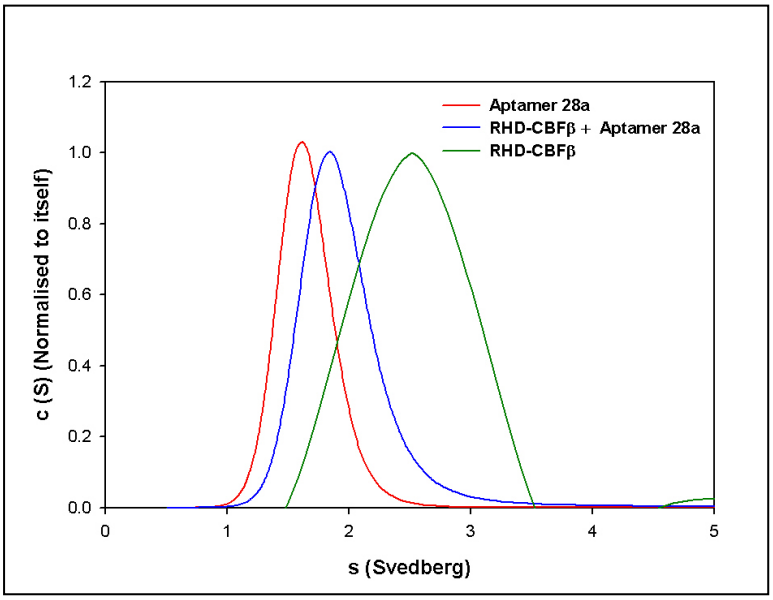

Figure 1. Sedimentation velocity analytical ultracentrifugation analysis of a minimal aptamer (red), the initial selection target RHD/CBFβ (green) and their complex (blue). S-values show a clear difference for all components studied and indicate that the minimal aptamer disrupts the heterodimer RHD/CBFβ forming a 1:1 complex with one of the subunits, that was shown to be the RHD biochemically.

Analysis of the selected aptamers revealed two dominant sequence families that each bind the selection target with high affinity. *In vitro* binding assays show that these aptamers disrupt DNA-binding by the purified protein and by proteins within nuclear extracts expressing wild-type RUNX-1/CBFβ. Minimal short stem-loop sequences encompassing the binding activity have been characterised and shown to work by binding to the DNA-binding motif within

RHD. Analysis of aptamer-RHD/CBFβ complexes by sedimentation velocity centrifugation show that the RHD/CBFβ dimer is disrupted in the presence of the aptamer fragments, which each seem to make a 1:1 complex with the RHD subunit (Figure 1).

We have also further characterised our aptamers against the amyloidogenic protein, beta-2-microglobulin (β2m). In previous studies, we demonstrated the ability of anti-β2m fibril aptamers to recognise different fibril morphologies, whilst not binding to the monomeric form of the protein. This suggested the presence of 'fibril specific epitopes'. Interestingly we also noted that the aptamers were able to bind to amyloid-like fibrils formed from some (but not all) other amyloidogenic proteins. This work has been extended to include binding assays of a number of *ex vivo* samples isolated from patients suffering from a range of amyloid associated diseases (Figure 2). Cross-reactivity of the anti-β2m fibril aptamers with clinical samples demonstrates the potential of aptamers as diagnostic reagents. We are currently attempting to isolate aptamers that specifically recognise the monomeric state of β2m with the aim of isolating inhibitors of fibrilogenesis.

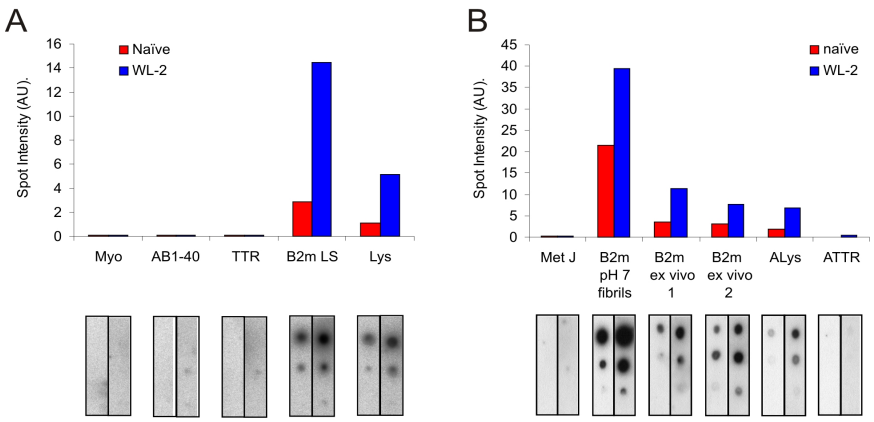

Figure 2. Dot-blots showing radiolabelled anti-β2m fibril aptamer WL-2 (blue) or the naïve pool (red), binding to various *in vitro* prepared, amyloid-like fibrils (A) or *ex vivo* fibrils (B).

Acknowledgements and funding

We would like to thank Dr. Glenys Tennent for supplying the *ex vivo* amyloid fibrils and for her continuing support of the amyloid aptamer project. These projects have been supported by grants from the Leukemia Research Fund and the UK Medical Research Council. The aptamer facilities within Leeds have been supported by funding from the UK Medical Research Council and The Wellcome Trust.

Publications

Bunka, D. H. J., Mantle B. J., Morten, I. J., Tennent, G. A., Radford, S. E., Stockley, P. G. (2007) Production and characterisation of RNA aptamers specific for amyloid fibril epitopes. *J. Biol. Chem.* **282**; 34500-34509

Targeting the functions of the Human Papilloma Virus 16 oncoproteins with RNA aptamers

Clare Nicol, G. Eric Blair and Nicola J. Stonehouse

Introduction

Human papilloma viruses (HPV) are DNA tumour viruses which can cause a variety of diseases ranging from benign warts and veruccas (the low-risk subtypes) to malignant lesions (the high-risk subtypes). There are currently thought to be more than 120 different HPV subtypes. Human papilloma virus 16 (HPV16) is a high-risk papilloma virus associated with the development of cervical cancer due to the actions of the oncoproteins E6 and E7. The most well characterised role of E6 in oncogenesis is the targeting of the tumor suppressor p53 for degradation. The major contribution of E7 to oncogenesis is in binding and destabilising the cell cycle control protein pRb. Despite their small size, both of these oncoproteins have been shown to bind to a large variety of additional cellular proteins (Figure 1) however their functions in many of these interactions are largely unknown.

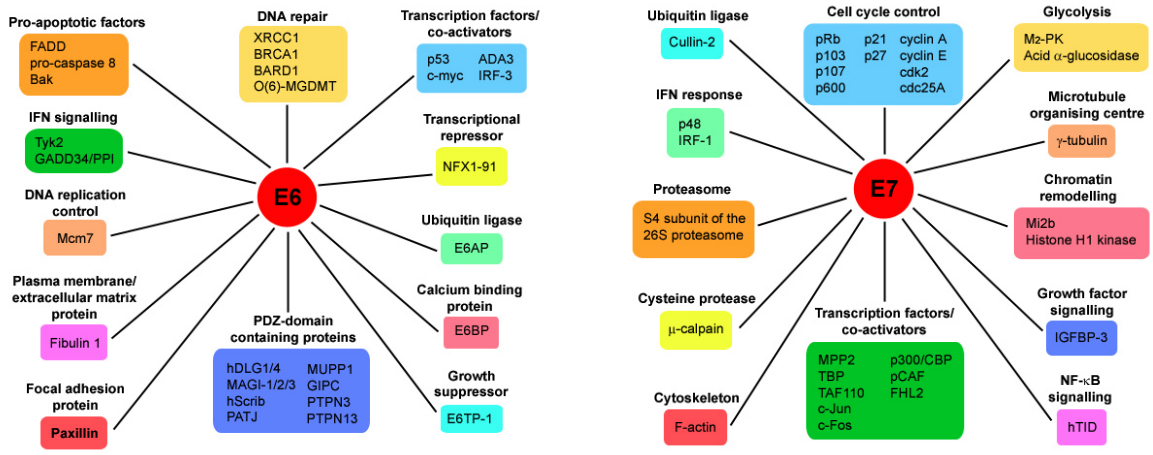

Figure 1 - The multiple interactions of HPV16 E6 and E7 with cellular factors

Aptamers are RNA molecules that are enriched from a random pool of molecules for high affinity binding to a target protein. Aptamers have been raised to both E6 and E7 of (HPV16) with the aim of using these molecules as tools to probe the activities of oncoproteins in cellular transformation.

Aptamers raised to GST-E7 induce apoptosis in cervical cancer cells

GST-E7 aptamers were transfected into a cell line derived from a human cervical cancer (SiHa) which contains the HPV genome integrated into chromosome 13. This cell line constitutively expresses both the E6 and E7 viral oncogenes. The E7 aptamers were shown to induce apoptosis in these cells but not in a control cell line (HaCaT). Apoptosis occurs within 18 hours post-transfection with aptamer. Aptamers have been shown to localise to the nucleus upon transfection, which is the site of the majority of the functions of E7 (Figure 2). Studies are ongoing to define the mechanism of action of the aptamers.

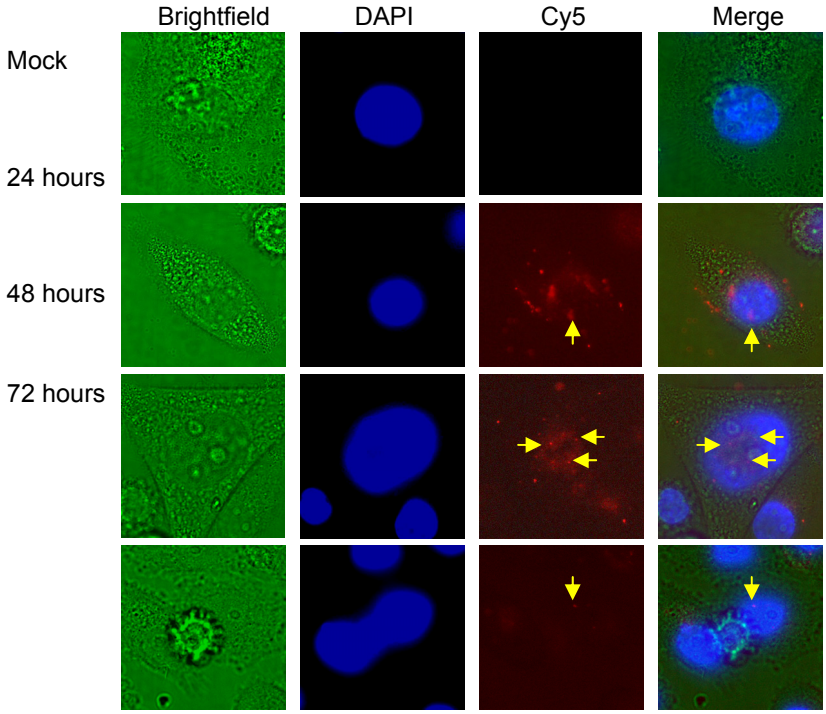

Figure 2 - Localisation of aptamer A2 to the nucleus of SiHa cells.

E6 has been cloned, expressed and purified

To produce aptamers to the second HPV16 oncoprotein, the E6 open reading frame was cloned into a GST-expression vector. Extensive optimisation of expression and purification has been carried out to produce sufficient quantities of E6 as a GST fusion protein. Aptamers to this protein have been generated and will subsequently be analysed for binding affinity for E6 and for effect in SiHa cells.

Collaborators

Prof Lawrence Banks, Trieste

Funding

Funding from Yorkshire Cancer Research is gratefully acknowledged.

Using RNA aptamers to study the replication of foot-and-mouth disease virus

Matthew Bentham, David J. Rowlands and Nicola J. Stonehouse

Introduction

Foot-and-mouth disease (FMD) has a global impact on animal husbandry; felt not only by the suffering of individual animals, but also in a wider economic sense. The total bill for the 2001 outbreak in the U.K. has been estimated at over £9 billion. Foot-and-mouth disease virus (FMDV), the etiological agent of FMD, has a relatively small (approx. 9Kb), single-stranded, RNA genome; which upon infection, is directly translated into one poly-protein. Subsequent cleavage gives rise to 13 fully mature proteins, though a number of the partial cleavage products are functional proteins in themselves. Despite this perceived simplicity, FMDV performs its entire life cycle over a remarkably short time period – in tissue culture it has been estimated that FMDV can under go a full round of infection in under 3 hours – indicative of a sophisticated interplay between virus and host.

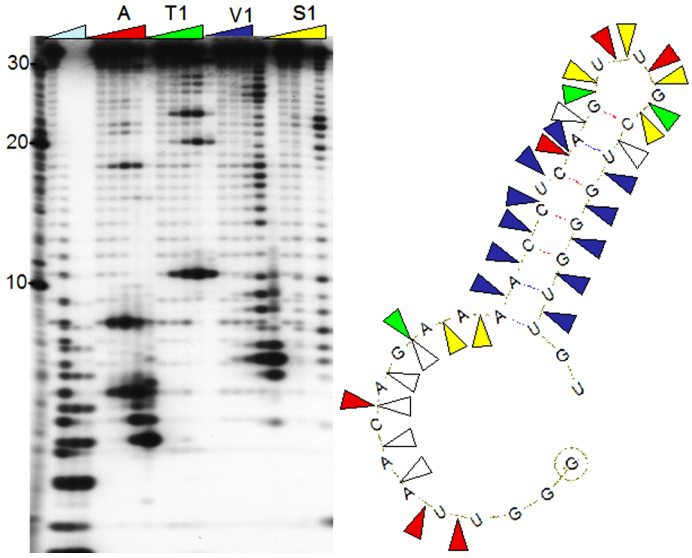

Figure 1 - Secondary structure probing of aptamer 47TR. Aptamer 47TR RNA was 5'end-labelled with 32P-ATP and incubated with a titration of; RNAse A (A: red triangles, cuts C+U), RNAse T1 (T1: green triangles, cuts ssG), RNAse V1 (V1: blue triangles, cuts base-paired RNA) and S1 nuclease (S1: yellow triangles, cuts single-stranded nucleic acid). The products were run on a denaturing gel and the banding pattern compared with the predicted mfold stucture.

Aptamers to study viral replication

A key stage in the life cycle of any virus is replication of its genome. In the case of FMDV, this is undertaken by a complex of both viral and cellular proteins centered on $3D^{pol}$, a virally encoded RNA-dependent-RNA polymerase. Previously, a series of aptamers have been raised against $3D^{pol}$, some of which have shown inhibitory function. We are currently building on this work by finding a 'minimal' aptamer sequence which still maintains an inhibitory ability. We have performed structure probing of the aptamer RNA, which confirmed mfold predictions, and foot-printing experiments to define the protein binding site on the aptamer RNA (Figure 1). We are now in a position to perform co-crystalisation of the truncated aptamer and 3Dpol to establish where these aptamers bind on $3D^{pol}$.

As well as elongation of the nascent strand $3D^{pol}$, and particularly its precursor 3CD, are involved in the priming of this reaction. In common with all other picornaviruses, of which FMDV is a family member, priming of the nascent strand is achieved using a virally encoded protein (VPg), covalently linked via a 5'uridine. Little is known about the mechanisms of this uridylyation reaction: a crucial first steps in genome replication. We hope to generate a range of aptamers, each specific to a protein component of the replication complex, in order to pare-apart both physically and temporally, the protein-protein and the protein-RNA interactions involved in uridylyation and subsequent genome replication.

Publications

Mark Ellingham, David H.J. Bunka, David J. Rowlands, and Nicola J. Stonehouse. Selection and characterization of RNA aptamers to the RNA-dependent RNA polymerase from foot-and-mouth disease virus. *RNA* (2006), 12:1970-1979

Collaborators

Prof Esteban Domingo, Madrid
Dr Nuria Verdaguer, Barcelona
Dr Graham Belsham, Denmark

Funding

Funding from BBSRC is gratefully acknowledged.

Understanding the recruitment and processivity of the staphylococcal helicase PcrA in the context of plasmid replication

Gerard P. Lynch, Neil H. Thomson and Christopher D. Thomas

Background

The helicase PcrA is not only essential for the viability of the Gram positive human pathogen, *Staphylococcus aureus*, but is also required for the rolling circle replication of staphylococcal plasmids such as pC221 – our model 4.6 kb plasmid encoding chloramphenicol resistance.

Work by our group and collaborators has previously centred on the interaction between the *Bacillus stearothermophilus* PcrA and the pC221 replication initiator protein, RepD. Advances in expression and purification of the staphylococcal helicase, resulting in greater yields of protein, have allowed us to return to a more homologous system to characterise the recruitment and processivity of the helicase by RepD.

Recent findings

RepD can nick and religate at its cognate *ori* sequence, *oriD*. In the presence of RepD the negatively supercoiled substrate pCER*oriD* is nicked and relaxed. RepD forms a covalent attachment to the nicked plasmid which is a prerequisite for unwinding by PcrA (Fig. 1). R189A is a mutant of RepD that can nick at *oriD* but cannot religate: this was used to generate a stable protein:DNA covalent adduct.

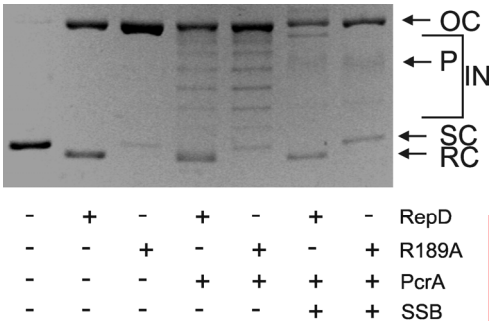

Fig. 1. Agarose gel showing nicking and unwinding of pCER*oriD*. OC, nicked open circular plasmid form; IN, partial unwound intermediates; SC, supercoiled; RC, relaxed covalently closed; P, main product in the presence of SSB.

Upon the addition of PcrA and ATP, partially unwound intermediates are observed. With further addition of single-strand DNA binding protein (SSB) these intermediate bands disappear, being replaced by a single, faint band (believed to be ssDNA, resulting from complete unwinding of the DNA) suggesting that this protein is also necessary for plasmid replication *in vivo*.

Fig. 2. Linear double stranded DNA is uniform in appearance (right). When linearised pCER*oriD* is incubated with R189K and PcrA the displaced, single strands forms a condensed, complex on the mica (top left). The scale bar represents 200 nm.

Recruitment of PcrA by RepD to a linear DNA substrate has also been visualised by AFM (Fig. 2). This approach will prove useful in future work characterising the dissociation of the helicase from the replisome at termination.

Publications

Zhang, W., Dillingham, M.S., Thomas, C.D., Allen, S., Roberts, C.J. & Soultanas, P. (2007) Directional loading and stimulation of PcrA helicase by the replication initiator protein RepD. *J. Mol. Biol.* **371,** 336-348.

Acknowledgements

We thank Neal Crampton, Jamie Caryl, Steve Carr and Simon Phillips (Leeds); Panos Soultanas (Nottingham), Martin Webb (Mill Hill) and Mark Dillingham (Bristol) for useful discussions and assistance.

Funding: This work was funded by the BBSRC.

Atomic force microscopy applications to living bacteria

Toby Tatsuyama-Kurk, Robert Turner, Simon D. Connell, David G. Adams, Deirdre Devine, Jennifer Kirkham and Neil H. Thomson

Introduction

Atomic force microscopy (AFM) provides the capacity to investigate live bacteria under liquid, such as physiological buffer or liquid growth media, and is able to resolve features as small as a few nanometres. It can also be used as a local force probe with piconewton sensitivity. We are working on two applications in this field; mapping molecular recognition events on the surface of bacteria present in the oral cavity and elucidating the mechanism of the surface gliding motility of cyanobacteria; a long standing mystery in microbiology.

Molecular recogntion force microscopy (MRFM)

Molecular recognition mapping is a technique complementary to labelling in confocal microscopy and allows the locations of target biomolecules to be identified in AFM images. The technique requires that a probe molecule (e.g. antibody) to be specifically linked to the end of an AFM tip. The force interactions it produces as the tip scans over a binding site can be used to map receptors on cell surfaces. It has a number of applications, for example, to study biopharmaceutical binding mechanisms and the modes of adhesion of clinically relevant bacteria to implants.

Staphylococcus aureus was selected as a species on which to develop molecular recognition mapping due to its clinical relevance. The scanning motion and local proximity of the AFM probe to the sample requires that cells are immobilised under liquid. Bacteria that are roughly spherical in shape, such as *S. aureus*, can be effectively trapped in the pores of a polycarbonate track etched (PCTE) filter membrane. The benefits of this method are that cells do not need to be dried, chemically treated, or exposed to adhesives; yielding a sample that is likely to be representative of *in vivo* conditions. Significant progress has been made in refining this technique using modified membranes with pore sizes tuned to suit the target bacteria (Fig. 1). Features of the cell wall, as small as 20 nm have been resolved.

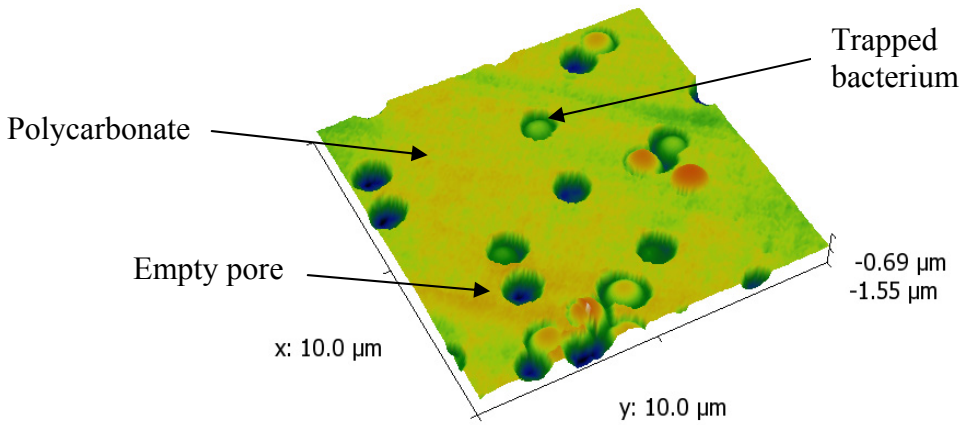

Fig. 1 – S. aureus (NCTC 8532) cells immobilised in a PCTE filter and imaged using tapping mode AFM under PBS. Scan size: xy = 10 µm; Height scale = 2.25 µm.

Cyanobacterial motility

Cyanobacteria are of huge ecological significance within the nitrogen and carbon cycles and are thought to have been critical for the development the today's oxygen-rich atmosphere. While most motile bacteria swim by means of flagella, many species of filamentous cyanobacteria are able to move on surfaces without flagella. This process is termed "gliding motility." Long filaments of conjoined cylindrical cells translocate lengthwise over surfaces

at rates of up to 10 μm s^{-1}, without flagella or other external organelles, and with no visible contractions or changes of shape. Translocation is accompanied by rotation around the filament axis, and frequent reversals of the direction of motion. It is proposed that the motile force is generated by travelling waves that are propagated over the cell surface by an unknown motor protein.

An array of 35 nm wide parallel fibrils that spans the cell surface, located between the outer membrane and peptidoglycan, has been observed in some species (Fig. 2). These fibrils are composed of a protein which is a likely candidate for the motor; recent sequence analysis of this protein indicated some homology with the motor protein that forms the contractile tail sheath of myoviruses.

Filamentous bacteria require a different immobilisation strategy to pore trapping, and the difficulty of immobilising cyanobacteria for AFM is further compounded by encapsulating layers of lubricating polysaccharide slime, as well as their motile nature. A novel solution is to mechanically trap the cyanobacterial filaments by partially embedding them in soft wax, and this has produced some of the first AFM images of living filamentous bacteria (Read *et al*., 2007). To test the surface wave motility hypothesis the AFM will be used as a local force probe to study the dynamics of the living cell surface with high temporal and spatial resolution. One of the obstacles to performing these experiments has been the unexpected degree of variability in the condition of the surface of these large and complex bacteria, and their encapsulating slime layers. This has been confirmed through the use of FEG-SEM imaging which is complementary to the local surface imaging of the AFM. New methods to orient and adhere cyanobacteria to surfaces for AFM investigation under buffer are now being explored.

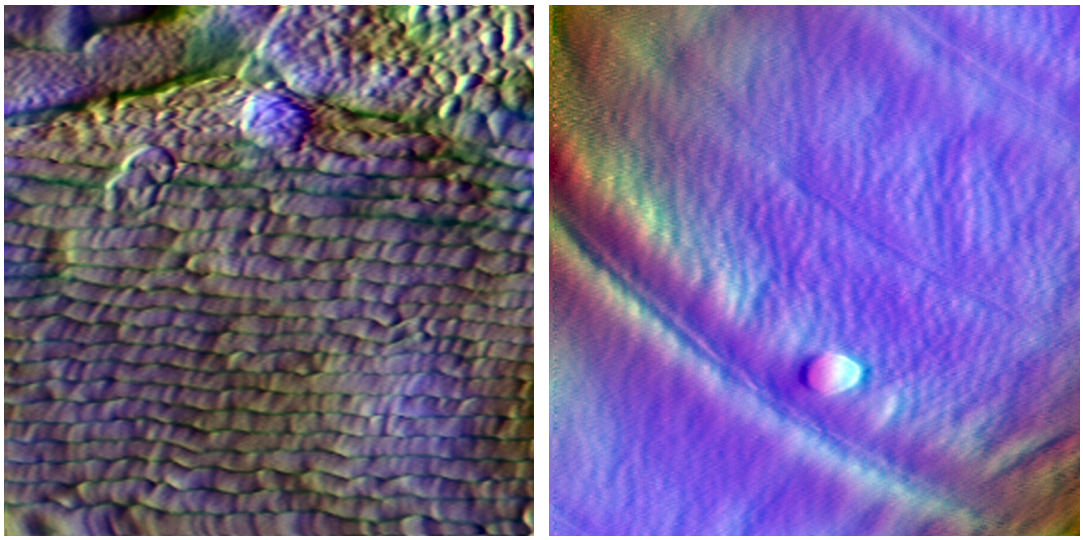

Fig. 2 - AFM of cyanobacteria, multi-channel false colour composite images. Left panel: Oscillatoria sp. A2 dried on mica imaged in air. Detail of surface fibrils. Scan size: xy = 1 μm; Height z = 100 nm. Right panel: *Oscillatoria princeps*, live under liquid growth media, immobilised in wax showing surface detail. Scan size: xy = 12 μm, z = 4.5 μm.

Publications

Read, N., Connell S., Adams, D.G. (2007) Nanoscale Visualization of a Fibrillar Array in the Cell Wall of Filamentous Cyanobacteria and Its Implications for Gliding Motility. *J. Bacteriol.* **189**, 7361 - 7366.

Funding

This work was funded by the EPSRC, MRC, The Leverhulme Trust and the University of Leeds.

The NMR solution structure and dynamics of K7: "A poxvirus protein that adopts a Bcl-2 fold"

Arnout P. Kalverda, Gary S. Thompson and Steve W. Homans

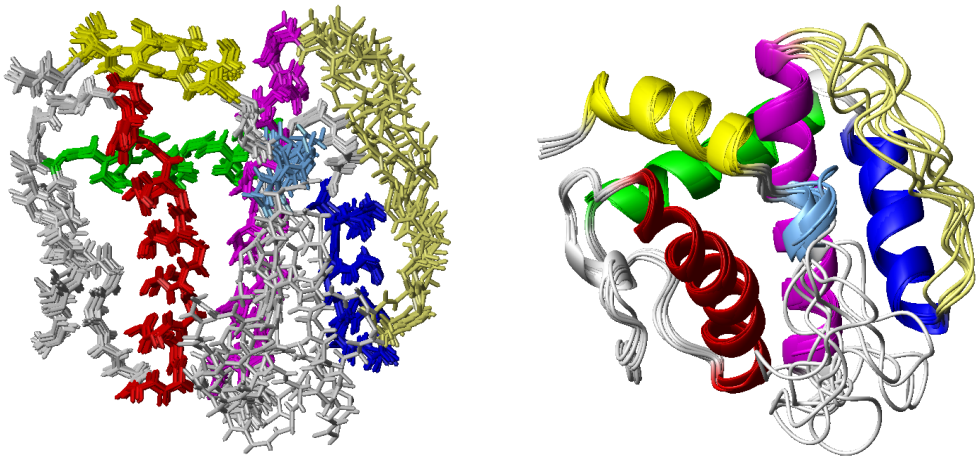

Poxviruses have evolved numerous strategies to evade host innate immunity. Vaccinia virus (VACV) proteins A46 and A52 were previously shown to antagonize Toll-like receptor (TLR) dependent signaling pathways. Vaccinia virus K7 is a 149-residue protein with previously unknown structure that is highly conserved in the orthopoxvirus family. K7 bears sequence and functional similarities to A52, which interacts with several cellular partners to suppress NF-κB anti-viral pathways and stimulate the secretion of the anti-inflammatory cytokine IL-10.

We determined the NMR solution structure of K7 using a novel protocol combining the Marvin/PASD approach of XPLOR-NIH for initial structure calculation with refinement via ARIA 2.2. This protocol did not require manual assignment of nOe spectra. The structure of K7 reveals an α-helical fold belonging to the Bcl-2 family despite having an unrelated primary sequence. ^{1}H-^{15}N dynamics measurements show fast dynamics and conformational exchange to be present in two disordered meander regions in the structure which are present as α̃ helices in the Bcl-2 family of structures. The high sequence homology of these regions in K7 and A52 suggests that they contain an interaction site which is common to the binding partners of both these proteins.

Funding & Collaborators

We would like to acknowledge our collaborators Andre Vogel, Raymond Chambers, Martina Schroder, Andrew G. Bowie, Amir R. Khan from School of Biochemistry and Immunology, Trinity College Dublin and funding by Science Foundation Ireland.

3D reconstruction of mammalian septin filaments

Natalya Lukoyanova, Stephen A. Baldwin and John Trinick

Introduction

Septins are a conserved family of GTP-binding proteins implicated in diverse processes, including cytokinesis, protein scaffolding, and vesicle trafficking. It has been hypothesized that septin exists as a cytoskeletal polymer. Here we present the 3D density map of septin filaments determined using single-particle analysis of images obtained by negative stain electron microscopy.

Methods

A mixture of septin isoforms 3, 5, 7a and 7b were isolated as from rat brain. The preparations were examined by negative stain electron microscopy and the images digitized and imported into the single particle image processing programs Spider and Eman.

Results

SDS-PAGE of the septin preparations showed four main bands with molecular weights 40-50 kDa. Identification of these bands as septins was by western blotting and N-terminal seq-uencing. Gel filtration chromatography indicated the size of the complex was ~240 kDa, consistent with the presence of two copies each of septins 3,5 and 7. Negative stain electron microscopy showed rod-like filaments with a variable length of 24-32 nm and width 7-8 nm. 3500 particle images were windowed out from digitized micrographs. Reference-free alignment and classification indicated a main group of filaments 27 nm long, together with a smaller group 32 nm long. The image averages showed considerably more detail than the raw data, where the filaments were featureless (Fig 1).

Figure 1. Image averages of the 27 nm septin filaments. Each panel contains the average of about 60 images

Figure 2. 3D reconstruction of septin filament.

3D reconstruction of 2115 shorter filaments was carried out using a row of spheres or continuous helical density as starting models. After approximately 40 iterations of refinement, both models of converged to very similar reconstructions. The reconstruction revealed the apparent presence of three subunits, each separated by a transverse cleft; these subunits were similar but not identical, possibly indicating multiple septin isoforms within each filament. In some views a smaller cleft appeared to separate the subunits into two smaller regions, perhaps reflecting the presence of septin dimmers (Fig 2). Subsequent iterations (40–60) yielded no changes in the structure, cross-correlation between raw images and the projections of reference volumes, or resolution of the reconstruction. A comparison of 3D volumes obtained using the different starting models revealed no major differences at

the final resolution of 27 Å. This structure was highly reproducible when the entire algorithm was repeated on multiple occasions. This is the first 3D reconstruction of the native septin assembly and appears compatible with the hypothesis that the septin complex is a hexamer consisting of dimers or heterotrimers.

Publications

Lukoyanova N, Baldwin SA & Trinick J. (2008). 3D reconstruction of mammalian septin filaments. *J Mol Biol* **376,** 1-7.

Funding

This work was supported by the BBSRC.

3D Reconstruction of a large protease complex from *Haemonchus contortus*

Stephen Muench, Chun Feng Song, Chris Kennaway and John Trinick

Introduction

The economically important nematode *Haemonchus contortus* is a blood feeding parasite that affects the stomach of ruminants, notably sheep. Substantial protection against the parasite has been achieved by immunising sheep with H-gal-GP, a large galactose containing glycoprotein complex located in its intestinal membranes. The complex is involved in the digestion of the parasite's blood meal and is composed of 4 zinc metalloendopeptidases, Cys protease galectins, cystatin, thrombospondin and a pepsinogen-like protein. Its overall molecular weight was determined by High-Mass MALDI ToF analysis to be 981 +/- 10 kDa. We have studied the structure of the complex by cryo-electron microscopy and image processing to obtain a 3D reconstruction.

Methods

Single particle/cryo-EM was conducted using 3mg/ml protein placed on glow discharged lacey carbon grids. The grids were imaged using a Technai F20 microscope, with data collected using a magnification of 69K on a Gatan 4K CCD camera. In total ~9,000 particles were windowed and processed. The resulting classes showed an apparent two fold symmetry (Figure 1). An initial model was generated using the angular reconstruction method in IMAGIC5, which was subsequently independently refined in both IMAGIC5 and EMAN6, with both programs converging on the same result. Resolution calculated with the Fourier shell correlation procedure was 17 Å using a 0.5 cut off.

Figure 1. The first 96 classes (left) and the corresponding reprojections (right) from the final refined H-gal-GP model.

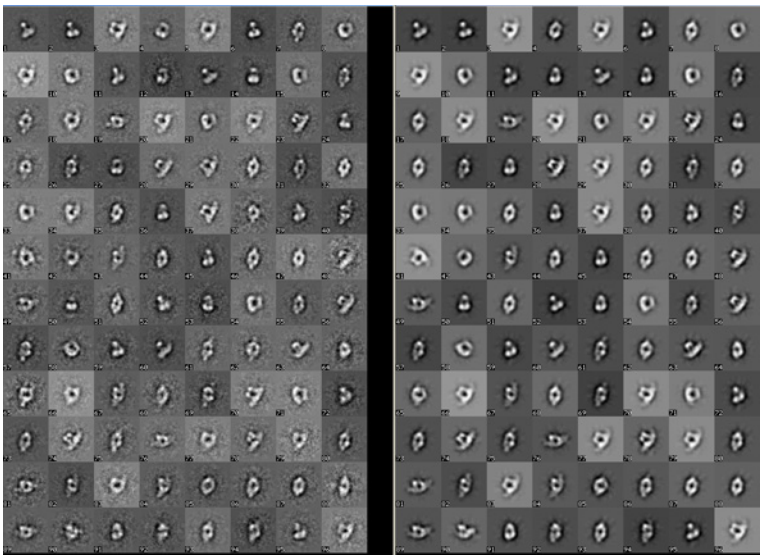

Results

The structure of the H-gal-GP complex reveals apparent 2-fold symmetry which contains a hole through the centre with the approximate dimensions of 3.5 x 6 nm (Figure 2). There is a large "arch" over the base which could accommodate the bulk of the haemoglobin substrate and the base is of an appropriate size for it to be easily accommodated by the intestinal membrane, which would expose the arch structure to the solvent allowing for substrate binding. The pepsinogen domains, which display vaccine protection and as such are likely to

be solvent-exposed, fit into the top of the arch region with their active sites facing inside the arch into the proposed active site. This is the first cryo-EM reconstruction of a large metalloendopeptidase complex and future work with bound substrates and antibody labelled subunits should allow more detailed characterisation of this important vaccine target.

Figure 2. The H-gal-GP complex as seen from the side(a), top (b), bottom (c) and front (d). The dimensions of the central "hole" are sufficient to accommodate the haemoglobin structure.

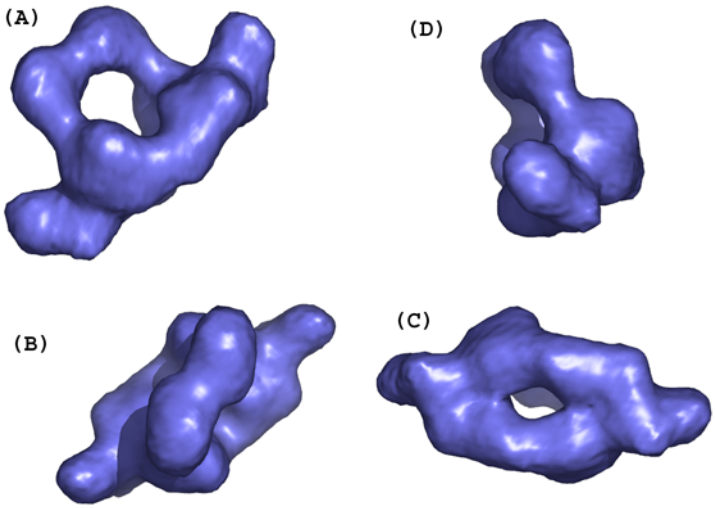

Collaborators

David Smith, George Newlands and Susan Taylor (all from the Moredun Research Institute, Edinburgh).

Structure and self-assembly of antennae pigments in green photosynthetic bacteria

Roman Tuma

Chlorosomes are large light harvesting complexes found in sulphur (*Chlorobiaceae*) and filamentous (*Chloroflexaceae*) green photosynthetic bacteria. Because of the high light harvesting efficiency of chlorosomes, species of green bacteria are capable of surviving under extremely low-light conditions, e.g. in depths of lakes and oceans. Hence, the chlorosome is considered a good model for developing highly efficient artificial light harvesting systems and other sensitive photonic devices.

A typical chlorosome is an ellipsoidal body (200 nm x 50 nm) which is attached to the inner leaflet of bacterial plasma membrane and contains on the order of 10^5 bacteriochlorophyll molecules (the major chlorosomal pigment), plus additional minor pigments (bacteriochlorophyll a, carotenoids and quinones) and several protein species. However, bacteriochlorophyll molecules are self-assembled into tightly packed, curved lamellar stacks (Fig. 1) without the support of structural proteins. The resulting dense packing assures strong excitonic coupling between pigments which, in turn, is the basis for fast energy transfer within the chlorosome.

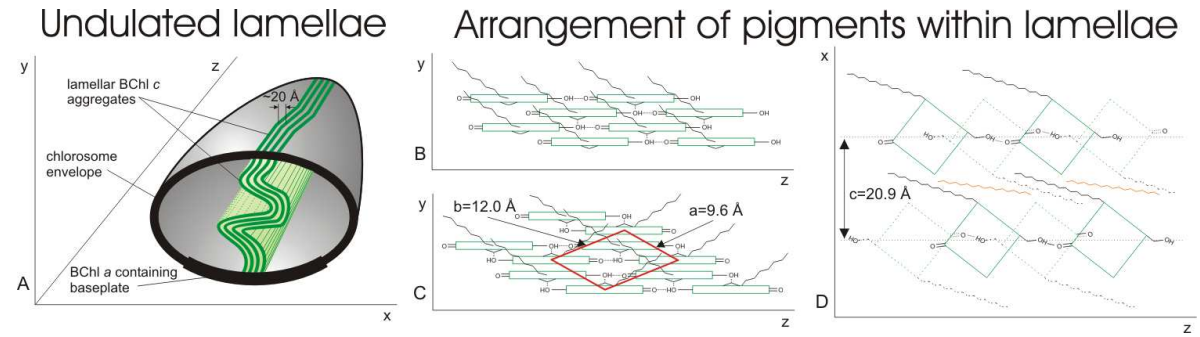

Figure 1: (A) A schematic cross-section through the chlorosome showing the internal lamellar structure. (B-C) The two-plausible arrangements (parallel in B and anti-parallel in C) of bacteriochlorophyll molecules (green) within the lamellar stacks. (D) Partitioning of carotenoids (red) within the hydrophobic phase of the lamellae. Lamellar spacing, c ~2.1 nm, for *Chlorobium tepidum* chlorosomes.

We use a combination of solution X-ray scattering, cryo-electron microscopy and optical spectroscopy to gain insight into chlorosome structure and self-assembly of chlorosomal pigments. The results demonstrated that carotenoids are essential for bacteriochlorophyll assembly. They partition into the hydrophobic phase created by the aliphatic chains of esterifying alcohols (e.g. farnesols) within the lamellae and augment the self-assembly process (Fig 1D). Consequently, lamellar spacing increases with the length of farnesol chains and the amount of carotenoids. Our recent results indicate that the short-range order of pigments can be reversibly restored *in vitro*. However, the long-range lamellar order that is often seen in intact chlorosomes is irreversibly lost upon disassembly in vitro and thus has to result from a template-assisted assembly. The results provide basis for engineering pigment systems suitable for directed self-assembly on surfaces and within prefabricated nanostructures.

Publications

Ikonen, T.P., Li, H., Psencik, J., Laurinmäki, P., Butcher, S.J., Frigaard, N.-U., Serimaa, R.E., Bryant, D.A. & Tuma, R. (2007) X-ray scattering and electron cryomicroscopy study on the effect of carotenoid biosynthesis to the structure of *Chlorobium tepidum* chlorosomes. *Biophys. J.* **93**, 620-28.

Arellano, J.B., Torkkeli, M., Tuma, R., Laurinmäki, P., Melø, T.B., Ikonen, T.P., Butcher, S.J., Serimaa, R.E. & Psencık, J. (2008) Hexanol-induced order-disorder transitions in lamellar self-assembling aggregates of bacteriochlorophyll *c* in *Chlorobium Tepidum* chlorosomes. *Langmuir* **24**, 2035-41.

Funding

This work was funded by Academy of Finland and the national agencies of the participating countries.

Acknowledgements

This is an ongoing collaboration between several groups: Profs. Sarah Butcher and Ritva Serimaa at the University of Helsinki, Finland, Dr. Jakub Psencik at Charles University, Prague, Czech Republic, and Dr. Juan Arellano at CSIC, Salamanca, Spain. The work on role of carotenoids in chlorosome biogenesis was done in collaboration with Prof. Donald Bryant at Penn State University, University Park, USA.

Structure, mechanism and application of viral RNA packaging motors

Roman Tuma

Molecular motors are nanoscale devices that convert chemical energy into mechanical work and motion. Helicases represent a special class of molecular motors that translocate along nucleic acids and unwind double helices into their parental strands at the expense of ATP hydrolysis. Helicases play essential role in all aspects of nucleic acid metabolism ranging from replication, transcription termination to repair. Many viruses utilize various helicases during their replication cycle. Double stranded (ds) RNA bacteriophages (*Cystoviridae* family) employ a hexameric helicase, protein P4, as their packaging motor, i.e. a device that translocates the genomic ssRNA precursors into preformed empty procapsids (Fig. 1A).

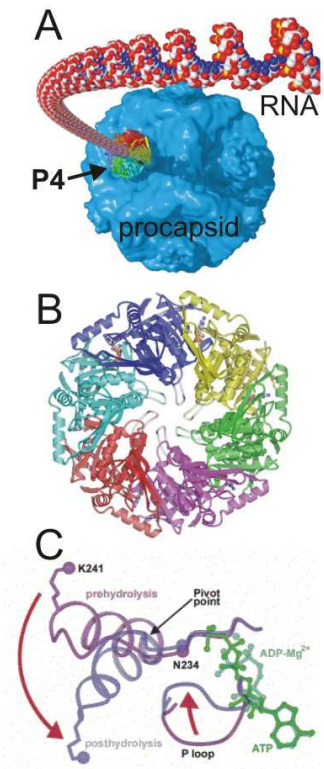

Figure 1: (A) P4 hexamer is located at each of the 12 five-fold vertices of the icosahedral procapsid (blue). One hexamer is highlighted and shown to package ssRNA. (B) Hexamer structure. (C) Conformational changes associated with ATP hydrolysis. The RNA binding site, K241, is located at the tip of α-helical lever position of which is controlled by the nucleotide occupancy of the active site.

The P4 hexamer is structurally related to the DnaB family of hexameric helicases (F4 super family) (Fig 1B). X-ray diffraction revealed conformational changes that may be associated with RNA translocation (Fig. 1C). Concerted structural and biophysical investigation of site directed mutants suggested a plausible mechanism of coupling between the mechanical motion and ATP hydrolysis. This mechanism is being tested by single molecule techniques.

The P4 motor represents one of the simplest nucleic acid "pumps" and thus may serve as a starting point for engineering "smart", self-assembling, molecular machines for detection and manipulation of single nucleic acid molecules. One example of such machine is a combination of P4 hexamer with α-hemolysin nanopore which constitutes a novel device for pumping ssRNA across membranes.

Publications

Wallin, A.E., Salmi, A. & Tuma, R. (2007) Step measurement - Theory and simulation for tethered bead constant-force single molecule assay. *Biophys. J.* **93**, 795-805.

Astier, Y., Kainov, D.E., Bayley, H., Tuma, R. & Howorka, S. (2007) Stochastic detection of motor protein-RNA complexes by single-channel current recording. *ChemPhysChem*, **8**, 2189-94.

Kainov, D.E., Mancini, E.J., Telenius, J., Lisal, J., Grimes, J.M., Bamford, D.H., Stuart, D.I. & Tuma, R. (2008). Structural basis of mechano-chemical coupling in a hexameric molecular motor. *J. Biol. Chem.* **283**, 3607-17.

Funding

This work was funded by Academy of Finland.

Acknowledgements

The biochemical and biophysical aspects of the work were carried out by present (Anders Wallin) and past (Drs. Jiri Lisal and Denis Kainov) members of my group at University of Helsinki. The structural work was carried out in collaboration with Dr. Erika Mancini and Prof. David Stuart, University of Oxford. Application to single molecule sensing was done in collaboration with Dr. Stefan Howorka at University College London and Prof. Hagan Bayley at University of Oxford.

Inhibiting bacterial toxin adhesion using protein aggregation

Cristina Sisu, Edward Hayes, Andrew Baron, Simon Connell and Bruce Turnbull

Introduction

Cholera and travellers' diarrhoea are still life threatening diseases in many parts of the world. These two diarrhoeal diseases are caused by protein toxins that share over 80% sequence identity; cholera toxin and *E. coli* heat-labile toxin. Their AB_5 hetero-oligomeric structures comprise a single toxic A-subunit and a pentameric B-subunit that interacts with the cell surface glycolipid ganglioside GM1. Inhibitors of the B-subunit-GM1 interaction could provide a prophylactic treatment for these debilitating diseases. It has been shown that compounds bearing multiple copies of GM1 are potent inhibitors of B-subunit adhesion, and have been shown to give up to 47,500 times more efficient inhibition than monovalent GM1. Theoretical models describing multivalent interactions of cholera or heat-labile toxin usually assume that the protein does not aggregate on binding to multivalent ligands as the binding sites are all on the same face of the multimeric protein.

Isothermal titration calorimetry studies of GM1 dimers and tetramers interacting with the *E. coli* heat-labile toxin B-pentamer (LTB) have revealed little inherent increase in affinity compared to that of the monovalent GM1 ligand. Analytical ultracentrifugation experiments indicated that the ligands induce protein aggregation at sub-stoichiometric concentrations of ligand groups. Subsequent dynamic light scattering studies confirmed that space-filling networks of protein aggregates can form when as little as 10% of the binding sites are occupied. The mechanism and kinetics of the aggregation process are dependent on the valency of the ligands. Atomic force microscopy has been used to demonstrate that a divalent inhibitor induces head-to-head dimerisation of the protein toxin en route to higher aggregates. These studies suggest that designing ligands to have valencies that are mismatched with their protein receptors may provide a general strategy for receptor inhibition by aggregative mechanisms.

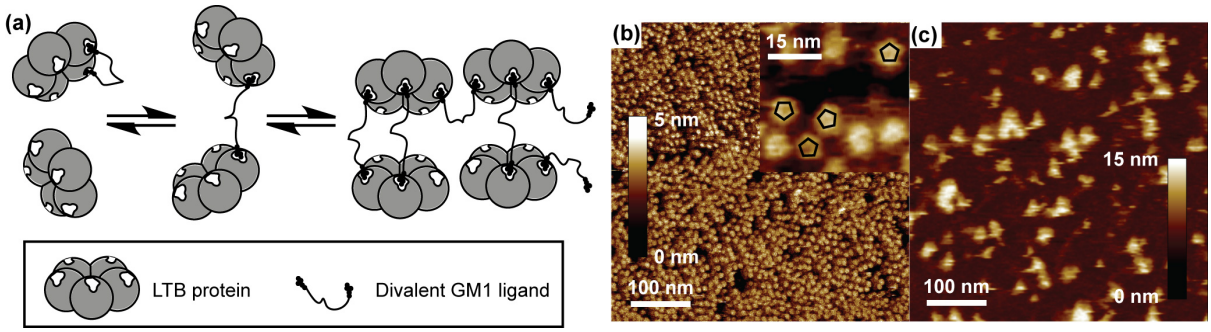

Fig. 1. (a) Cartoon representation of LTB aggregation by a divalent ligand. (b) AFM image of LTB pentamers on a mica surface. (c) LTB aggregates in the presence of one equivalent of the divalent ligand.

Collaborators

Gerben Visser, Han Zuilhof and Renko de Vries, Wageningen University, The Netherlands.
Roland Pieters, Utrecht University, The Netherlands

Funding

This work is supported by the Royal Society and the European Union COST programme.

Gene function and network prediction

James Bradford, Andy Bulpitt, Matthew Care, Chris Needham, Philip Tedder,
Elizabeth Webb and David Westhead

Introduction

With the growing size of sequence databases containing genes with little or no annotation, there is a pressing need for accurate, automated methods to predict gene function. Sequence homology based methods such as BLAST are now well established but are restricted to those sequences for which homologues exist. Therefore, a key task is to develop methods that use other data sources and provide added value over and above sequence information. With this in mind, much of the group's recent work, in collaboration with colleagues in the School of Computing, has focused on developing novel methods to predict aspects of gene function. Significant progress has also been made in tackling the related, but complex problem of reverse engineering gene networks from high-throughput co-expression data.

Gene function prediction using a naïve Bayes classifier

In this study, we have integrated five data types (sequence motifs, co-expression, protein-protein interactions, phylogenetic profiles and gene neighbourhood) into a naïve Bayes classifier in order to predict gene function in five example organisms: the plant *Arabidopsis thaliana*, *Homo sapiens* (human), *Mus Musculus* (mouse), the yeast *S. cerevisiae* and the malarial parasite *Plasmodium falciparum*. The key to the method is our functional classification scheme which exploits the terms and structure of the Gene Ontology (GO). Briefly, we cluster genes according to a semantic similarity measure between their GO annotations to create sets of organism-dependent functional classes representing 8 different levels of functional specificity (8=sharing the same highly specific function, 1=sharing a much less specific function). The strategy allows us to address three important questions:

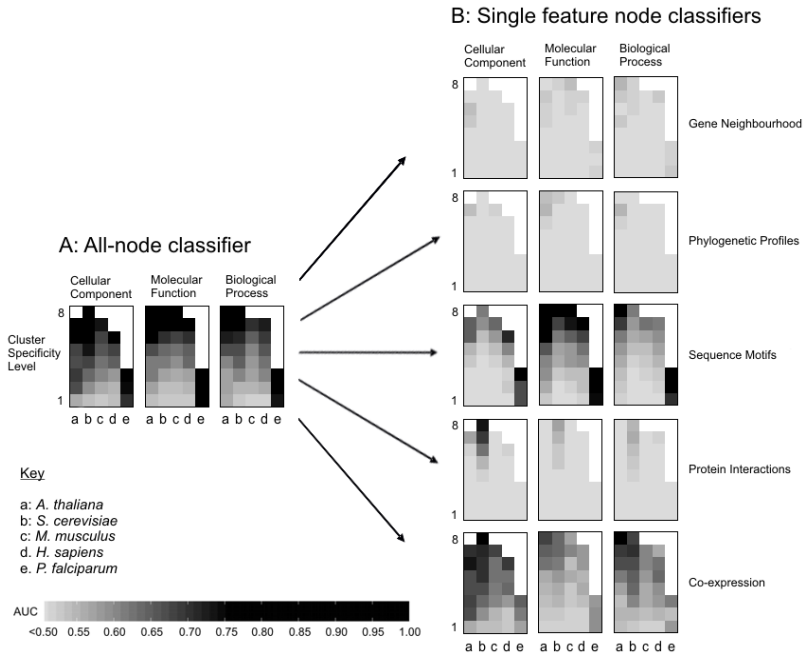

Figure 1: Performance of the Bayes classifier, A: integrating all data types, B: on each separate data type. Since this is a binary classification problem (do gene pairs occupy the same cluster or not?) we can assess performance using the area under ROC curve (AUC) statistic (perfect classification has AUC=1, no better than random has AUC=0.5). Separate analyses are presented for each GO category. Results cover the five different species, use five different sources of data, and are presented at the 8 different levels of functional specificity.

1. Can we distinguish gene pairs sharing cluster membership from those that do not? In other words, how well can our classifier predict functionally linked genes?
2. How does classifier performance compare between GO categories, cluster specificity levels and the five example organisms?
3. What are the individual contributions of each data type, and are some data types more applicable to certain situations than others?

Several conclusions can be drawn from Figure 1. First, it is clear that each of the data sources is predictive of

gene function, but the most predictive are sequence motifs and microarray co-expression data, with protein interaction data also highly predictive in the species where it is higher quality (*S. cerevisiae*). Information on the phylogenetic profile of the genes and their chromosomal location (gene neighbourhood) is less predictive, but above random. When information from all the data sources is integrated using an all node Bayes classifier, the performance is much better than any of the classifiers working on a single data type. As would be expected, sequence motifs are more predictive in the molecular function ontology than biological process or cellular location. Microarray co-expression data on the other hand is more predictive in the biological process and cellular component ontologies, again as might be expected. Future work will involve using these results to optimize the classifier for each organism and assign genes of unknown function to functional clusters.

PAGODA: Gene function prediction in *Plasmodium falciparum*

Malaria, caused by the parasite *Plasmodium falciparum*, is one of the world's most deadly diseases, and with growing resistance to conventional drugs, new treatments and vaccines are urgently needed. Accurate annotation of *P. falciparum* genes of unknown function is essential to facilitating this task, particularly since *P. falciparum* remains one of the most poorly annotated of all organisms with a sequenced genome. One of the main reasons for this is around 60% of its genes lack the orthologs required to infer function by established sequence homology methods such as BLAST. To circumvent this difficulty, we have developed a novel protein function prediction program called PAGODA (Protein Assignment by Gene Ontology Data Associations) that uses multiple sources of data such as co-expression and protein-protein interactions to augment available sequence information and annotate genes of unknown function with Gene Ontology (GO) terms across all three functional categories: molecular function, biological process and cellular component. Following promising results, the data and methods used in PAGODA are now being further developed to 'hole-fill' metabolic pathways by suggesting protein candidates for enzymes that are believed to exist in the *P. falciparum* genome, but have yet to be found. We plan to make the original PAGODA program and the 'hole-filling' method available online and accessible to the malaria research community.

Prediction of transcriptional associated proteins across species

Transcription is an essential process in DNA replication, repair, repackaging, recombination and regulation of gene expression. As such, proteins involved in these activities are potential drug targets and so their identification in pathogenic organisms like *P. falciparum* is an important goal. Consequently, we have developed TFHUNTER, a sensitive sequence based method that uses protein domain content and decision trees to predict proteins with the parent/child Gene Ontology (GO) terms "transcription", and "transcriptional regulator activity". Previous attempts to predict these terms have largely relied on information derived from protein structure, which is often unavailable. In contrast, TFHUNTER requires no such a priori knowledge, can be applied to raw un-annotated DNA sequence and is transferable between organisms.

Initially, TFHUNTER was applied to proteins of *S. cerevisiae*, assigning them to highly specific transcription-related GO terms with low error rates that outperform simple BLAST or InterPro Scan methods. The information learnt from these decision tree rules was then applied to other model organisms with encouraging early results. Successful transferability of this method between organisms will be crucial when applying confidence to less well annotated genomes like *P. falciparum* and newly sequenced genomes.

Disease gene prediction

There has been an increasing effort to develop computational methods to prioritize candidate genes within chromosomal linkage-intervals associated with human genetic disorders. One such method is to use 'interactome' information: the disease gene can often be located by looking at the known interaction partners of the genes in the interval and identifying those genes interacting with partners already implicated in similar disorders. Whilst this has proved effective when such partners exist, coverage is limited. A separate but related research area is the prediction of deleterious single nucleotide polymorphisms (SNPs). Methods have been developed by this group and others to attack this problem demonstrating high accuracies of 80% or above in cross-validation.

Given these findings, and that a protein with a deleterious SNP prediction is potentially involved in disease, it is natural to ask whether information about predicted deleterious SNPs can add value to current disease gene prediction methods. We have therefore augmented an existing and successful disease gene prediction method that uses interaction data with our own deleterious SNP prediction method that identifies non-synonymous SNPs within both the proteins in the linkage-interval and their interaction partners. We carried out in-depth benchmarking with increasingly stringent data-sets, reaching precisions of up to 75% (19% recall) for 10Mb linkage-intervals (averaging 100 genes). For the most stringent (worst-case) data we attained an overall recall of 6%, yet were still able to gain precisions of up to 90% (4% recall). At all levels of stringency and precision we demonstrate that known disease proteins have more deleterious SNPs than 'neutral' proteins, and that this is also true of their interaction partners. In summary, the inclusion of information about predicted deleterious SNPs improves recall at all values of precision of existing computational methods to prioritize candidate genes within chromosomal linkage-intervals associated with human genetic disorders.

Inferring gene regulatory networks from microarray data

We are currently developing Bayesian network methods, facilitated by the use of High End Computing services, to identify possible causal connections in genetic regulatory networks from very large microarray datasets. Within the Bayesian network, nodes represent genes and edges represent regulatory interactions. Using an initial dataset containing around 20,000 *A. thaliana* genes in over 3000 experimental conditions, a structure learning algorithm identifies the network structure which is statistically most likely to have originated from the observed data. We have applied these computational inferences to learning networks involving a number of largely uncharacterized GATA transcription factors. Preliminary results shown in Figure 2 indicate reasonable learned connections between genes of the *A. thaliana* circadian clock, GATA factors and genes localised in the chloroplast.

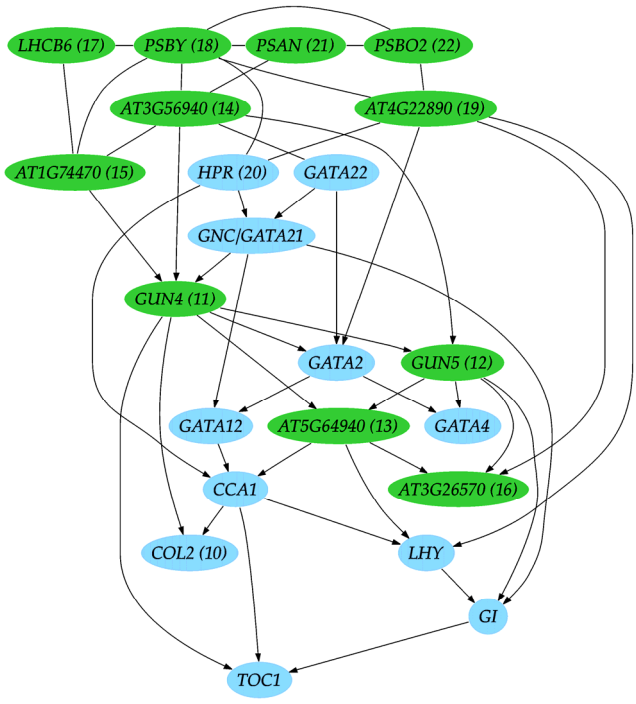

Figure 2: Learned connections between *A. thaliana* circadian clock genes, GATA transcription factors (all blue), and genes localized in the chloroplast.

Publications

Care, M.A., Needham, C.J., Bulpitt, A.J. & Westhead, D.R. (2007) Deleterious SNP prediction: Be mindful of your training data! *Bioinformatics*. **23**, 664-672.

Needham, C.J., Bradford, J.R., Bulpitt, A.J. & Westhead, D.R. (2007) A primer on learning in Bayesian networks for computational biology. *PLoS Computational Biology*. **3**, e129.

Manfield, I.W., Devlin, P.F., Jen, C.-H., Westhead, D.R. & Gilmartin, P.M. (2007) Conservation, convergence, and divergence of light-responsive, circadian-regulated, and tissue-specific expression patterns during evolution of the Arabidopsis GATA Gene Family. *Plant Physiology*. **143**, 941-958.

Funding

This work was funded by the BBSRC.

Identification of the ribonucleoprotein complex required for efficient export of herpesvirus intronless mRNAs

James Boyne, Kevin Colgan and Adrian Whitehouse

Introduction

The nuclear export of mRNA composes one part of a larger network of molecular events that begin with transcription of the mRNA in the nucleus and end with its translation and degradation in the cytoplasm. During trafficking to the cytoplasm, a nascent mRNA undergoes numerous co-transcriptional processing steps, including 5' capping, splicing to remove introns and 3' polyadenylation. Of these events it has become clear that splicing is particularly important for mRNA nuclear export, as recruitment of multiprotein complexes required for mRNA export are bound to mRNA in a splicing dependent manner. Two multiple protein complexes, namely, hTREX and the EJC bind at separate locations on spliced mRNA. hTREX, which comprises Aly, UAP56 and the multiprotein ThoI complex, is recruited exclusively to the 5' end of the first exon, providing 5'-polarity and therefore directionality observed in mRNA export.

However, in contrast to the majority of mammalian genes, analysis of herpesvirus genomes has highlighted that most lytically expressed viral genes lack introns. Herpesviruses replicate in the nucleus of the host mammalian cell, and therefore require their intronless mRNAs to be exported out of the nucleus to allow viral mRNA translation in the cytoplasm. This therefore leads to an intriguing question concerning the mechanism by which the viral intronless mRNAs are exported out of the nucleus in the absence of splicing. To circumvent this problem, and to facilitate viral mRNA export, γ-2 herpes viruses encode the ORF 57 protein. ORF 57 interacts with Aly, binds viral RNA, shuttles between the nucleus and the cytoplasm and promotes the nuclear export of viral mRNA.

We are currently investigating how an intronless viral mRNP is assembled in KSHV and what role ORF57 plays in that process. We have shown that ORF57 interacts with hTREX and is essential for the recruitment of hTREX onto intronless viral mRNA transcripts. Importantly, ORF57 does not recruit the EJC to intronless viral transcripts. Moreover, we are currently determining how ORF 57 recognises the viral mRNA and allows recruitment of hTREX. This is the first system that has distinguished between hTREX and EJC *in vivo* and demonstrates that recruitment of hTREX alone to mRNA transcripts is sufficient for their nuclear export. Therefore, we believe this viral system is an exciting model to further study mRNA export mechanisms. We propose a model for herpesvirus mRNA export, whereby ORF57 mimics splicing in order to recruit the mRNA export machinery to intronless viral mRNAs.

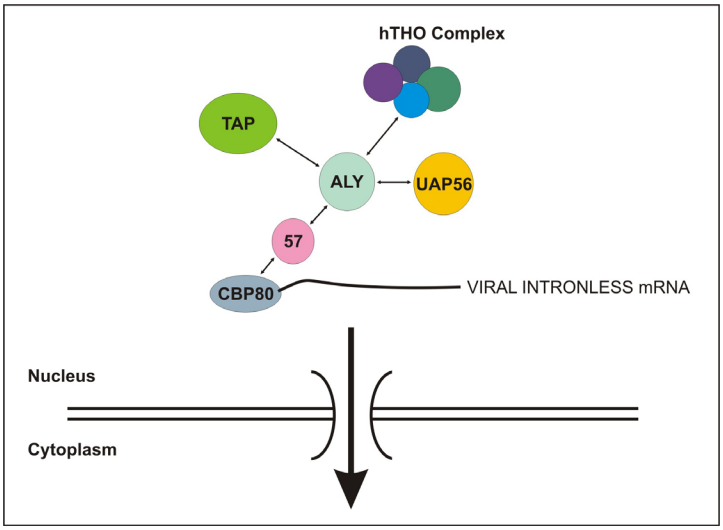

Figure: Assembly of the ribonucleoprotein complex required for efficient export of herpesvirus intronless mRNA

Publications

Boyne, J.R. & Whitehouse, A. (2006). Gamma-2 herpesvirus post-transcriptional gene regulation. *Clinical Microbiology and Infection,* 12, 110-117.

Boyne, J.R. & Whitehouse, A. (2006). Nucleolar trafficking is essential for nuclear export of intronless herpesvirus mRNAs. *Proc. Natl. Acad. Sciences, USA,* 103, 15190-15195.

Boyne, J.R. Colgan, K.J. & Whitehouse, A. (2008). Herpesvirus saimiri ORF57: a post-transcriptional regulatory protein. *Frontiers in Bioscience,* 13, 2928-2938.

Acknowledgements
This project is funded by the BBSRC and we wish to thank Professor Reed, Harvard University for providing hTREX reagents.

Development of a herpesvirus-based bionanosubmarine

Stuart McNab, Julian Hiscox and Adrian Whitehouse

Introduction

The continuing advances and understanding in the field of molecular and cellular biology, and the underpinning genetic control mechanisms, has allowed the creation and development of non-traditional means for treating disease to be pursued such as gene therapy and bionanomedicine. We are currently developing a bionanosubmarine which delivers therapeutic genes to the correct cell types. The bionanosubmarine is based on elements of Herpesvirus saimiri (HVS). We have previously shown that HVS can infect a variety of human cell types and upon infection the viral genome can persist as a non-integrated episome in both *in vitro and in vivo* studies. Therefore, HVS has great potential to be developed as a bionanosubmarine. To achieve this, the infectious delivery system of HVS needs to be retained, but the viral genes need to be deleted and replaced with therapeutic genes.

The bionanosubmarine comprises a two tier system created in tissue culture. It utilises the biosafety of an amplicon vector plasmid coupled with the natural infectivity of the wild type virus. The system creates a virus like particle (VLP) containing the transgene of interest expressed from an amplicon vector. The VLP particle is essentially the wild type viral coat preferably lacking, or with minimal immuno-stimulatory antigens exposed. The VLP is generated by a helper-virus genome which contains all the necessary structural genes while remaining replication deficient.

An amplicon is a gutless vector derived from a viral genome. The amplicon contains a transgene, the related expression sequences, and the *cis*-acting sequences required for replication, cleavage, and packaging into the VLP. The amplicon carries no transacting virus genes and consequently does not induce synthesis of virus proteins. Therefore, these vectors are non-toxic for the infected cells and non-pathogenic for the inoculated organisms. Another major advantage of the amplicon system is the removal of most of the virus genome, this consequently creates a transgene capacity equivalent in size to the wild type virus genome.

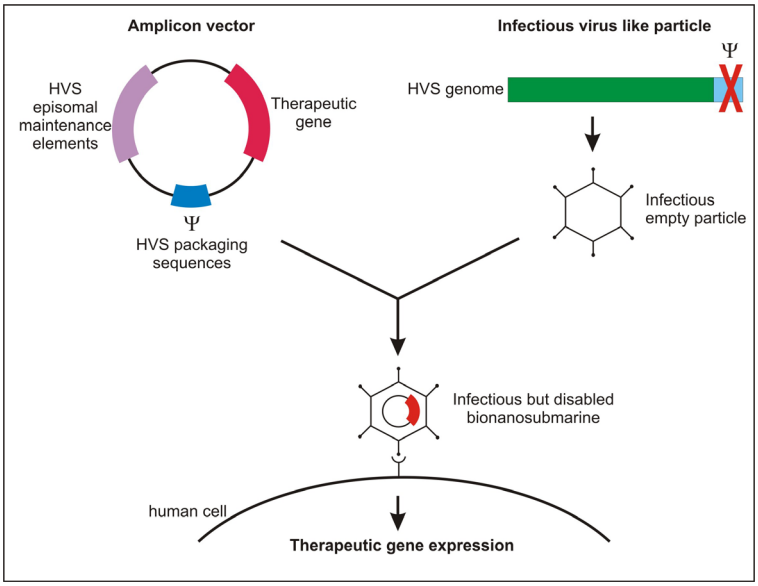

Figure: Methodology to produce a HVS-based bionanosubmarine

To date, we have produced a bionanosubmarine, namely the VLP containing the amplicon. We have demonstrated that the bionanosubmarine is exported from the culture cell in the normal manner of the wild type virus and can then be harvested from the culture system and is still infectious. In particular, we have delivered the transgene to multiple human carcinoma cell types. We are now improving the bionanosubmarine production system to produce submarines in higher quantities.

Publications

Griiffiths, R.A., Boyne, J.R. & Whitehouse, A. (2006). Herpesvirus saimiri-based gene delivery vectors. *Current Gene Therapy,* 6, 1-15.

Whitehouse, A. (2006). Gamma-2 Herpesvirus saimiri-based vectors, p 255-264. In Gene Transfer: Delivery and expression of DNA and RNA, a laboratory manual. *Cold Spring Harbor Laboratory Press.*

Griffiths, R.A. & Whitehouse, A. (2007). The interaction between ORF 73 and MeCP2 is essential for HVS episomal persistence. *Journal of Virology*, 81, 4021-4032.

Macnab, S., White, R.E., Hiscox, J.A. & Whitehouse, A. (2008). Production of an infectious Herpesvirus saimiri-based episomally maintained amplicon system *Journal of Biotechnology,* 134, 287-296.

Acknowledgements

This project is funded by the University of Leeds Interdisciplinary Institute of Bionanoscience.

Repressosome formation and disruption regulates the KSHV latent-lytic switch

Faye Gould and Adrian Whitehouse

Introduction

The etiological agent of Kaposi's Sarcoma, Kaposi's sarcoma associated herpesvirus virus (KSHV), is the most recently identified human tumour virus. KSHV has two distinct forms of infection, latent persistence and lytic replication. The switch between these phases is important as lytic replication plays an essential part in the pathogenesis and spread of KSHV infection. The KSHV ORF 50 protein is the key gene product which regulates viral lytic gene expression as sustained transient expression of ORF 50 in a KSHV-latently infected cell line leads to the stimulation of its own expression and consequently viral lytic replication. This implicates the ORF 50 protein as the molecular switch for reactivation and initiation of the KSHV lytic replication cycle.

We are currently investigating the host cell-ORF 50 interactions to further understand the role of KSHV ORF 50 in the latent-lytic switch. We have demonstrated that KSHV ORF 50 interacts with the cellular protein, Hey-1. Hey-1 functions as a transcriptional repressor, acting as adapter protein that binds to specific DNA binding sites within gene promoters, and subsequently recruits transcriptional repressosome complexes.

The interaction between KSHV ORF 50 and the transcriptional repressor protein Hey-1 is a particular intriguing one. Why would ORF 50 interact with a transcriptional repressor protein, given the role of ORF 50 in transcriptional activation and initiating the lytic replication cycle? However, we have shown that the Hey-1-ORF 50 interaction is an essential interaction playing a pivotal role in regulating the KSHV latent-lytic switch.

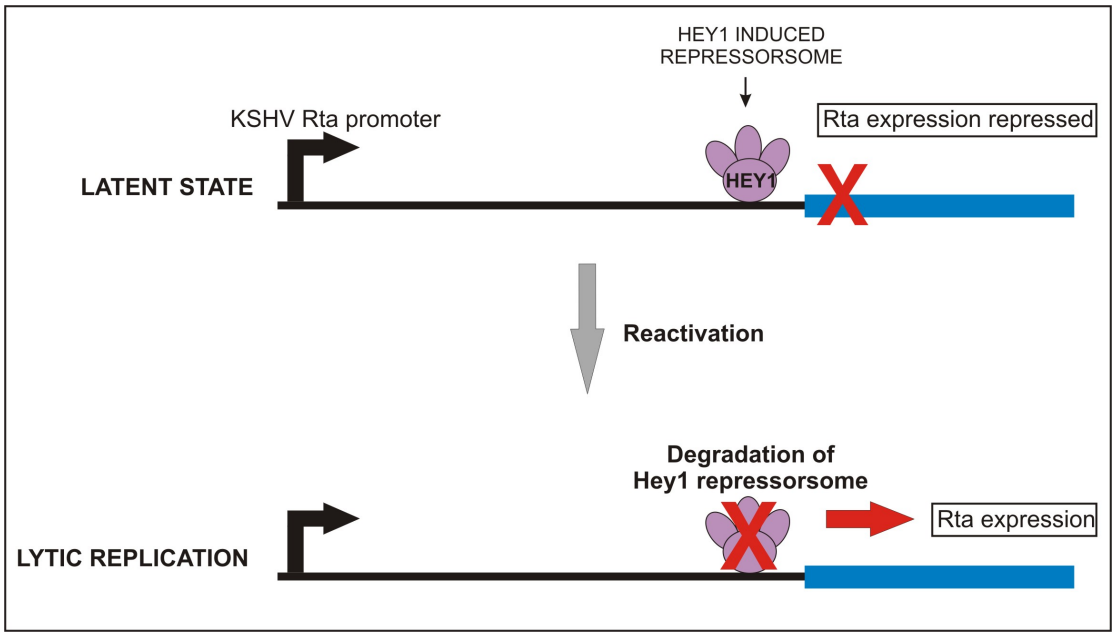

Figure: Repressosome assembly and disassembly regulates the KSHV latent-lytic switch

We have shown that Hey-1 specifically represses ORF 50 expression by binding the ORF 50 promoter and recruiting a functional repressosome, thus helping KSHV to remain in the latent state. However, we have also demonstrated that KSHV ORF 50 can act as an ubiquitin E3 ligase, which results in the degradation of Hey-1 via a proteasome-degradation pathway.

This disrupts the repressosome and allows ORF 50 expression leading to KSHV lytic replication.

We now aim to further characterise the DNA/protein and protein/protein interactions involved in KSHV reactivation and in the regulation of lytic gene expression. This analysis will also give further insights into the role of the cellular Hey-1 protein in transcriptional repression. Moreover, this project will provide valuable information on KSHV reactivation that may ultimately lead to the identification of specific antiviral targets to inhibit ORF 50–host cell interactions which may be developed as a novel treatment for this important human pathogen.

Publications

Wilson, S.J., Tsao, E., Webb, B.L., Ye, H., Dalton-Griffin, L., Tsantoulas, C., Gale, C.V., Du, D., Whitehouse, A. & Kellam, P. (2007). XBP-1 transactivates the KSHV ORF50 promoter, linking plasma cell differentiation to KSHV reactivation from latency. *Journal of Virology,* **81**, 13578-13586.

Acknowledgements
This project is funded by the Wellcome Trust and BBSRC.

Synthesis of α-helix mimetics: inhibitors of protein-protein interactions

Fred Campbell, Jeff Plante, Bara Malkova, Stuart Warriner,
Thomas Edwards and Andrew Wilson

Introduction

Although many cellular processes depend upon enzymatic reactions, protein-protein interactions (PPIs) mediate a large number of important regulatory pathways - thus an explosion of interest in their study mirrors a pivotal role in diseased states. Inhibition of protein function is traditionally achieved using molecules that masquerade as enzyme substrates. What is not clear is how to effectively target protein-protein interfaces with high affinity and selectivity using a small molecule; given that it must cover 800-1100Å of a protein surface and complement the poorly defined projection of hydrophobic and charged domains on a flat or moderately convex surface. We have initiated a program directed towards inhibition of α- helix mediated PPI's using small molecule scaffolds amenable to library synthesis

Synthesis and design

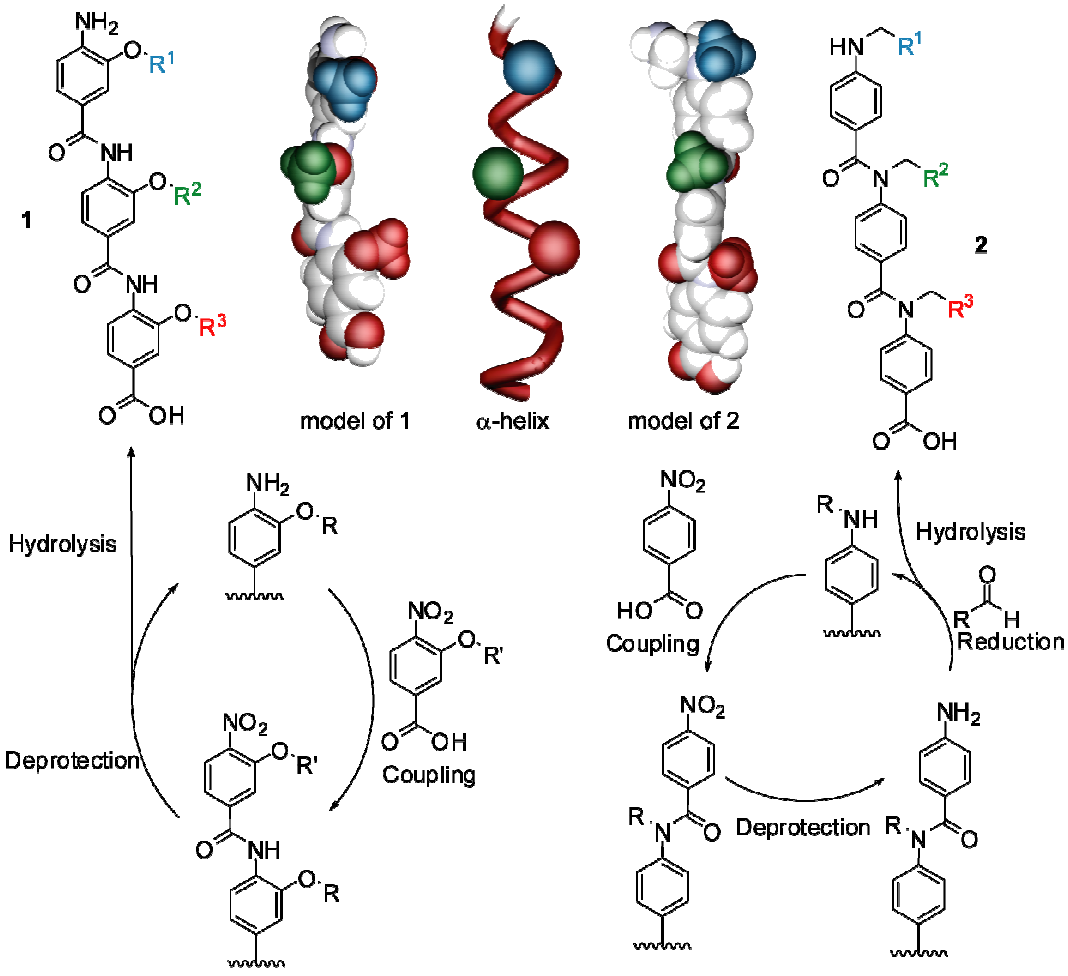

Figure 1. Design and synthesis of α-helix mimetics

A key motif observed at the interface of protein-protein interactions is the binding of an α-helix from one protein binding through it's i, i +3 (or 4) and i + 7 (or 8) residues to a cleft on its partner. We have designed two aromatic oligoamide scaffolds that project side chains in an identical 3D projection to mimic these key interfacial α-helix side chains (Figure 1). A solution phase strategy towards both has been optimised, allowing for inclusion of a multitude of functionality that mimics α-amino acid side chains (Figure 1). The *O*-alklyated

scaffold is held in a rigid rod like conformation as a consequence of the preferred *trans* conformation of the secondary benzamide. The scaffold is further rigidified by an intramolecular H-Bond from the amide NH to the alkoxy O - this restricts rotation about the aryl-NH bond. In contrast the preferred conformation of the *N*-alkylated tertiary benzamide is *cis* and the *N*-alklyated scaffold therefore adopts a helical conformation – although this does not preclude its use as an α-helix mimetic we expect protein affinities to be lower.

Inhibition of protein-protein interactions

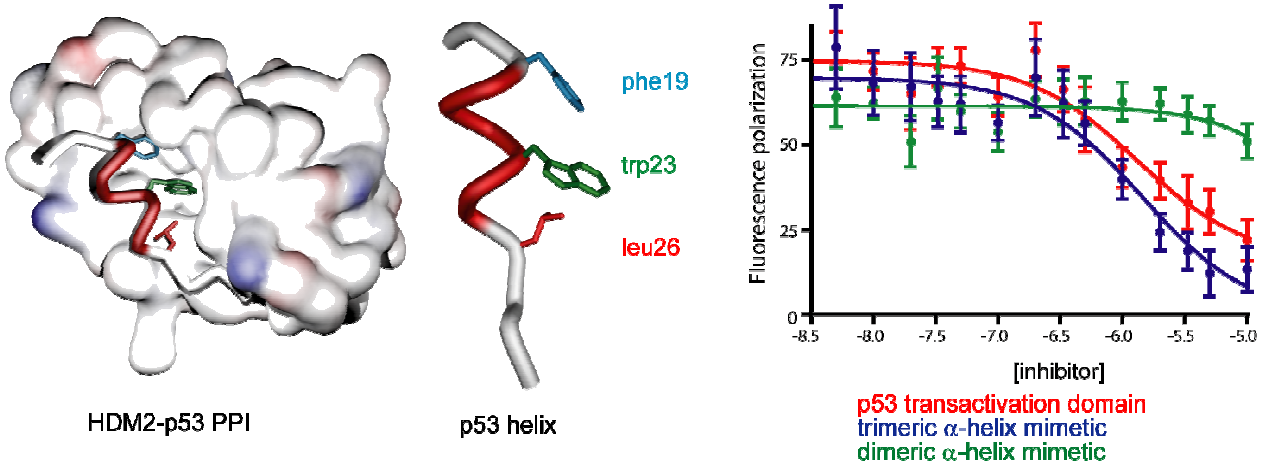

Figure 2. p53-HDM2 PPI and inhibition using synthetic molecules as evidenced by fluorescence polarisation assay

We selected the p53-HDM2 interaction as a model system with which to test our α-helix mimetics as inhibitors of protein-protein interactions. HDM2 is over-expressed in several cancers and so this interaction represents an important therapeutic target. The p53 binds in an α-helical conformation to HDM2 through three key residues (phe19, Trp23 and Leu26) as shown in Figure 2. The HDM2 clone was expressed in *E. coli* and used in a fluorescence polarization displacement assay. In this assay, polarization recovery on displacement of fluoresceine labelled p53 transactivation domain by synthetic ligands is used to determine K_i's (Figure 2). Our initial screening results indicate that trimers are able to inhibit the interaction with low μM affinity comparable to the native α-helix whereas dimers that do not mimic three full turns of an a-helix bind with low affinity.

Collaborators

We gratefully acknowledge the donation of the HDM2 clone from Prof J. Robinson University of Zurich

Publications

Plante, J., Campbell, F., Malkova, B., Kilner, C. A., Warriner, S. L. & Wilson A. J. (2008) Synthesis of Functionalised Aromatic Oligamide Rods. *Org. Biomol. Chem.* **6,** 138-146.

Campbell, F., Plante, J., Carruthers, C., Hardie, M. J., Prior, T. J. & Wilson, A. J. Macrocyclic Scaffolds Derived From Para-Aminobenzoic Acid. *Chem. Commun.* 2240-2242.

Funding

We gratefully acknowledge EPSRC, the University of Leeds and The Wellcome Trust for financial support of this research.

The end is not always in sight: multiple single-stranded segments can stimulate rapid cleavage by *Escherichia coli* RNase E

Louise Kime, Stefanie S. Jourdan, Jonathan A. Stead and Kenneth J. McDowall

Introduction

The factors that determine the longevity of transcripts in cells are central to gene regulation. RNase E, a single-strand-specific endonuclease, initiates the degradation of many mRNAs in *Escherichia coli*. It is widely described as being a 5'-end-dependent enzyme that requires a monophosphate group at the 5' end of its substrates in order to effect their efficient cleavage. Recently, a pocket that can bind a 5'-phosphate group has been identified in X-ray crystal structures of RNase E and evidence has been obtained by others that *E. coli* contains a pyrophosphatase that can process the 5'-triphosphate group of newly synthesized transcripts. These high profile publications have led to the notion that the efficient cleavage of RNA by RNase E can only proceed after the generation of a 5' end with a monophosphate group. Here we report for the first time that *E. coli* RNase E is capable of the rapid cleavage of substrates that lack a 5'-monophosphate group.

Results and discussion

While assaying the cleavage of a 5'-hydroxylated substrate by a preparation of RNase E, we noticed that the reaction appeared to biphasic: there was an initial phase (5-10 min) in which cleavage was rapid (Fig. 1). Further investigations revealed that (i) the addition of another aliquot of substrate, but not enzyme resulted in another phase of rapid cleavage; (ii) reducing the amount of enzyme significantly affected the amount of substrate that was cleaved rapidly, but not the duration of the first phase, and (iii) rapid cleavage could be eliminated by pre-warming the substrate to 37°C. This suggested that when heated the 5'-hydroxylated substrate underwent a relatively slow conformational change and that the conformation at low temperature was highly susceptible to RNase E cleavage, despite the substrate not having a monophosphate group at its 5' end.

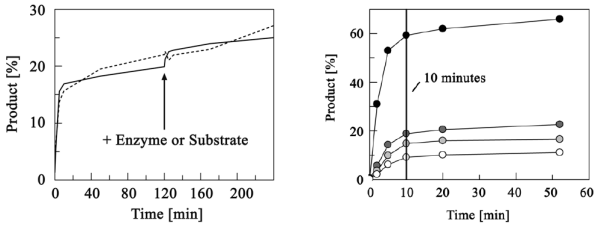

Fig. 1. Left panel, effects of adding an additional aliquot of enzyme (broken line) or substrate (solid). Right panel, effect of enzyme concentration on amount of rapidly cleaved substrate.

The substrate used in the above assays was a 3' fluorescein-labelled oligonucleotide that had three guanosines at the 5' end so that is sequence was identical to that of a transcript made by *in vitro* transcription. Circular dichroism revealed that the G-triplet allows BR13 to form a temperature-labile, tetramolecular quadruplex (Fig. 2). The positive maximum at ~264 nm and the negative minimum at ~240 nm are characteristic of a parallel topology. Additional experiments that include the characterisation of natural substrates suggest that the substrate requirement for rapid, 5'-end-independent cleavage is the presence of multiple single-stranded segments. This relatively simple requirement provides an explanation for why hindering translation can greatly increase the susceptibility of transcripts to degradation by RNase E. We propose that the tetrameric arrangement of *E. coli* RNase E permits multivalent interactions that greatly increase the affinity for RNA. Thus, although the decay of many transcripts in *E. coli* requires functional RNase E, not all cleavages are necessarily highly 5'-end dependent. Indeed, 'internal entry' may represent a major pathway for initiating mRNA in bacteria.

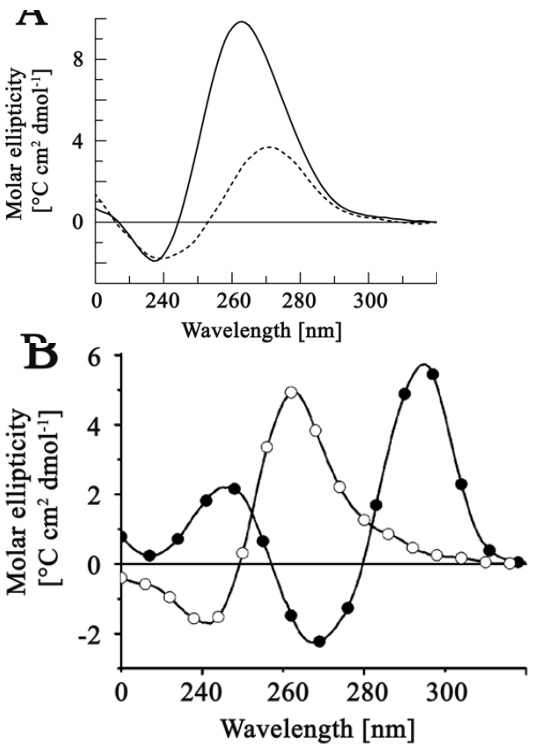

Fig. 2. CD spectra. Panel A, spectra of $_{HO}$-BR13-Fl at 4 and 37°C. Panel B, characteristic spectra of parallel (white circles) and antiparallel (black circles) quadruplexes.

Publications

Kime, L., Jourdan, S.S. & McDowall, K.J. (2008) Identifying and characterizing substrates of the RNase E/G family of enzymes. In *RNA Turnover in Prokaryotes, Archaea and Organelle: Methods in Enzymology,* Vol. 448. Eds. Maquat L.M. and Arraiano C.M..

McDowall, K.J. (2008) The chemistry, measurement, and modulation of RNA stability. In *Wiley Encyclopedia of Chemical Biology*, Vol 1. Ed. Begley T.P.

Funding

This work was funded by the European Union through the Marie Curie Actions and a BBSRC grant to K. J. M.

5’ sensing stimulates the decay of functional mRNA transcripts *in vivo*

Stefanie S. Jourdan and Kenneth J. McDowall

Introduction

The RNase E/G family of endoribonucleases is evolutionarily conserved in bacteria and plastids. Its members have a central role in RNA turnover in all organisms that have been studied. *Escherichia coli* encodes two homologues that participate in both the processing and the decay of RNA. The best studied to date is RNase E, which is essential for cell viability, but it is now known that its paralogue, RNase G cooperates in the maturation of 16S rRNA and is required for the normal decay of several transcripts including functional forms of *adhE* and *eno* mRNA. It has been shown, by us and others, that the cleavage of RNA by these enzymes *in vitro* can be enhanced by the presence of a 5’ monophosphate on the RNA, provided this group is immediately followed by a short segment that is single-stranded. 5’ monophosphate groups are accommodated in a pocket that is at the end of a channel leading to the active site. It has been proposed that the binding of a 5’ monophosphate induces an allosteric change in the protein that favours cleavage of the RNA. To investigate the importance of this 5’ interaction on the overall pattern of RNA processing and decay *in vivo* and the mechanism by which it stimulates cleavage by *E. coli* RNase E and related enzymes, we have constructed mutations in the 5’ monophosphate-binding pocket. Here we summarise our characterisation of these mutations within the context of *E. coli* RNase G, which unlike RNase E is non-essential. Thus, the analysis *in vivo* was not complicated by effects on overall growth.

Results and discussion

We found that the stimulation of endonucleolytic cleavages by a 5’ monophosphate makes a significant contribution to the decay of functional mRNA in *E. coli* and that this stimulation is the result of a substantial increase in the affinity of RNA binding as measured using fluorescence anisotropy and inferred from Michaelis-Menten parameters (Fig. 1). In mutants defective in 5’ end sensing, we detected an increase in the levels of AdhE and Enolase. Moreover, this was associated with increases in the abundance and stability of the corresponding transcripts (Fig. 2). The magnitudes of these increases were similar to those associated with complete disruption of the gene encoding RNase G. Thus, the ability to bind 5’ monophosphorylated RNA with high affinity appears critical to the function of RNase G and probably other members of its family.

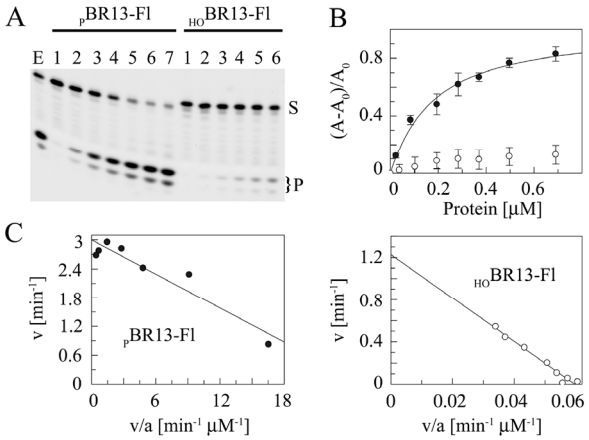

Fig. 1. Assay of RNA cleavage and binding by RNase G. Panel A, assay of 5’ monophosphorylated and 5’ hydroxylated substrate. Panel B, fluorescence anisotropy analysis of RNA binding via titration of protein. 5’ monophosphate and hydroxyl RNA are represented by closed and open symbols, respectively. The continuous line represents the best fit to a 1:1 binding model. Panel C, Eadie-Hofstee plots of RNA cleavage by RNase G. Taken from Jordan & McDowall (2008).

The finding that a 5’ monophosphate group stimulates association with RNA gives renewed credence to the notion that members of the RNase E/G family can degrade or process transcripts containing multiple cleavage sites that are separated from each other with a degree of processivity. The channel that links the 5’ monophosphate-binding pocket and the site of catalysis, which generates downstream products that have a 5’ monophosphate group, does

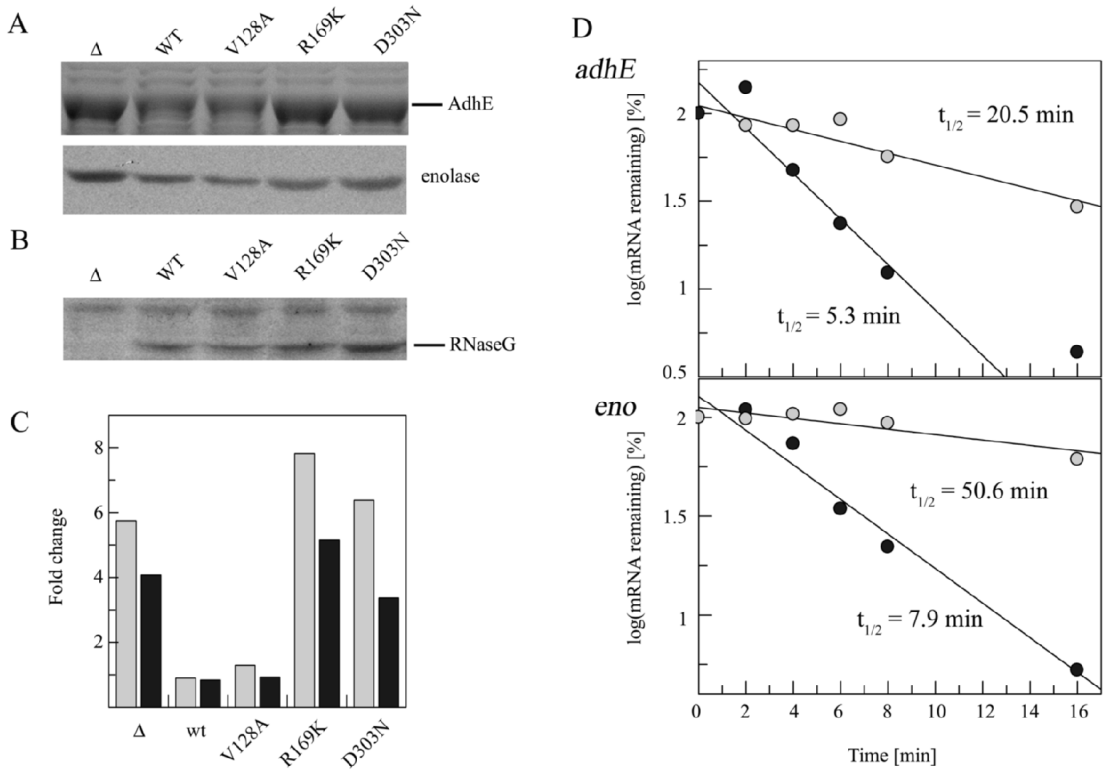

Fig. 2. Characterisation of the R169K sensor mutant. Panel A, levels of AdhE and enolase assayed by SDS-PAGE and Westerns, respectively. Panel B, Westerns of RNase G levels. Panel C, q RT-PCR analysis of *adhE* (light grey) and *eno* (black) mRNA. Panel D, decay of *adhE* and *eno* mRNA in cells containing wild-type RNase G (black circles) or the R169K mutant (grey circles). Taken from Jordan & McDowall (2008).

not appear from the crystal structure to make substantial sequence-specific contacts. Thus, following cleavage of a transcript at a particular site, it can be envisaged that the newly formed 5' end is well placed to engage with the monophosphate-binding pocket by moving along the channel and need not dissociate from the enzyme. The upstream product could dissociate passively or be actively removed by the action of exonucleases *in vivo*. This, and other, models are currently being tested using mutants that are defective in '5' end sensing'.

Publications

Jourdan, S.S. & McDowall, K.J. (2008) Sensing of 5 ' monophosphate by *Escherichia coli* RNase G can significantly enhance association with RNA and stimulate the decay of functional mRNA transcripts *in vivo*. *Mol. Microbiol*. **67**, 102-115.

Funding

This work was funded by the European Union through the Marie Curie Actions and a BBSRC grant to K. J. M.

Two-dimensional gel electrophoresis for identifying nucleic acid-binding proteins

Jonathan A. Stead and Kenneth J. McDowall

Introduction

The electrophoretic mobility shift assay (EMSA) has been used extensively to analyse nucleic acid–protein interactions for two decades. It is based on the finding that when a fragment of nucleic acid (the 'probe') is bound by protein, its electrophoretic mobility is retarded when compared to its free state. Thus, the final position of a labelled probe when bound by protein appears shifted. Accordingly, the EMSA is also referred to as the gel shift or gel retardation assay. Even relatively labile nucleic acid–protein complexes (with apparent dissociation constants in the range of hundreds of nM) can be analysed using EMSAs as the gel matrices provide a stabilising 'caging effect'. Complexes are also stabilised by the use of electrophoresis buffers with relatively low ionic strength.

Although the EMSA is used widely to detect the presence of nucleic acid-interacting factors and to assess the specificity and affinity of interactions, for the purpose of identifying the actual polypeptide(s) that interacts with a particular probe, many laboratories, including our own, have resorted to purifying the binding factor. This is often a laborious and time-consuming process; thus, we developed an identification method that circumvents the need for extensive purification. The approach utilises the resolving power of SDS–polyacrylamide gel electrophoresis to allow the identification of protein that, in a prior EMSA step, has altered mobility because it binds a probe. In principle, the approach need not be limited to the identification of DNA-binding proteins as the EMSA can be used to study proteins that bind RNA. We were recently invited to provide a detailed protocol for our method.

Methods for the identification of DNA-binding proteins are important as they allow function to be studied *in vivo* using reverse genetic approaches. They also aid biochemical and structural studies by allowing comparison with database entries of known properties and structure, and permitting the overexpression and manipulation of the corresponding genes in the natural or a heterologous host.

Overview of technique

The protocol is applicable to cases where the following three conditions are met; (i) an EMSA has already revealed the existence of a nucleic acid-interacting factor of interest, (ii) the interaction with probe produces a tight band that can migrate to a central position within a gel and (iii) sufficient complex is formed to allow detection of the protein component by Coomassie staining. With regard to the latter, the rule-of-thumb is that if a protein band (spot) can be detected by a standard Coomassie-staining protocol, it should be readily identifiable by peptide mass fingerprinting (PMF).

The level of purification required before the identification of protein by our approach is dependent on the number of copies of the nucleic acid-binding factor per cell. In our experience, we are able to assay binding activity in bacterial samples containing approximately 100 μg of protein. This amount is equivalent to the total protein content of approximately 6×10^8 *Escherichia coli* cells. Although we have no experience of working with samples from eukaryotic sources, we estimate using published values that the same amount of protein could be obtained from 2×10^7 haploid yeast cells. The amount of protein that can be detected readily by Coomassie staining is 0.5 pmol or more, which is equivalent to 3×10^{11} molecules. Given the aforementioned estimates and assuming that the majority of the molecules of a nucleic acid-interacting factor can be shifted, factors present at 500 or 15,000 copies per cell of *E. coli* or yeast, respectively, should be identifiable in cell extracts

using our approach. While transcription factors such as the cAMP receptor protein of *E. coli* and Sp1 of yeast are present in numbers in excess of these levels, many are not. Indeed, a recent analysis of protein expression in yeast indicates that the average copy number of its transcription factors is approximately 1,000. While in many cases, protein purification will be required before the adoption of our approach to identify a nucleic acid-interacting factor, the level of purification required should be easily obtainable in a single step such as ion-exchange chromatography.

An EMSA is run within a tube gel as is a control that lacks probe. The tubes are then place on top of separate SDS-polyacrylamide gels and the proteins resolved. Gels corresponding to an experimental and mock analysis are shown in Figure 1.

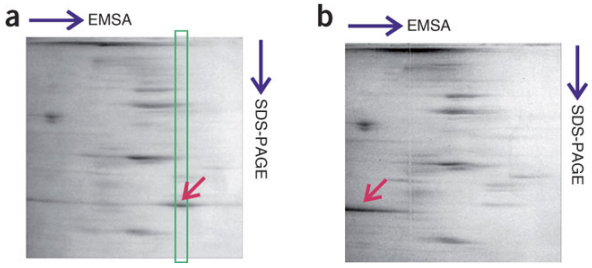

Fig. 1. Two-dimensional gel electrophoresis for identifying nucleic acid-binding proteins. Panel A, experimental sample. The green box indicates those polypeptides that are in line with the position of the complex at the end of running the first dimension, whereas the arrow indicates the position within this box of the unique band (spot) that corresponds to the nucleic acid-interacting factor. Panel B, mock sample. The arrow indicates the position of the free protein factor. Taken from Stead & McDowall (2007).

Publications

Stead, J.A., Keen J.N., & McDowall, K.J. (2007) Two-dimensional gel electrophoresis for identifying proteins that bind DNA or RNA. *Nature Prot.*, **2**, 1839-1848.

Stead, J.A. & McDowall, K.J. (2006) The identification of nucleic acid-interacting proteins using a simple proteomics-based approach that directly incorporates the electrophoretic mobility shift assay. *Mol. Cell. Proteomics*. **5**, 1697-1702.

Funding

This work was funded by a BBSRC grant and studentship to K. J. M.

Astbury Seminars 2007

11th January 2007
Dr Margarida Archer, Instituto de Tecnologia Quimica e Biologica, New University of Lisbon
"X-ray structure of the membrane-bound cytochrome c nitrite reductase complex NrfHA"

15th January 2007
Prof Haruki Nakamura, Institute for Protein Research, Osaka University, Japan
"Structural bioinformatics towards understanding protein functions"

8th February 2007
Prof Kazuhiro Oiwa, National Institute of Information and Communications Technology and University of Hyogo, Japan
"Force-generating mechanism of axonemal dyneins studied by cryoelectron tomography and x-ray fiber diffraction analysis"

8th March 2007
Prof So Iwata, Faculty of Life Sciences, Imperial College London
"Towards the structure determination of human membrane receptors"

19th April 2007
Prof Colin Robinson, Department of Biological Sciences, University of Warwick
"Transport of folded proteins by the twin-arginine translocation system in bacteria and chloroplasts"

17th May 2007
Prof Gabriel Waksman, Institute of Structural Molecular Biology, Birkbeck and University College London
"Structural biology of pilus biogenesis and bacterial host recognition"

7th June 2007
Dr Helen Walden, Cancer Research UK
"Mechanisms of ubiquitination"

21st June 2007
Dr Venki Ramakrishnan, MRC Laboratory of Molecular Biology
"The ribosome in action: structures of defined states of the ribosome"

12th July 2007
Dr Tim Hunt FRS, Cancer Research UK
"ANNUAL ASTBURY LECTURE - Getting into and out of mitosis "

6th September 2007
Dr Dejian Zhou, School of Chemistry, University of Leeds
"Fabrication and manipulation of functional biological nanostructures"

11th October 2007
Prof Ian Robinson, UCL and Diamond Light Source
"Coherent X-ray diffraction methods in biology"

18th October 2007
Dr Jonathan Essex, School of Chemistry, University of Southampton
"Coarse grained modelling of membrane systems"

1st November 2007
Prof Ted Baker, Department of Chemistry, The University of Auckland
"Discovering the structure and function of secreted and cell-surface virulence proteins of Staphylococcus and Streptococcus "

8th November 2007
Dr Sonia Contera, Bionanotechnology IRC, University of Oxford
"Using AFM to study the molecular forces and mechanical properties that control membrane protein function"

4th December 2007
Prof Stephen Martin, Chemistry and Biochemistry Department, The University of Texas at Austin
"Preorganization in Biological Systems: Are Conformational Constraints Really Worth the Energy?"

6th December 2007
Dr Jennifer Potts, Department of Biology, University of York
"Unusual interactions: the structural biology of Staphylococcus aureus invasion of human cells "

7th December 2007
Prof Arthur Olson, Department of Molecular Biology, The Scripps Research Institute
"Tangible Interfaces for Molecular Biology"

Publications by Astbury Centre Members 2007

Allen, L. R. & Paci, E. (2007). Transition states for protein folding using molecular dynamics and experimental restraints. *J. Phys.: Condens. Matter* **19**, Jul 18.

Ansell, R. J., Barrett, S. A., Meegan, J. E. & Warriner, S. L. (2007). On the interactions of alkyl 2-hydroxycarboxylic acids with alkoxysilanes: Selective esterification of simple 2-hydroxycarboxylic acids. *Chem. Eur. J.* **13**, 4654-4664.

Baldwin, S. A., McConkey, G. A., Cass, C. E. & Young, J. D. (2007). Nucleoside transport as a potential target for chemotherapy in malaria. *Curr. Pharm. Des.* **13**, 569-580.

Borysik, A. J., Morten, I. J., Radford, S. E. & Hewitt, E. W. (2007). Specific glycosaminoglycans promote unseeded amyloid formation from beta(2)-microglobulin under physiological conditions. *Kidney Int.* **72**, 174-181.

Bracey, K. & Wray, D. (2007). Effect of tubulin binding on the heag2 potassium channel. *Biophys. J.*, 126A-127A.

Brockwell, D. J. (2007). Force denaturation of proteins - an unfolding story. *Current Nanoscience* **3**, 3-15.

Brockwell, D. J. (2007). Probing the mechanical stability of proteins using the atomic force microscope. *Biochem. Soc. Trans.* **35**, 1564-1568.

Brockwell, D. J. & Radford, S. E. (2007). Intermediates: ubiquitous species on folding energy landscapes? *Curr. Opin. Struct. Biol.* **17**, 30-37.

Bunka, D. H. J., Mantle, B. J., Morten, I. J., Tennent, G. A., Radford, S. E. & Stockley, P. G. (2007). Production and characterization of RNA aptamers specific for amyloid fibril epitopes. *J. Biol. Chem.* **282**, 34500-34509.

Burgess, S. A., Yu, S. Z., Walker, M. L., Hawkins, R. J., Chalovich, J. M. & Knight, P. J. (2007). Structures of smooth muscle myosin and heavy meromyosin in the folded, shutdown state. *J. Mol. Biol.* **372**, 1165-1178.

Burnley, B. T., Kalverda, A. P., Paisey, S. J., Berry, A. & Homans, S. W. (2007). Hadamard NMR spectroscopy for relaxation measurements of large (> 35 kDa) proteins. *J. Biomol. NMR* **39**, 239-245.

Campbell, F., Plante, J., Carruthers, C., Hardie, M. J., Prior, T. J. & Wilson, A. J. (2007). Macrocyclic scaffolds derived from p-aminobenzoic acid. *Chemical Communications*, 2240-2242.

Care, M. A., Needham, C. J., Bulpitt, A. J. & Westhead, D. R. (2007). Deleterious SNP prediction: be mindful of your training data! *Bioinformatics* **23**, 664-672.

Carr, S. B., Makris, G., Phillips, S. E. V. & Thomas, C. D. (2007). Crystallization and preliminary X-ray diffraction analysis of two N-terminal fragments of the DNA-cleavage domain of topoisomerase IV from *Staphylococcus aureus*. *Acta Cryst F - Struct Biol & Crystal Commun* **63**, 59-59.

Caryl, J. A. & Thomas, C. D. (2007). The pC221 relaxosome: essential interactions for nicking and mobilization. *Plasmid* **57**, 195-195.

Casey, T. M., Meade, J. L. & Hewitt, E. W. (2007). Organelle proteomics. *Molecular & Cellular Proteomics* **6**, 767-780.

Cawood, R., Harrison, S. M., Dove, B. K., Reed, M. L. & Hiscox, J. A. (2007). Cell cycle dependent nucleolar localization of the coronavirus nucleocapsid protein. *Cell Cycle* **6**, 863-867.

Cockell, S. J., Oliva, B. & Jackson, R. M. (2007). Structure-based evaluation of *in silico* predictions of protein-protein interactions using comparative docking. *Bioinformatics* **23**, 573-581.

Craven, C. J., Al-Owais, M. & Parker, M. J. (2007). A systematic analysis of backbone amide assignments achieved via combinatorial selective labelling of amino acids. *J. Biomol. NMR* **38**, 151-159.

Dalton, J. A. R. & Jackson, R. M. (2007). An evaluation of automated homology modelling methods at low target-template sequence similarity. *Bioinformatics* **23**, 1901-1908.

Damaraju, V. L., Elwi, A. N., Hunter, C., Carpenter, P., Santos, C., Barron, G. M., Sun, X. J., Baldwin, S. A., Young, J. D., Mackey, J. R., Sawyer, M. B. & Cass, C. E. (2007). Localization of broadly selective equilibrative and concentrative nucleoside transporters, hENT1 and hCNT3, in human kidney. *Am. J. Physiol. - Renal Physiol.* **293**, F200-F211.

Damiano, T., Morton, D. & Nelson, A. (2007). Photochemical transformations of pyridinium salts: mechanistic studies and applications in synthesis. *Organic & Biomolecular Chemistry* **5**, 2735-2752.

Davies, J. R., Jackson, R. M., Mardia, K. V. & Taylor, C. C. (2007). The Poisson Index: a new probabilistic model for protein ligand binding site similarity. *Bioinformatics* **23**, 3001-3008.

Dodd, K., Morton, D., Worden, S., Narquizian, R. & Nelson, A. (2007). Desymmetrisation of a centrosymmetric molecule by carbon-carbon bond formation: Asymmetric aldol reactions of a centrosymmetric dialdehyde. *Chem. Eur. J.* **13**, 5857-5861.

Duarte, A. M. S., Wolfs, C., van Nuland, N. A. J., Harrison, M. A., Findlay, J. B. C., van Mierlo, C. P. M. & Hemminga, M. A. (2007). Structure and localization of an essential transmembrane segment of the proton translocation channel of yeast H^+-VATPase. *Biochimica Et Biophysica Acta-Biomembranes* **1768**, 218-227.

Embery, J., Graham, R. S., Duckett, R. A., Groves, D., Collis, M., Mackley, M. R. & McLeish, T. C. B. (2007). Tearing energy study of "oriented and relaxed" polystyrene in the glassy state. *Journal Of Polymer Science Part B-Polymer Physics* **45**, 377-394.

Erbe, A., Bushby, R. J., Evans, S. D. & Jeuken, L. J. C. (2007). Tethered bilayer lipid membranes studied by simultaneous attenuated total reflectance infrared spectroscopy and electrochemical impedance spectroscopy. *Journal Of Physical Chemistry B* **111**, 3515-3524.

Espinosa, M. & Thomas, C. D. (2007). Replication - Summary. *Plasmid* **57**, 183-185.

Garner, A. E., Smith, D. A. & Hooper, N. M. (2007). Sphingomyelin chain length influences the distribution of GPI-anchored proteins in rafts in supported lipid bilayers. *Mol. Membr. Biol.* **24**, 233-242.

Garnett, J. A., Baumberg, S., Stockley, P. G. & Phillips, S. E. V. (2007). A high-resolution structure of the DNA-binding domain of AhrC, the arginine repressor/activator protein from *Bacillus subtilis*. *Acta Cryst F -Struct Biol & Crystal Commun* **63**, 914-917.

Garnett, J. A., Baumberg, S., Stockley, P. G. & Phillips, S. E. V. (2007). Structure of the C-terminal effector-binding domain of AhrC bound to its corepressor L-arginine. *Acta Cryst F -Struct Biol & Crystal Commun* **63**, 918-921.

Garrow, A. G. & Westhead, D. R. (2007). A consensus algorithm to screen genomes for novel families of transmembrane beta barrel proteins. *Proteins-Structure Function And Bioinformatics* **69**, 8-18.

Gold, N. D., Deville, K. & Jackson, R. M. (2007). New opportunities for protease ligand-binding site comparisons using SitesBase. *Biochem. Soc. Trans.* **35**, 561-565.

Griffiths, R. & Whitehouse, A. (2007). Herpesvirus saimiri episomal persistence is maintained via interaction between open reading frame 73 and the cellular chromosome-associated protein MeCP2. *J. Virol.* **81**, 4021-4032.

Gunn, S. J., Baker, A., Bertrarn, R. D. & Warriner, S. L. (2007). A novel approach to the solid-phase synthesis of peptides with a tetrazole at the C-terminus. *Synlett*, 2643-2646.

Gutmann, D. A. P., Mizohata, E., Newstead, S., Ferrandon, S., Henderson, P. J. F., Van Veen, H. W. & Byrne, B. (2007). A high-throughput method for membrane protein solubility screening: The ultracentrifugation dispersity sedimentation assay. *Protein Sci.* **16**, 1422-1428.

Hadden, J. M., Declais, A. C., Carr, S. B., Lilley, D. M. J. & Phillips, S. E. V. (2007). The structural basis of Holliday junction resolution by T7 endonuclease. *Nature* **449**, 621-U615.

Hamming, I., Cooper, M. E., Haagmans, B. L., Hooper, N. M., Korstanje, R., Osterhaus, A., Timens, W., Turner, A. J., Navis, G. & van Goor, H. (2007). The emerging role of ACE2 in physiology and disease. *J. Pathol.* **212**, 1-11.

Hann, E., Kirkpatrick, N., Kleanthous, C., Smith, D. A., Radford, S. E. & Brockwell, D. J. (2007). The effect of protein complexation on the mechanical stability of Im9. *Biophys. J.* **92**, L79-L81.

Harrison, S. M., Dove, B. K., Rothwell, L., Kaiser, P., Tarpey, I., Brooks, G. & Hiscox, J. A. (2007). Characterisation of cyclin D1 down-regulation in coronavirus infected cells. *FEBS Lett.* **581**, 1275-1286.

Harrison, S. M., Tarpey, I., Rothwell, L., Kaiser, P. & Hiscox, J. A. (2007). Lithium chloride inhibits the coronavirus infectious bronchitis virus in cell culture. *Avian Pathology* **36**, 109-114.

Heikkila, T., Ramsey, C., Davies, M., Galtier, C., Stead, A. M. W., Johnson, A. P., Fishwick, C. W. G., Boa, A. N. & McConkey, G. A. (2007). Design and synthesis of potent inhibitors of the malaria parasite dihydroorotate dehydrogenase. *J. Med. Chem.* **50**, 186-191.

Henderson, P., Szakonyi, G., Leng, D., Ma, P., Blessie, H. Y. V. & Phillips-Jones, M. (2007). Bacterial membrane drug efflux and receptor proteins. *Drugs Of The Future* **32**, 6-6.

Hiscox, J. A. (2007). RNA viruses: hijacking the dynamic nucleolus. *Nature Reviews Microbiology* **5**, 119-127.

Hodgson, R., Kennedy, A., Nelson, A. & Perry, A. (2007). Synthesis of 3-sulfonyloxypyridines: Oxidative ring expansion of alpha-furylsulfonamides and N -> O sulfonyl transfer. *Synlett*, 1043-1046.

Homans, S. W. (2007). Dynamics and thermodynamics of ligand-protein interactions in Bioactive Conformation I. *Top. Curr. Chem.* **272**, 51-82.

Homans, S. W. (2007). Water, water everywhere - except where it matters? *Drug Discovery Today* **12**, 534-539.

Hong, B., Phornphisutthimas, S., Tilley, E., Baumberg, S. & McDowall, K. J. (2007). Streptomycin production by Streptomyces griseus can be modulated by a mechanism not associated with change in the adpA component of the A-factor cascade. *Biotechnol. Lett.* **29**, 57-64.

Huysmans, G. H. M., Radford, S. E., Brockwell, D. J. & Baldwin, S. A. (2007). The N-terminal helix is a post-assembly clamp in the bacterial outer membrane protein PagP. *J. Mol. Biol.* **373**, 529-540.

Ironmonger, A., Whittaker, B., Baron, A. J., Clique, B., Adams, C. J., Ashcroft, A. E., Stockley, P. G. & Nelson, A. (2007). Scanning conformational space with a library of stereo- and regiochemically diverse aminoglycoside derivatives: the discovery of new ligands for RNA hairpin sequences. *Organic & Biomolecular Chemistry* **5**, 1081-1086.

Isguder, S. Z., Hooper, N. M. & Naim, H. Y. (2007). GPI-Anchor dictates trafficking of membrane dipeptidase. *FASEB J.* **21**, A610-A610.

Jeuken, L. J. C., Bushby, R. J. & Evans, S. D. (2007). Proton transport into a tethered bilayer lipid membrane. *Electrochemistry Communications* **9**, 610-614.

Jeuken, L. J. C., Daskalakis, N. N., Han, X. J., Sheikh, K., Erbe, A., Bushby, R. J. & Evans, S. D. (2007). Phase separation in mixed self-assembled monolayers and its effect on biomimetic membranes. *Sensors And Actuators B-Chemical* **124**, 501-509.

Khatri, B. S., Kawakami, M., Byrne, K., Smith, D. A. & McLeish, T. C. B. (2007). Entropy and barrier-controlled fluctuations determine conformational viscoelasticity of single biomolecules. *Biophys. J.* **92**, 1825-1835.

Khatri, B. S. & McLeish, T. C. B. (2007). Rouse model with internal friction: A coarse grained framework for single biopolymer dynamics. *Macromolecules* **40**, 6770-6777.

Kotani, N., Sakakibara, H., Burgess, S. A., Kojima, H. & Oiwa, K. (2007). Mechanical properties of inner-arm dynein-F (dynein I1) studied with *in vitro* motility assays. *Biophys. J.* **93**, 886-894.

Legrand, B., Ashcroft, A. E., Buchaillot, L. & Arscott, S. (2007). SOI-based nanoelectrospray emitter tips for mass spectrometry: a coupled MEMS and microfluidic design. *Journal Of Micromechanics And Microengineering* **17**, 509-514.

Linse, S., Cabaleiro-Lago, C., Xue, W. F., Lynch, I., Lindman, S., Thulin, E., Radford, S. E. & Dawson, K. A. (2007). Nucleation of protein fibrillation by nanoparticles. *Proc. Natl. Acad. Sci. U. S. A.* **104**, 8691-8696.

Liu, B. B., Westhead, D. R., Boyett, M. R. & Warwicker, J. (2007). Modelling the pH-dependent properties of Kv1 potassium channels. *J. Mol. Biol.* **368**, 328-335.

MacRaild, C. A., Daranas, A. H., Bronowska, A. & Homans, S. W. (2007). Global changes in local protein dynamics reduce the entropic cost of carbohydrate binding in the arabinose-binding protein. *J. Mol. Biol.* **368**, 822-832.

Manfield, I. W., Devlin, P. F., Jen, C. H., Westhead, D. R. & Gilmartin, P. M. (2007). Conservation, convergence, and divergence of light-responsive, circadian-regulated, and tissue-specific expression patterns during evolution of the Arabidopsis GATA gene family. *Plant Physiol.* **143**, 941-958.

Mardia, K. V., Nyirongo, V. B., Green, P. J., Gold, N. D. & Westhead, D. R. (2007). Bayesian refinement of protein functional site matching. *Bmc Bioinformatics* **8**.

Maruta, F., Akita, N., Nakayama, J., Miyagawa, S., Ismail, T., Rowlands, D. C., Kerr, D. J., Fisher, K. D., Seymour, L. W. & Parker, A. L. (2007). Bacteriophage biopanning in human tumour biopsies to identify cancer-specific targeting ligands. *J. Drug Target.* **15**, 311-319.

Mathai, M., Radford, S. E. & Holland, P. (2007). Progressive glycosylation of albumin and its effect on the binding of homocysteine may be a key step in the pathogenesis of vascular damage in diabetes mellitus. *Med. Hypotheses* **69**, 166-172.

McLeish, T. C. B. (2007). A theory for heterogeneous states of polymer melts produced by single chain crystal melting. *Soft Matter* **3**, 83-87.

Morten, I. J., Gosal, W. S., Radford, S. E. & Hewitt, E. W. (2007). Investigation into the role of macrophages in the formation and degradation of beta(2)-microglobulin amyloid fibrils. *J. Biol. Chem.* **282**, 29691-29700.

Morton, V. L., Friel, C. T., Allen, L. R., Paci, E. & Radford, S. E. (2007). The effect of increasing the stability of non-native interactions on the folding landscape of the bacterial immunity protein Im9. *J. Mol. Biol.* **371**, 554-568.

Nagalingam, A. C., Radford, S. E. & Warriner, S. L. (2007). Avoidance of epimerization in the synthesis of peptide thioesters using Fmoc protection. *Synlett*, 2517-2520.

Needham, C. J., Bradford, J. R., Bulpitt, A. J. & Westhead, D. R. (2007). A primer on learning in Bayesian networks for computational biology. *Plos Computational Biology* **3**, 1409-1416.

Noronha, M., Lima, J. C., Paci, E., Santos, H. & Macanita, A. L. (2007). Tracking local conformational changes of ribonuclease A using picosecond time-resolved fluorescence of the six tyrosine residues. *Biophys. J.* **92**, 4401-4414.

Numata, N., Roberts, A., Burgess, S. A., Kon, T., Okura, R., Knight, P. & Sutoh, K. (2007). Are six AAA modules sufficient to form the AAA ring of dynein? *Biophys. J.*, 496A-496A.

Parkin, E. T., Watt, N. T., Hussain, I., Eckman, E. A., Eckman, C. B., Manson, J. C., Baybutt, H. N., Turner, A. J. & Hooper, N. M. (2007). Cellular prion protein regulates beta-secretase cleavage of the Alzheimer's amyloid precursor protein. *Proc. Natl. Acad. Sci. U. S. A.* **104**, 11062-11067.

Perazzolo, C., Verde, M., Homans, S. W. & Bodenhausen, G. (2007). Evidence of chemical exchange in recombinant Major Urinary Protein and quenching thereof upon pheromone binding. *J. Biomol. NMR* **38**, 3-9.

Pinney, J. W., Papp, B., Hyland, C., Warnbua, L., Westhead, D. R. & McConkey, G. A. (2007). Metabolic reconstruction and analysis for parasite genomes. *Trends In Parasitology* **23**, 548-554.

Rahman, M., Ismat, F., McPherson, M. J. & Baldwin, S. A. (2007). Topology-informed strategies for the overexpression and purification of membrane proteins. *Mol. Membr. Biol.* **24**, 407-U416.

Reed, M. L., Howell, G., Harrison, S. M., Spencer, K. A. & Hiscox, J. A. (2007). Characterization of the nuclear export signal in the coronavirus infectious bronchitis virus nucleocapsid protein. *J. Virol.* **81**, 4298-4304.

Reig, N., del Rio, C., Casagrande, F., Ratera, M., Gelpi, J. L., Torrents, D., Henderson, P. J. F., Xie, H., Baldwin, S. A., Zorzano, A., Fotiadis, D. & Palacin, M. (2007). Functional and structural characterization of the first prokaryotic member of the L-

amino acid transporter (LAT) family - A model for APC transporters. *J. Biol. Chem.* **282**, 13270-13281.

Rella, M., Elliot, J. L., Revett, T. J., Lanfear, J., Phelan, A., Jackson, R. M., Turner, A. J. & Hooper, N. M. (2007). Identification and characterisation of the angiotensin converting enzyme-3 (ACE3) gene: a novel mammalian homologue of ACE. *Bmc Genomics* **8**.

Rogers, M. S., Tyler, E. M., Akyumani, N., Kurtis, C. R., Spooner, R. K., Deacon, S. E., Tamber, S., Firbank, S. J., Mahmoud, K., Knowles, P. F., Phillips, S. E. V., McPherson, M. J. & Dooley, D. M. (2007). The stacking tryptophan of galactose oxidase: A second-coordination sphere residue that has profound effects on tyrosyl radical behavior and enzyme catalysis. *Biochemistry* **46**, 4606-4618.

Sader, K., Reedy, M., Popp, D., Lucaveche, C. & Trinick, J. (2007). Measuring the resolution of uncompressed plastic sections cut using an oscillating knife ultramicrotome. *J. Struct. Biol.* **159**, 29-35.

Say, Y. H. & Hooper, N. M. (2007). Contamination of nuclear fractions with plasma membrane lipid rafts. *Proteomics* **7**, 1059-1064.

Shibayama, K., Wachino, J., Arakawa, Y., Saidijam, M., Rutherford, N. G. & Henderson, P. J. F. (2007). Metabolism of glutamine and glutathione via gamma-glutamyltranspeptidase and glutamate transport in *Helicobacter pylori*: possible significance in the pathophysiology of the organism. *Mol. Microbiol.* **64**, 396-406.

Slugoski, M. D., Loewen, S. K., Ng, A. M. L., Smith, K. M., Yao, S. Y. M., Karpinski, E., Cass, C. E., Baldwin, S. A. & Young, J. D. (2007). Specific mutations in transmembrane helix 8 of human concentrative Na^+/nucleoside cotransporter hCNT1 affect permeant selectivity and cation coupling. *Biochemistry* **46**, 1684-1693.

Smith, D. P., Giles, K., Bateman, R. H., Radford, S. E. & Ashcroft, A. E. (2007). Monitoring copopulated conformational states during protein folding events using Electrospray ionization-ion mobility spectrometry-mass spectrometry. *J. Am. Soc. Mass Spectrom.* **18**, 2180-2190.

Smith, F. M., Slugosic, M. D., Cass, C. E., Baldwin, S. A., Karpinsi, E. & Young, J. D. (2007). Cation coupling properties of human concentrative nucleoside transporters hCNT1, hCNT2 and hCNT3. *Mol. Membr. Biol.* **24**, 53-64.

Song, C. F., Kendrick-Jones, J. & Trinick, J. (2007). Electron microscopy of negatively stained myosin VI molecules. *Biophys. J.*, 494A-494A.

Spencer, K. A., Dee, M., Britton, P. & Hiscox, J. A. (2007). Role of phosphorylation clusters in the biology of the coronavirus infectious bronchitis virus nucleocapsid protein. *Virology* **370**, 373-381.

Spencer, K. A., Osori, F. A. & Hiscox, J. A. (2007). Recombinant viral proteins for use in diagnostic ELISAs to detect virus infection. *Vaccine* **25**, 5653-5659.

Stead, J. A. & McDowall, K. J. (2007). Two-dimensional gel electrophoresis for identifying proteins that bind DNA or RNA. *Nature Protocols* **2**, 1839-1848.

Stead, M. A., Trinh, C. H., Garnett, J. A., Carr, S. B., Baron, A. J., Edwards, T. A. & Wright, S. C. (2007). A beta-sheet interaction interface directs the tetramerisation of the Miz-1 POZ domain. *J. Mol. Biol.* **373**, 820-826.

StGelais, C., Tuthill, T. J., Clarke, D. S., Rowlands, D. J., Harris, M. & Griffin, S. (2007). Inhibition of hepatitis C virus p7 membrane channels in a liposome-based assay system. *Antiviral Res.* **76**, 48-58.

Stockley, P. G., Rolfsson, O., Thompson, G. S., Basnak, G., Francese, S., Stonehouse, N. J., Homans, S. W. & Ashcroft, A. E. (2007). A simple, RNA-mediated allosteric switch controls the pathway to formation of a T=3 viral capsid. *J. Mol. Biol.* **369**, 541-552.

Syme, N. R., Dennis, C., Phillips, S. E. V. & Homans, S. W. (2007). Origin of heat capacity changes in a "Nonclassical" hydrophobic interaction. *Chembiochem* **8**, 1509-1511.

Szakonyi, G., Leng, D., Ma, P., Bettaney, K. E., Saidijam, M., Ward, A., Zibaei, S., Gardiner, A. T., Cogdell, R. J., Butaye, P., Kolsto, A. B., O'Reilly, J., Hope, R. J., Rutherford, N. G., Hoyle, C. J. & Henderson, P. J. F. (2007). A genomic strategy for cloning, expressing and purifying efflux proteins of the major facilitator superfamily. *J. Antimicrob. Chemother.* **59**, 1265-1270.

Taylor, D. R. & Hooper, N. M. (2007). The low-density lipoprotein receptor-related protein 1 (LRP1) mediates the endocytosis of the cellular prion protein. *Biochem. J.* **402**, 17-23.

Taylor, D. R. & Hooper, N. M. (2007). Role of lipid rafts in the processing of the pathogenic prion and Alzheimer's amyloid-beta proteins. *Semin. Cell Dev. Biol.* **18**, 638-648.

Tedbury, P. R. & Harris, M. (2007). Characterisation of the role of zinc in the hepatitis C virus NS2/3 auto-cleavage and NS3 protease activities. *J. Mol. Biol.* **366**, 1652-1660.

Teixeira, P. I. C., Read, D. J. & McLeish, T. C. B. (2007). Demixing instability in coil-rod blends undergoing polycondensation reactions. *J. Chem. Phys.* **126**.

Thomas, C. D. & Joce, C. M. (2007). The inverted complementary repeat is a consequence of, not a requirement for, the action of a replication initiator protein at a replication origin. *Plasmid* **57**, 186-186.

Thomson, N. H., Crampton, N., Bonass, W. A., Kirkham, J. & Rivetti, C. (2007). RNA polymerase collisions in the atomic force microscope. *Biophys. J.*, 411A-411A.

Trinh, C. H., Liu, Y., Phillips, S. E. V. & Phillips-Jones, M. K. (2007). Structure of the response regulator VicR DNA-binding domain. *Acta Crystallographica Section D-Biological Crystallography* **63**, 266-269.

Tuthill, T. J., Rowlands, D. J. & Killington, R. A. (2007). Picornavirus entry. *Future Virology* **2**, 343-351.

Vardy, E., Rice, P. J., Bowie, P. C. W., Holmes, J. D., Grant, P. J. & Hooper, N. M. (2007). Increased circulating insulin-like growth factor-1 in late-onset Alzheimer's disease. *Journal Of Alzheimers Disease* **12**, 285-290.

Visser, F., Sun, L. J., Damaraju, V., Tackaberry, T., Peng, Y. S., Robins, M. J., Baldwin, S. A., Young, J. D. & Cass, C. E. (2007). Residues 334 and 338 in transmembrane segment 8 of human equilibrative nucleoside transporter 1 are important determinants of inhibitor sensitivity, protein folding, and catalytic turnover. *J. Biol. Chem.* **282**, 14148-14157.

Vohra, R. S., Murphy, J., Walker, J. H., Homer-Vanniasinkam, S. & Ponnambalam, S. (2007). Refolding and functional characterization of the lectin-like oxidized low-density lipoprotein scavenger receptor (LOX-1). *FASEB J.* **21**, A852-A852.

Vohra, R. S., Murphy, J. E., Walker, J. H., Homer-Vanniasinkam, S. & Ponnambalam, S. (2007). Functional refolding of a recombinant C-type lectin-like domain containing intramolecular disulfide bonds. *Protein Expr. Purif.* **52**, 415-421.

Watt, N. T., Routledge, M. N., Wild, C. P. & Hooper, N. M. (2007). Cellular prion protein protects against reactive-oxygen-species-induced DNA damage. *Free Radic. Biol. Med.* **43**, 959-967.

White, H. D. & Ashcroft, A. E. (2007). Real-time measurement of myosin-nucleotide noncovalent complexes by electrospray ionization mass spectrometry. *Biophys. J.* **93**, 914-919.

Whittaker, S. B. M., Spence, G. R., Grossmann, J. G., Radford, S. E. & Moore, G. R. (2007). NMR analysis of the conformational properties of the trapped on-pathway folding intermediate of the bacterial immunity protein Im7. *J. Mol. Biol.* **366**, 1001-1015.

Wijma, H. J., Jeuken, L. J. C., Verbeet, M. P., Armstrong, F. A. & Canters, G. W. (2007). Protein film voltammetry of copper-containing nitrite reductase reveals reversible inactivation. *J. Am. Chem. Soc.* **129**, 8557-8565.

Wilson, A. J. (2007). Non-covalent polymer assembly using arrays of hydrogen-bonds. *Soft Matter* **3**, 409-425.

Wilson, S. J., Tsao, E. H., Webb, B. L. J., Ye, H. T., Dalton-Griffin, L., Tsantoulas, C., Gale, C. V., Du, M. Q., Whitehouse, A. & Kellam, P. (2007). X box binding protein XBP-1s transactivates the Kaposi's sarcoma-associated herpesvirus (KSHV) ORF50 promoter, linking plasma cell differentiation to KSHV reactivation from latency. *J. Virol.* **81**, 13578-13586.

Wozniak, A. L., Griffin, S., Rowlands, D., Harris, M. & Weinman, S. A. (2007). Hepatitis CP 7 protein alters the proton conductance of intracellular membrane vesicles. *Hepatology* **46**, 452A-452A.

Yao, S. Y. M., Ng, A. M. L., Slugoski, M. D., Smith, K. M., Mulinta, R., Karpinski, E., Cass, C. E., Baldwin, S. A. & Young, J. D. (2007). Conserved glutamate residues are critically involved in Na^+/Nucleoside cotransport by human concentrative nucleoside transporter 1 (hCNT1). *J. Biol. Chem.* **282**, 30607-30617.

Yoon, H. J., Park, S. W., Lee, H. B., Im, S. Y., Hooper, N. M. & Park, H. S. (2007). Release of renal dipeptidase from glycosylphosphatidylinositol anchor by insulin-triggered phospholipase C/intracellular Ca^{2+}. *Arch. Pharm. Res.* **30**, 608-615.

You, J. H., Reed, M. L. & Hiscox, J. A. (2007). Trafficking motifs in the SARS-coronavirus nucleocapsid protein. *Biochem. Biophys. Res. Commun.* **358**, 1015-1020.

Zhang, J., Visser, F., King, K. M., Baldwin, S. A., Young, J. D. & Cass, C. E. (2007). The role of nucleoside transporters in cancer chemotherapy with nucleoside drugs. *Cancer Metastasis Rev.* **26**, 85-110.

Zhang, W. K., Dillingham, M. S., Thomas, C. D., Allen, S., Roberts, C. J. & Soultanas, P. (2007). Directional loading and stimulation of PcrA helicase by the replication initiator protein RepD. *J. Mol. Biol.* **371**, 336-348.

UNIVERSITY OF LEEDS

Leeds, United Kingdom
LS2 9JT
Tel. 0113 243 1751
www.leeds.ac.uk